

VILNIUS UNIVERSITY  
CENTER FOR PHYSICAL SCIENCES AND TECHNOLOGY

LUKAS TAUJENIS

IDENTIFICATION AND ENANTIOSELECTIVE DETERMINATION OF  
PROTEIN AMINO ACIDS IN FERTILIZERS BY HYDROPHILIC  
INTERACTION AND CHIRAL CHROMATOGRAPHY COUPLED TO  
TANDEM MASS SPECTROMETRY

Doctoral dissertation

Physical Sciences, Chemistry (03 P)

Vilnius, 2016

The research was carried out at Vilnius University in the period of 2011 - 2015.

Scientific supervisor – prof. habil. dr. Audrius Padarauskas (Vilnius University, physical sciences, chemistry – 03 P)

## TABLE OF CONTENTS

ABBREVIATIONS .....	5
INTRODUCTION .....	6
1. LITERATURE REVIEW .....	9
1.1. HPLC – a brief history .....	9
1.2. Hydrophilic interaction chromatography .....	11
1.3. Chiral HPLC stationary phases .....	13
1.3.1. Polysaccharide based CSPs .....	15
1.3.2. Cyclodextrin based CSPs.....	17
1.3.3. Brush/Pirkle-type CSPs .....	19
1.3.4. Macrocyclic antibiotic based CSPs .....	20
1.4. Mass spectrometry .....	22
1.4.1. Ion sources .....	24
1.4.2. Mass analyzers.....	28
1.4.3. Tandem mass spectrometry (MS/MS).....	34
1.5. Hydrolyzed protein fertilizers .....	36
1.6. Determination of amino acids .....	38
1.7. Enantioselective HPLC determination of amino acids .....	41
1.8. Determination of amino acids in HPF .....	42
1.9. Method validation .....	43
2. EXPERIMENTAL.....	46
2.1. Equipment .....	46
2.2. Materials.....	46
2.3. Sample preparation .....	47
2.4. Method validation .....	48
3. RESULTS AND DISSCUSIONS.....	49
3.1. Characterization of amino acids.....	49
3.2. Tandem mass spectrometry parameters .....	51
3.3. HILIC separation.....	55
3.4. Enantioselective HPLC separation.....	69

3.5. Validation of the methods .....	83
3.5.1. HILIC-MS/MS .....	83
3.5.1. Chiral LC-MS/MS .....	85
3.6. Sample Analysis .....	89
CONCLUSIONS .....	97
Publications summarized in doctoral dissertation.....	98
ACKNOWLEDGEMENT .....	98
REFERENCES .....	100

## **ABBREVIATIONS**

APCI – atmospheric pressure chemical ionization

CD – cyclodextrin

CEC – capillary electrochromatography

CRM – certified reference material

CSP – chiral stationary phase

CTA – cellulose triacetate

ESI – electrospray ionization

FWHM – full width at half maximum

GC – gas chromatography

HILIC – hydrophilic interaction chromatography

HPF – hydrolyzed protein fertilizers

HPLC – high performance liquid chromatography

IS – ion source

LOD – limit of detection

LOQ – limit of quantification

MRM – multiple reaction monitoring

MS – mass spectrometry

MS/MS – tandem mass spectrometry

NP – normal phase chromatography

QqQ – triple quadrupole

RP – reversed phase

TOF – time of flight

## INTRODUCTION

Various types of fertilizers have been used in agriculture for the centuries. Compost, manure and other kinds of natural fertilizing materials have been replaced by synthetic inorganic nitrogen and phosphorous sources during technological development era. However, the use of large scale of the synthetic fertilizers has a huge negative impact to environment and food quality. Therefore developed countries encourage and support eco-farming. The problem is that increased food demand not always can be satisfied without growth stimulants. Novel fertilizer materials that meet eco and quality standards are currently produced from sources of natural origin. One of those are hydrolyzed protein fertilizers (HPF). The amino acids that are obtained during protein hydrolysis is an alternative nitrogen source for plants. In addition, natural amino acids can be easily processed by microorganism and do not interrupt ecosystem.

In order to evaluate and control HPF products fast and effective analytical techniques are of a great significance. High performance liquid chromatography (HPLC) is perhaps the best choice for the determination of a large number of nonvolatile analytes having very similar properties. However, the determination of amino acids by the most popular reversed phase HPLC coupled to photo diode array detector is associated with two problems. The first one is related to detection: most of the amino acids cannot be detected using conventional UV detector due to lack of chromophore. A more serious problem is that conventional reversed phase (RP) stationary phases do not provide sufficient retention of very hydrophilic analytes. Pre-column derivatization is therefore required to improve detectability and increase retention of the amino acids. Although this approach is well understood and has been historically well received, it is labor intensive and time-consuming.

Above mentioned problems can usually be avoided by using hydrophilic interaction chromatography (HILIC) coupled to mass spectrometry (MS). HILIC technique uses a polar stationary phase in conjunction with a mobile

phase consisting of a polar organic solvent (typically acetonitrile) containing an appreciable amount of water. The main advantage of HILIC is that it well retains very polar and ionizable compounds such as amino acids. In addition, the large percentage of acetonitrile ( $\geq 60\%$ ) in the HILIC mobile phase enables facilitated solvent evaporation in MS source and thus often an increase in analyte response when compared to water-rich mobile phase systems. Taking all these factors into account, the HILIC technique coupled to MS seems to be very promising for the determination of amino acids.

Amino acids have at least one chiral carbon atom (except of glycine), therefore these compounds can undergo racemization during fertilizers manufacturing. However, only L-amino acids can be effectively assimilated by plants, and D-amino acids are not involved in enzymatic growth processes or might even be toxic in some cases. Therefore analytical methods are also necessary to assess the enantiopurity of amino acids. For the chiral separation of amino acids, HPLC is perhaps the most popular and reliable technique among all chromatographic and electromigration separation methods. There are two main approaches for HPLC separation of enantiomers: indirect, which uses derivatization prior to analysis, and direct, which uses chiral stationary phases or, more rarely, chiral mobile phase additives. By far, the most successful enantioselective separations of various chiral compounds were achieved on chiral stationary phases.

**The aim of the doctoral thesis** was to develop fast, reliable and effective liquid chromatography-tandem mass spectrometry techniques for the identification and enantioselective determination of protein amino acids in hydrolyzed protein fertilizers.

**The following main tasks** were set to achieve the aim:

1. Optimization of the HILIC-MS/MS method for the separation and identification of protein amino acids.

2. Development of the chiral HPLC-MS/MS method based on teicoplanin stationary phase for the enantioselective determination of protein amino acids.
3. Validation and application of the developed methods for the identification and enantioselective determination of protein amino acids in commercial hydrolyzed protein fertilizers.

**Statements for defense:**

1. Among the three stationary phases investigated a silica-based amide bonded phase exhibits the best performance for the separation of amino acids in HILIC mode.
2. Under HILIC conditions amino acids are retained by the mixed partition/adsorption retention mechanism.
3. Amino acids on teicoplanin based chiral stationary phase show typical HILIC retention behavior.
4. Tandem mass spectrometry operating in multiple reaction monitoring mode enables selective and sensitive detection of amino acids.
5. Developed HILIC-MS/MS and chiral HPLC-MS/MS techniques are well suited for the fast analysis of commercial fertilizers.



## **1. LITERATURE REVIEW**

### **1.1. HPLC – a brief history**

The first steps of chromatography science often is dated back to 1903 [1,2], when Mikhail S. Tswett presented a lecture “On a new category of adsorption phenomena and their application to biochemical analysis”. He was the first who used the term “chromatography”. In his paper he explained chromatogram and its development using different eluents for the separation of chlorophylls a and b [3]. Despite the fact that Tswett have discussed his ideas on chromatography with leading scientists of European countries, chromatography was largely ignored until the early 1930s. Later, the principle of chromatography was applied for the separation of carotenoids and for the purification for naturally occurring organic products [4]. Tswet`s technique is now described as normal phase (NP) chromatography and basically all early stage chromatographic separations were related to this separation mode [5]. NP separation technique uses columns packed with polar stationary phases combined with nonpolar or moderately-polar mobile phases. The retention is resulted by the analytes adsorption on the stationary phase surface and analytes are eluted from the column in order of increasing polarity. Polar cellulose or inorganic oxide (e.g., silica gel, aluminium oxide) stationary phases combined with nonpolar organic mobile phases were the main chromatographic systems till mid-1960s, when non-polar alkyl chains bonded stationary phases started to appear and reversed phase (RP) chromatography mode was introduced [5,6]. The use of a hydrophobic stationary phase in combination with polar mobile phase can be considered the opposite, or "reverse", of normal phase chromatography. Consequently, the term "reversed-phase chromatography" was accepted to designate chromatography of this type. In RP separation mode of chromatography the retention increases with decreasing analyte polarity. The popularity of novel RP separation mode was inevitable, taking into account that at that time NP inorganic oxide sorbents suffered from slow equilibrium and site heterogeneity that resulted nonlinear adsorption isotherms. Peak tailing and retention time shifting, when different concentration samples were injected, was also a great problem. In addition, rapid

development of pharmaceutical industry promoted popularity of the RP mode, because large scale molecules of interest were well separated on nonpolar stationary phases using aqueous buffers with water miscible organic solvents as the mobile phases.

In the late 1960s Horvath demonstrated the chromatographic separation on packed column with mobile phases that were delivered by high pressure pumps [7]. Commercial development of in-line detectors and reliable injectors allowed liquid chromatography to become a sensitive and quantitative technique leading to an explosive growth of applications [1]. The acronym HPLC (high performance liquid chromatography) was born. It is not clear if HPLC originally meant high performance liquid chromatography (as it usually does today) or high pressure liquid chromatography (which was required to get the superior performance). In either case, HPLC is usually used to distinguish between the new, modern mode of operation as opposed to the old Tswett method. Such technological accomplishment was a huge breakthrough for the liquid chromatography. 5<sup>th</sup> symposium on “Advances in Chromatography” in 1969 (Miami) became a fast-track for HPLC. Special session for HPLC was organized and several companies already introduced their HPLC instrumentation [1]. The development of HPLC instrumentation was accompanied by the development of novel column packing technologies. During the next two decades many novel stationary phases with various surface phase chemistry and polarity have been designed and synthesized for the separations in different HPLC modes. Analytes applicable for HPLC separations can be classified from extremely hydrophobic compounds such as carotenoids to highly hydrophilic like carbohydrates. However, the separation of small, very polar and ionized compounds was challenging for a long time. NP-HPLC separation mode is not suitable for such compounds due to their low solubility in nonpolar mobile phases. The use of RP-HPLC is hampered by two important drawbacks: (1) the resolution of very polar and ionized compounds is difficult because these compounds are weakly or even not retained on conventional RP stationary phases; and (2) significant

peak tailing takes place by the separation of ionized analytes due to the electrostatic interactions with ionized residual silanol groups.

The above mentioned problems can usually be avoided by using hydrophilic interaction chromatography (HILIC) technique first introduced in 1990 by Alpert [8]. However, for a couple of years HILIC has been almost forgotten and only since the early 2000s it became one of the fastest growing chromatographic techniques employed for the separation of wide range of polar compounds.

## **1.2. Hydrophilic interaction chromatography**

Hydrophilic interaction chromatography is a chromatographic technique which in a way combined both RP and NP separation modes. The separation in this method is performed on the polar stationary phases and the mobile phases are polar organic solvents. The acronym of this mode - “Hydrophilic Interaction Chromatography” (HILIC) - was introduced only in 1990 by Alpert [8], although this separation technique had been already used for oligosaccharide analysis since 1975 [9].

As already mentioned above, HILIC mode has some features of RP and NP separation modes [10]. In RP chromatography retention is considered to be controlled by partition mechanism only. In contrast, in NP chromatography retention is based on adsorption of the analytes on stationary phase surface. In HILIC analytes are separated on polar stationary phases with polar mobile phase composed of an aqueous-organic (acetonitrile in most cases) mixture usually containing approximately 5% to 40% of water. From chromatographic point of view such phase combination seemed to be inappropriate: water molecules would shield stationary phase surface silanol groups and, consequently, would prevent the interaction of the analytes with stationary phase. But the key concept of HILIC separation lies in formation of aqueous sublayer. Due to hydrogen bonding, water molecules are immobilized on polar stationary phase surface and form liquid stationary phase. Alpert believed that partition is the dominant mechanism in HILIC [8], where separation of polar or charged analytes is

resulted by partition between bulk eluent and a water-rich layer. He made this assumption based on previous experiments that were carried out for the separation of carbohydrates on unbonded and amino bonded silica phases [11] and on similarity of analytes retention behavior with those observed for DNA separation on microgranular cellulose using two phase partition system [12].

In his first HILIC article Alpert suggested that the retention can also be influenced by other factors, such as hydrogen bonding, ion-exchange or dipole-dipole interactions [8]. Later, in 2006, Hemstrom and Irgum [5] applied partition and adsorption models for previously published data and demonstrated that HILIC in fact exhibits much more complex retention mechanism (Figure 1.1.), which depends on nature of the stationary phase, analyte properties (neutral, acidic, basic) and mobile phase composition. Although HILIC is investigated extensively in the last decade, the exact mechanism of HILIC separation is still under debate.

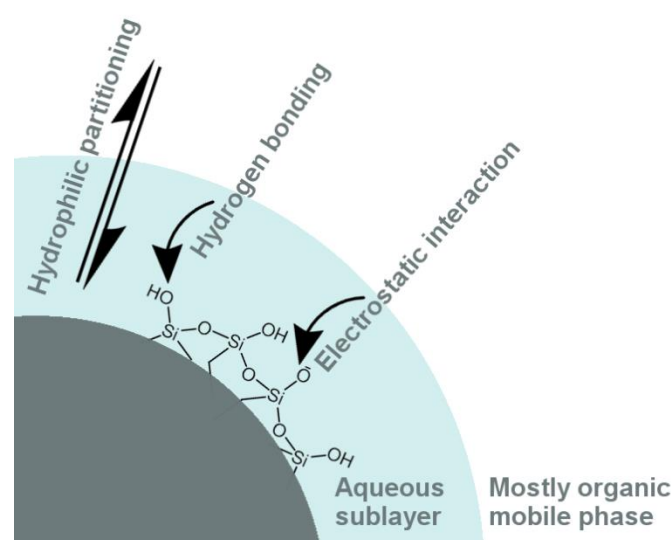


**Figure 1.1.** Partition and adsorption interactions on bare silica stationary phase under HILIC conditions.

Bare silica and amino-silica were the two stationary phases commonly employed for HILIC separations till early 2000s. Since then, a number of commercially

available phases designed especially for HILIC have been commercialized. Novel hydroxylated silica, hybrid silica-organic and polymeric silica phases have been designed [6]. Probably the most popular HILIC stationary phase is hydroxylated silica. In this type of stationary phases bare silica is hydroxylated by replacement of Si-OH groups to Si-H. The other type of HILIC phases contains organic modifier with polar or ionizable groups covalently linked to silica surface. There is a vast variability of such sorbents and probably the most popular are amino, amide, diol, sulfoalkylbetaine groups containing stationary phases. It is important to note that HILIC stationary phases containing expressed charge may be also employed as a weak anion or cation exchangers in ion exchange chromatography.

### **1.3. Chiral HPLC stationary phases**

Chiral separations are one of the major areas of interests in the pharmaceutical and agrochemical analysis fields. The ability of the enantiomers to have a different biochemical effect on the organisms has been known for a long time and probably the most tragic illustration on that is the Thalidomide tragedy [13]. Although the first successful resolution of the enantiomers on chiral selector was demonstrated in 1951 [14], the commercial chiral stationary phases (CSP) became available only after the Thalidomide events [15]. By the late 90`s the list of commercial CSP`s was exceeding 40 [16]. With the increase of the chiral HPLC popularity the need to classify chiral sorbents arose. Modern CSPs generally rely on spherical, porous silica gel as the underlying support particle. Silica has advantages of efficiency, stability, and ease of modification over synthetic polymer particles. So, although there are some exceptions, the most CSPs for modern chiral HPLC are silica particles covalently bonded or physically adsorbed with native, modified, or mimetic chiral selector. Producers offered various types of chiral selectors with individual sorbent surface chemistry, retention and enantioseparation properties. However, the names of the commercial products would not always be informative for consumers. For example, Enantiopac® or Resolvosil® does not tell much about the sorbent

origin and enantioseparation trends, whereas the knowledge of the processes that are responsible for enantioseparation is usually a crucial for advanced analyst/scientist. Therefore US born Irving W. Wainer suggested the classification of chiral columns according to their interaction mechanism with chiral analyte [17]. This CSP classification was introduced in 1987 [17] and was followed by a booklet “A Practical Guide to the Selection and Use of HPLC Chiral Stationary Phases”.

**Table 1.1.**

The Wainer CSP classification.

Type	Mechanism	CSPs [17]	Novel CSPs (post-1988) [16]
<b>I</b>	Complexes are formed by attractive interactions. H-bonding, $\pi$ - $\pi$ interaction, dipole stacking, etc.	Brush/Pirkle-type.	Aromatic cyclofructans (NP).
<b>II</b>	The primary mechanism is based on attractive interactions together with inclusion complexes.	Cellulose and Amylose derivatives.	Macrocyclic antibiotics (RP), higher generation Brush/Pirkle-type, aryl-modified cyclodextrins.
<b>III</b>	The analytes are separated due to the formation of inclusion complexes in the chiral cavities.	Cyclodextrins, crown ethers, helical polymers.	Alkylated cyclofructans.
<b>IV</b>	Chiral ligand-exchange chromatography. Analytes are part of diastereomeric metal complexes.	Conventional achiral stationary phase with enantioselective mobile phase modifier.	
<b>V</b>	CSP is protein and analyte-CSP complex formation is based on multiple hydrophobic and polar interactions.	Human $\alpha$ acid glycoprotein (AGP), bovine serum albumin (BSA)	Macrocyclic antibiotics.

According to the formation of the analyte-CSP complex, five CSPs categories were highlighted (Table 1.1). This classification was applied for commercial columns and was a guide until further attempts to imply suggested model for

newly developed stationary phases. Other possible classification is based on the origin of CSP. There are over 100 brands of commercially available chiral HPLC stationary phases [18], though at least 20-30 of them are mostly employed for the majority separations. The most common chiral selector classes based on the origin of the stationary phase are:

- ❖ Polysaccharide CSPs.
- ❖ CSPs based on synthetic polymers.
- ❖ Protein CSPs.
- ❖ Cyclodextrin CSPs.
- ❖ Macrocyclic antibiotic CSPs.
- ❖ Chiral crown-ether CSPs.
- ❖ Brush/Pirkle-type CSPs.
- ❖ Chiral ion-exchange CSPs.
- ❖ Chiral-ligand exchange CSPs.

In this section the most common CSP`s employed for enantioselective separations are briefly described.

### **1.3.1. Polysaccharide based CSPs**

Saccharides and polysaccharides were the starting stationary phase materials for the development of enantioselective chromatography. The attempts to separate optical isomers on natural biopolymers such as silk and wool were conducted in 1904, by Willstätter [19]. Later, the first partial chiral separation of the terpenoid enantiomers was demonstrated on the lactose chiral selector. Following the research on enantioseparation of ephedrine, Troeger`s base and some other enantiomers, the overview of chiral separations on the saccharide based CSPs was published [19]. However, the real potential of saccharide CSPs was demonstrated when derivatized cellulose was introduced, first by Lüttringhaus et al. in 1966 [15], followed by Hesse and Hegel, who five years later introduced fully acetylated cellulose (triacetylcellulose) as a new efficient chiral CSP [20]. Microcrystalline cellulose triacetate (CTA) became a widely employed

commercial CSP in preparative enantioseparations for many applications [21]. However, the CTA suffers from instability, due to moderate solubility of the triacetylcellulose in most of the organic solvents used for HPLC separations. Therefore CTA stationary phases found its application only in preparative scale. Novel generation polysaccharide CSPs containing derivatized polysaccharides were developed by Okamoto's group [22,23] and Daicel company in Japan. Various polysaccharides, namely cellulose, amylose, inulin, curdlan, chitosan, xylan, dextran and their derivatives (mainly phenylcarbamates) have been evaluated for enantioselectivity properties. However, only several of them, mostly cellulose and amylose based polysaccharide phenylcarbamates were commercialized. The physically coated derivatized polysaccharide materials were commercialized under trademarks of Chiralcel™ by Daicel and LUX™ by Phenomenex, whereas covalently bonded derivatized polysaccharide CSPs - as Chiralpak™ by Daicel. Figure 1.2 represents structural features of the most common cellulose and amylose tris-phenylcarbamate derivatives used for CSPs.

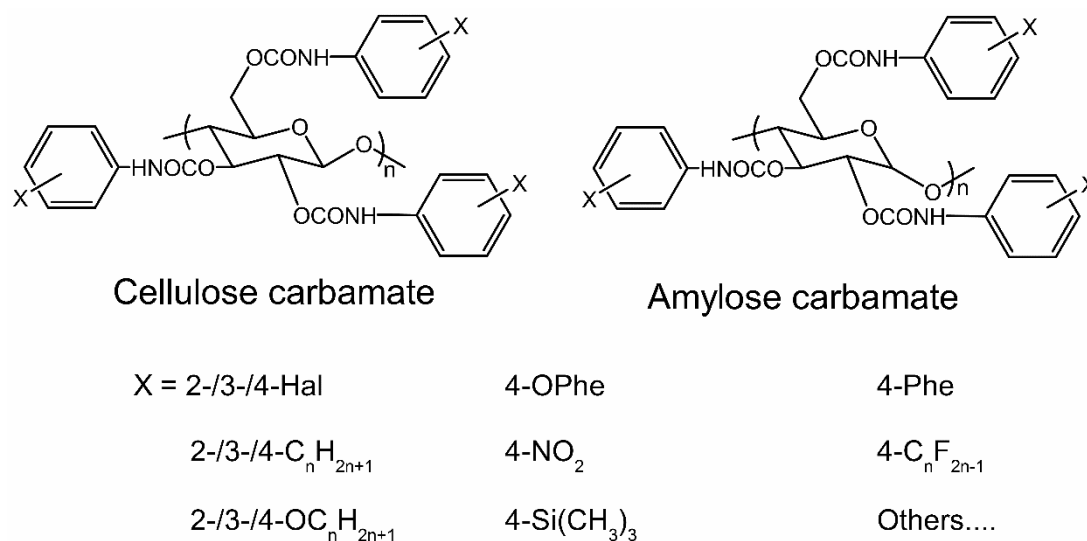


**Figure 1.2.** Structure of tris-phenylcarbamate derivatives of cellulose and amylose.

According to the Wainer's classification [17], polysaccharide stationary phases belong to Type-II CSP class, where enantioresolution is resulted by multiple attractive interactions between analyte and stationary phase surface (hydrogen



bonding,  $\pi$ - $\pi$  interactions and dipole stacking) together with inclusion in chiral cavities. Although the detailed chiral recognition mechanism is not yet fully understood [24], the effect of the substituents on the phenyl moiety as well as the chromatographic conditions for the CSP performance is well studied [15]. Polysaccharide based chiral phases found their application not only in various HPLC modes but also in gas chromatography (GC), capillary electrochromatography (CEC) and supercritical fluid chromatography.

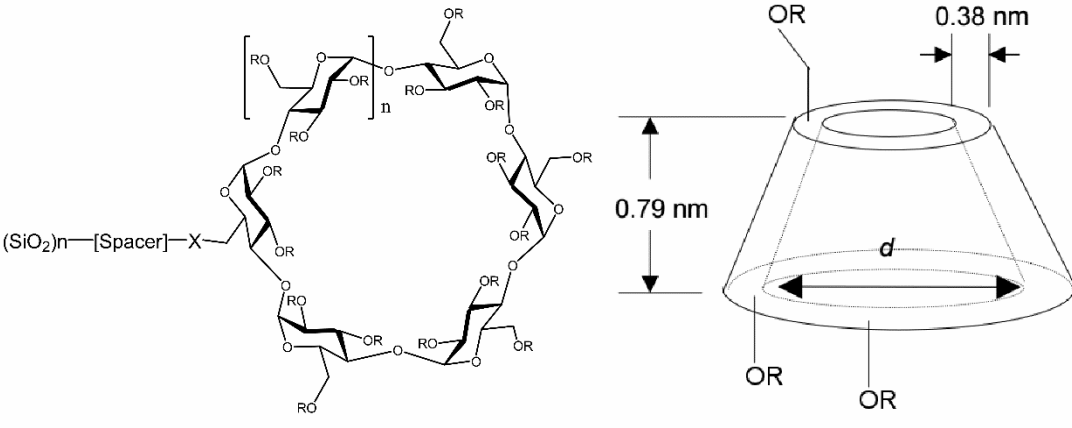
### **1.3.2. Cyclodextrin based CSPs**

Cyclodextrins (CDs) are one of the most popular CSPs, first introduced by Koscielsky et al. [25] in 1983. Their commercial availability, UV transparency and relatively low cost make them an attractive alternative for chiral separations. CDs are cyclic oligosaccharides that are composed of D-glucose units linked via  $\alpha(1,4)$ -glucosidic bonds. Although CD CSPs have structural similarities to polysaccharide CSPs, the CD CSPs belong to different group (Type-III) chiral selectors according to Wainer's classification [17]. The central cavity of the cylindrical shape CD acts as molecular capsule that can accommodate so-called "guest molecule" of appropriate shape, size and polarity. Such structural feature of CD provides enantioseparation of the analytes due to the formation of inclusion complexes in the chiral cavities [26].

Among the CD homologs, only  $\alpha$ -,  $\beta$ - and  $\gamma$ -cyclodextrins have practical importance and are produced industrially as chiral selectors. Structural model of the CD is presented in Table 1.2.

**Table 1.2.**

## Structural model of cyclodextrins.



n	Nomenclature	Inner diameter d, nm
1	$\alpha$ - cyclodextrin	0.57
2	$\beta$ - cyclodextrin	0.78
3	$\gamma$ - cyclodextrin	0.95

The inner diameter together with inclusion properties of the torus-shaped CD cylinder depends on the number of the glucose units involved in the CD ring formation. The  $\alpha$ -CD contains 6 D-glucose units,  $\beta$ -CD - 7 and  $\gamma$ -CD - 8, where the inner diameter increases from 0.57 nm to 0.95 nm, respectively. The primary hydroxyl groups at C-6 are situated close to narrow ring and the wider rim contains secondary hydroxyl groups forming hydrophobic inner cavity and hydrophilic outside [21].

First applications of CD as chiral selectors was described for the enantioseparation of  $\alpha$ - and  $\beta$ - pinene on underivatized  $\alpha$ - and  $\beta$ -CD CSPs [27]. This work was followed up by separation of ethylbenzene and xylene regioisomers [28] demonstrating high potential of the CDs for CSPs. Although the resolution factor was adequate, the initial CD stationary phases suffered from

low stability and reduced lifetime [29]. These drawbacks could be overcome by crosslinking of CDs with various linkers and applying modern coating/bonding technologies. In addition, sugar molecules of the CD phases have three hydroxyl groups that are available for derivatizations, such as alkylation or acylation [30,31]. This improves physical and chemical properties of the CDs. As already mentioned above, the primary chiral recognition mechanism is based on the inclusion of the lipophilic analyte moiety into hydrophobic CD cavity, whereas secondary interactions such as H-bonding; dipole-dipole,  $\pi$ - $\pi$  interactions or ion exchange can occur between the analyte and hydroxyl group substitutes. Neutral together with negatively and positively charged CD derivatives are commercialized and widely used as chiral selectors or chiral mobile phase additives for CEC, GC and HPLC separations. Astec, BGB Analytik, Restek, Supelco and some other companies provide huge variety of CD based CSPs for different applications [32,33].

### **1.3.3. Brush/Pirkle-type CSPs**

William F. Pirkle pioneered novel, bonded stationary phases for chiral resolution of broad spectrum optical isomers including sulfoxides, lactones, and derivatives of alcohols, amines, amino acids and mercaptans [34]. The key concept of this type CSPs is to provide at least three simultaneous interaction sites between enantiomer and stationary phase. Enantio-discrimination of enantiomers occurs due to differences in their shape, charge, hydrophobicity or hydrophilicity [34]. Large variety of such chiral selectors was synthesized by Pirkle and other groups [33]. Figure 1.3 represents two examples of BrushPirkle-type CSPs.

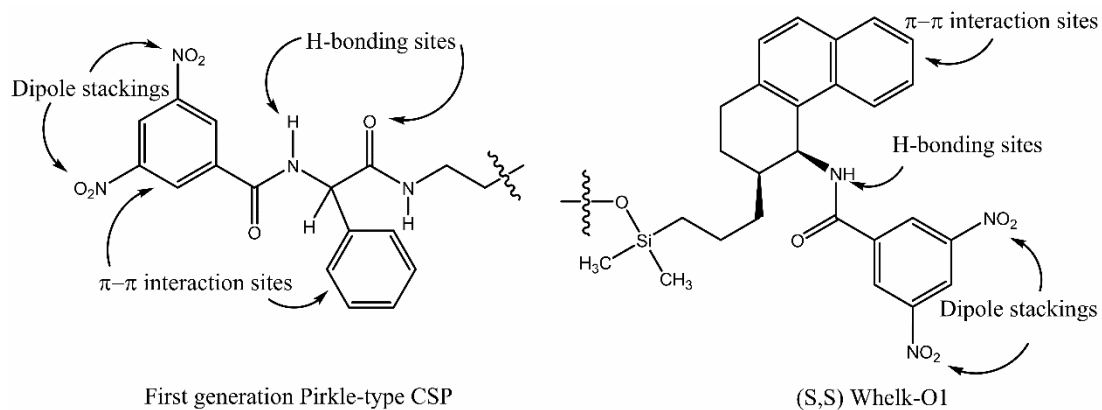


**Figure 1.3.** Brush/Pirkle type (multiple interaction sites) CSPs.

Probably the most widely applicable Pirkle type CSPs, namely (R,R) Whelk-O1 and (S,S) Whelk-O1, were developed by Pirkle and Welch [35,36] and commercialized by Regis Technologies. Synthetic chiral selectors are covalently bonded to solid support, usually silica, therefore these CSPs possess several benefits, compared to natural origin CSPs, such as chemical and physical inertness, compatibility to any mobile phase, faster kinetics and elevated sample loading capacities [37].

According to Wainer's classification, first generation Brush/Pirkle type CSPs were classified as Type-I chiral selectors [17]. The next generation Brush/Pirkle type chiral selectors provide complex enantio-discrimination mechanisms, where due to bulky molecular moieties additional inclusion processes can be involved in enantioseparation. Therefore novel Pirkle type CSPs could also be attributed to Type-II class [16].

#### 1.3.4. Macrocyclic antibiotic based CSPs

Macrocyclic antibiotic based chiral stationary phases were first proposed by Armstrong et al. in 1994 [38,39]. In this paper Armstrong and co-workers introduced three covalently bonded to silica macrocyclic antibiotics (Rifamycin B, Thiostrepton and Vancomycin) for enantioseparation of over 70 chiral compounds [38]. In addition, Armstrong's and other research groups demonstrated that macrocyclic antibiotics have great application potential as chiral selectors for CEC [43-45], thin layer chromatography [43] and

conventional HPLC [44]. The high variety of macrocyclic antibiotics that includes anamycins, glycopeptides, macrolides, lincosamides, and several others has been employed as chiral selectors [45,46]. They all possess several characteristics that allow them to interact with different classes compounds and serve as universal enantio-discrimination agents. The multiple stereogenic centers is one common feature for all macrocyclic antibiotics. For example, teicoplanin aglycone contains 8 stereogenic centers [47], whereas Ristocetin A – 38 [45,47]. The straightforward attribution of macrocyclic CSPs to Wainers [17] classification can be complicated. These CSPs can operate in different separation modes, namely normal-phase, polar-organic or reversed-phase, therefore the enantio-discrimination mechanism differs within different separation mode. Nevertheless, Lough in his revised Wainers classification review [16] attributed the macrocyclic antibiotic stationary phases to Type-II and Type-V, due to their ability to form multiple interactions together with inclusion complexes and protein like combination of hydrophilic and hydrophobic interactions, respectively.

Macrocyclic glycopeptide antibiotics are one of the most popular chiral selectors. They include avoparcin, teicoplanin, ristocetin A, vancomycin and their analogs [47]. For chiral HPLC separations Astec provides CHIROBIOTIC™ CSPs based on macrocyclic glycopeptides that have been bonded through multiple covalent linkages to silica. These include Chirobiotic T™ – teicoplanin chiral selector, Chirobiotic V™ – vancomycin, Chirobiotic R™ – Ristocetin A and Chirobiotic TAG™ – teicoplanin aglycone. Figure 1.4 represents a structural formula of teicoplanin molecule.

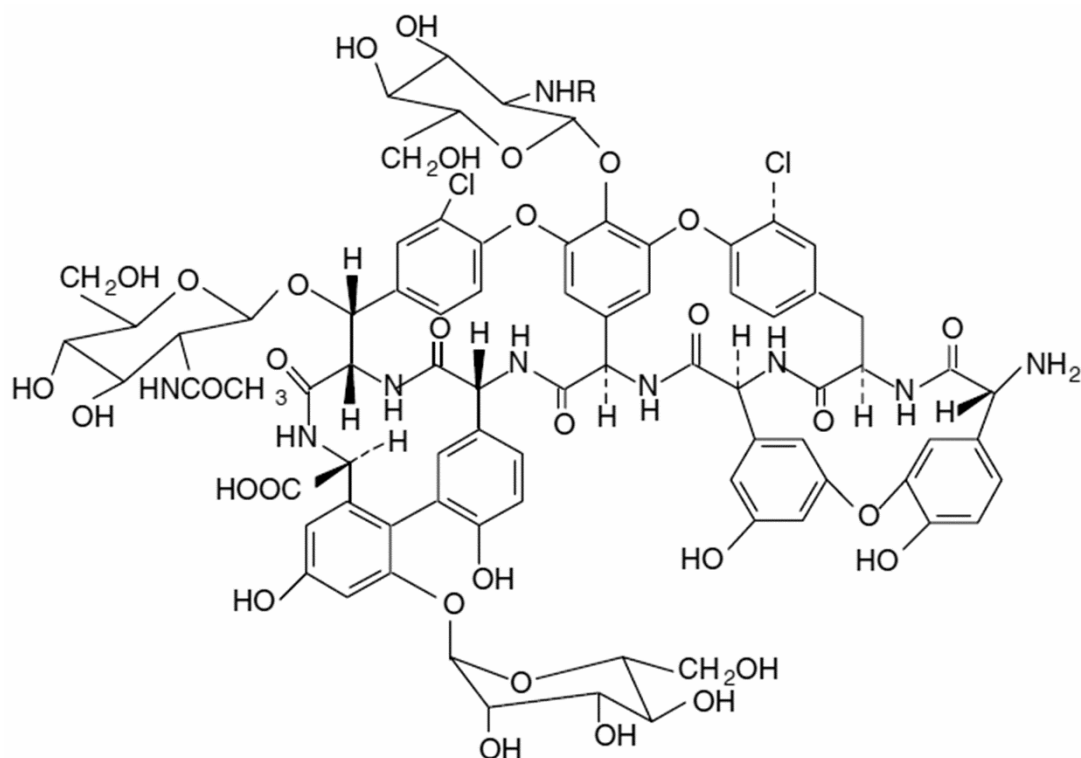


**Figure 1.4.** Structural formula of teicoplanin.

Teicoplanin is glycopeptide that contains seven aromatic rings where two of them have chloro-substituents, three - sugar moieties and hydrophobic hydrocarbon chain attached to one sugar molecule. The secondary and tertiary teicoplanin structural properties provide appropriate H-bonding, dipole-dipole, hydrophobic and steric interaction sites. In addition, ionizable amino and carboxyl groups supply electrostatic interactions [38].

Currently macrocyclic antibiotic based CSPs are widely used in different fields of enantioselective analysis [41,48–50].

#### 1.4. Mass spectrometry

The glorious era of mass spectrometry began in the beginning of the 20th century, when, in 1912 a British born physicist Joseph J. Thomson first designed a mass spectrograph and in 1913 identified neon isotopes on photographic plate [51]. Already at that time Thomson recognized the potential of mass spectrometry and in one of his comments he wrote: “I feel sure that there are many problems in chemistry which could be solved with far greater ease by

this than by any other method” [52]. Although Thompson received Nobel Prize not for the first mass spectrometer, his famous scholar Francis W. Aston was later recognized by Nobel committee for the discovery of 212 naturally occurring isotopes using mass spectrometry technique [53]. At its early stage mass spectrometry was mostly employed for isotope mass spectrometry, until 1929, when Bleakney, following the pioneering work of Dempster, developed electron impact ion source [54]. These improvements enabled the application of mass spectrometry for organic molecules such as hydrocarbons.

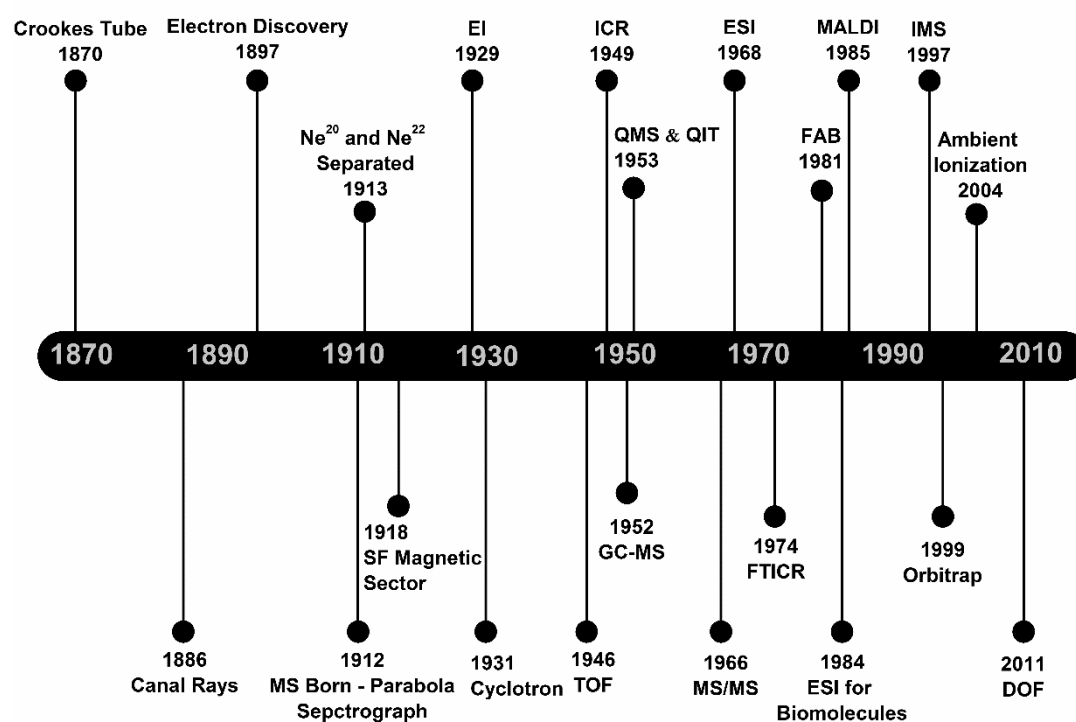


**Figure 1.5.** Time line of the major developments in mass spectrometry [52].

Over past 100 years (Figure 1.5) mass spectrometry has become one of the most important analytical techniques in almost every field of science and technology [53]. Remarkable MS applications made this technique versatile and irreplaceable in many research areas.

Whether we take the first mass spectrograph, designed by Thompson, or the latest MS system, all the MS instruments have at least three essential common

parts. First, analytes must be ionized in ion source, then separated by mass to charge ratio in mass analyzer, and finally quantitatively and/or qualitatively detected. In this part only most important ion sources and mass analyzers employed in conjunction with liquid chromatography are briefly described.

#### **1.4.1. Ion sources**

The development of the atmospheric pressure ionization interface is perhaps the most important factor in the successful combination of HPLC and mass spectrometry. MS analyzers manipulate and detect ions in the gaseous phase, so for the MS to be useful as an HPLC detector, the mobile phase must be effectively evaporated and analyte ions must be generated. This is the function of the MS instrument interface or so called ion source. The two most common atmospheric pressure ionization techniques used in HPLC-MS are electrospray ionization (ESI) and atmospheric pressure chemical ionization (APCI).

Originally the electrospray process has been known from Dole experiments already in 1968, but the first electrospray application as ion source interface for MS was demonstrated in 1984 by Yamashita and Fenn [55]. The electrospray principle is based on the generation of gas-phase ions from a solution flowing through a small outlet, when a high voltage is applied [56,57]. Unlike other ionization techniques the energy required for analyte ionization is not absorbed by the analyte directly, but firstly is absorbed by surroundings that initiate ionization. This makes ESI a very soft ion source that induce very low or no fragmentation during ionization process [56]. In addition, the ionization in most cases occurs due to protonation/deprotonation reactions, therefore multiple charge species are formed when high molecular mass compounds, such as proteins or nucleic acids, are analyzed. Together with straightforward online coupling to liquid chromatography, ESI-MS became a versatile and very powerful tool for analysis of small compounds and biomolecules, including their non-denatured state or non-covalent biocomplexes [58].



The analyte diluted in mobile phase that has sufficient dielectric permittivity is pumped through capillary. The high voltage applied to the capillary induce charge separation at liquid phase`s surface. When the solution reaches the end of the capillary tip, it forms somewhat called “Taylor cone” (Figure 1.6). Taylor cone reaches the Rayleigh limit and the droplet detaches the tip and the ESI spray is formed [59]. Based on the ESI source construction the additional nebulizer gas flow must be employed for better spray formation. The highly charged droplet travels to the counter electrode and is evaporated by heated curtain gas. The act of droplet evaporation and fission repeats until the singly or multiply charged ion are formed.

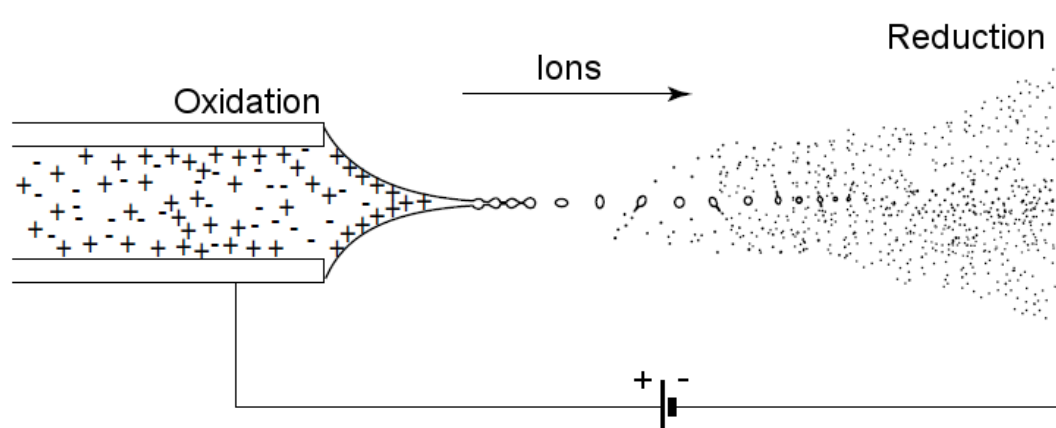


**Figure 1.6.** Schematic of the processes occurring in atmospheric pressure ESI ionization.

Two ion formation models have been suggested (Figure 1.7). The ion evaporation model proposed by Iribone and Thomson (1976) assumes that the increased charge density that results from solvent evaporation eventually causes coulombic repulsion to overcome the liquid's surface tension, resulting in a release of ions from the droplet surfaces [59,60].

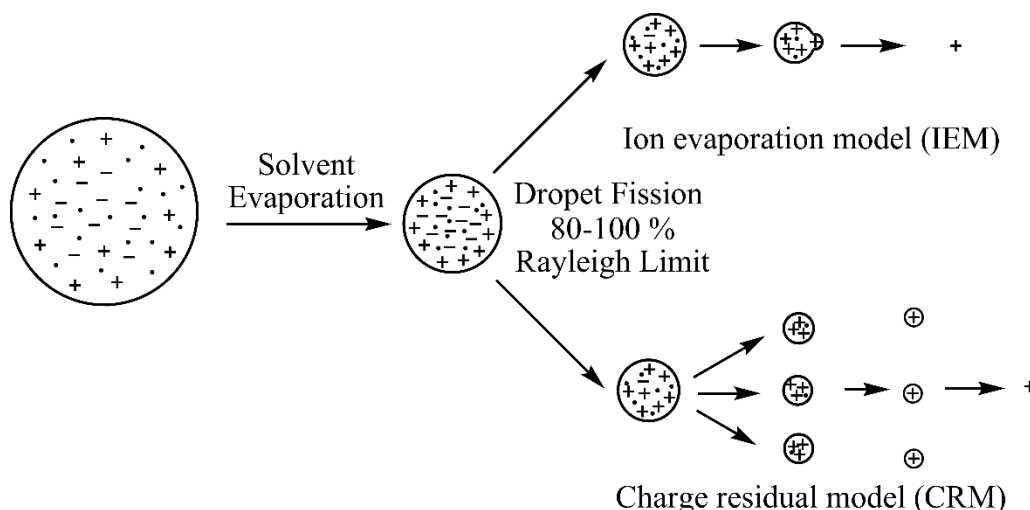


**Figure 1.7.** The two models of ions generation in ESI ions source.

The explanation of ion formation by charge residual model mechanism is attributed to Dole [57], but the roots of understanding, what happens to the charged droplet when the solvent evaporates, was formulated by Rayleigh years earlier [61]. In his paper, Rayleigh postulated that at certain point the shrinking charged droplet would reach the point, where, due to the columbic repulsion forces it would break into the smaller offspring droplets – now known as Rayleigh limit. Dole understood that this process would repeat until the droplet containing only one charged analyte molecule is formed. At this moment the last solvent molecules evaporate and most of the charge would remain on the analyte producing the gas-phase ion [61]. Nevertheless, series of studies have been conducted for better ESI mechanism understanding in terms of charge separation, droplets formation, solvent evaporation, droplet fission and ion formation the ESI mechanism has not been fully resolved [62].

ESI is the most popular but not the only ionization technique that operates in atmospheric pressure. Atmospheric pressure chemical ionization utilizes additional technical feature, compared to ESI, which enables ionization of less polar compounds [63]. In APCI solution is spayed pneumatically to ion source chamber where solvent is evaporated by heated inert gas. The high voltage corona discharge needle initiates ionization. Schematic illustration of APCI ion source is demonstrated in Figure 1.8.

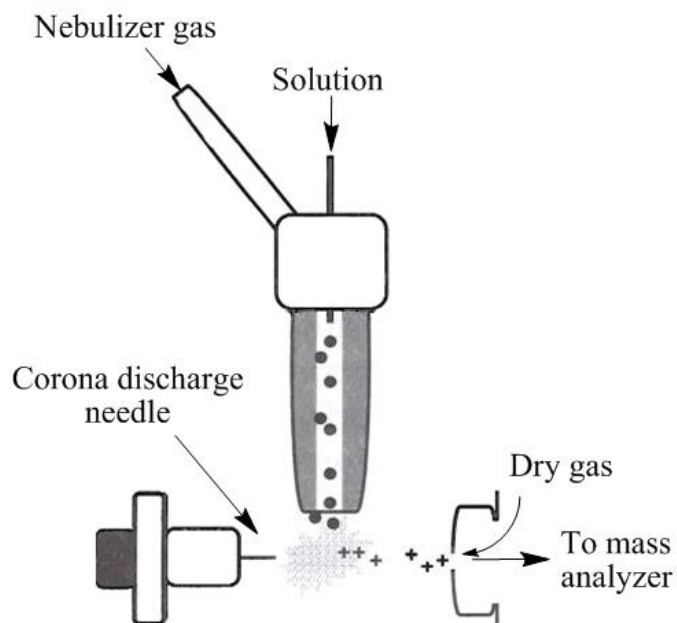


**Figure 1.8.** Schematic illustration of APCI ion source.

In positive ion mode ionization occurs by proton transfer, adduct formation or charge exchange from solvent component to analyte. Negative ions are formed due to proton abstraction, anion adduct formation, associative or dissociative electron capture. Generally APCI is a bit harsher ionization technique compared to ESI. The main advantages of APCI are that it enables ionization of less polar compounds, can operate at higher mobile phase flow rates and tolerates higher concentration of volatile buffers.

APCI is a most common alternative for ESI, but not the only one. Atmospheric pressure photoionization ion source [64] is similar to APCI, just instead of corona discharge needle ionization is boosted by photo irradiation. Recently, matrix assisted laser desorption ionization technique has been adapted for operation in atmospheric pressure. However, this ionization method is hardly suited for online coupling with chromatographic or electromigration separation techniques.

### 1.4.2. Mass analyzers

The ions from ion source are delivered to the mass analyzer through couple vacuum stages and all mass analyzers operate in highly reduced pressure environment. The primary function of mass analyzers is to separate ions by their mass to charge ratio. This can be done by magnetic or electric fields, or combination of both. In this section most important mass analyzers are briefly described.

Magnetic sector instruments were the first mass analyzers commercialized in 1950s. Although these instruments required advanced user skills, they provided the analytical information that chemists had been seeking for [65]. Introduced double-focusing technologies made magnetic sector instruments accurate and precise, capable of operating with a wide variety of ion sources.

The MS separation of charged particle in constant magnetic field can be described by Lorentz force law, where the Lorentz force ( $F_L$ ) directly depends on ion charge  $z$ , ion velocity  $v$ , and magnetic field momentum  $B$ . The ion travelling through a homogeneous magnetic field perpendicular to velocity direction, follow a circular path with radius  $r$  (Figure 1.9).

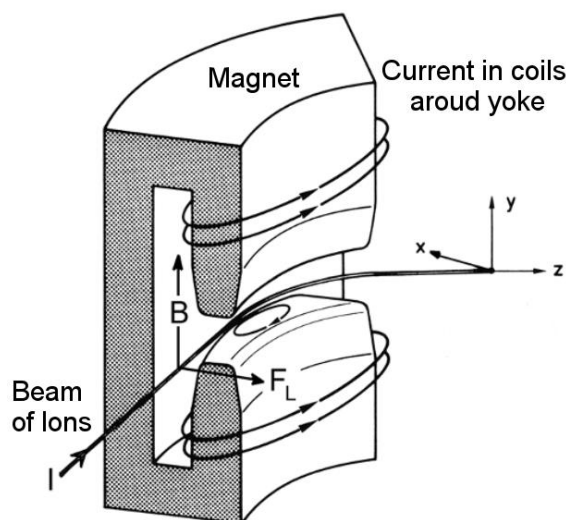


**Figure 1.9.** Schematics of magnetic sector mass analyzer and the direction of Lorentz force.

Therefore the principal of magnetic sector instrument is: “the radius  $r$  depends on the momentum  $mv$  of an ion, which itself depends on  $m/z$ ” [65]. The magnet is scanned over the range of  $B$  to produce mass spectrum. These magnetic sector instruments are combined to electric field sectors, and the result is enhanced resolution up to 150,000 with the dynamic range as high as  $10^7$  [66].

Another device that uses either combination of electric and magnetic fields or only electric field for focusing charged particles is ion trap. One of the ion traps application areas is mass spectrometry. For the discovery of electromagnetic traps for charged and neutral particles German physicist Wolfgang Paul was awarded with Noble Prize in 1989 [67,68]. The idea of building ion traps came from molecular beam physics, particles physics and mass spectrometry experiment in which W. Paul was involved during 1960s. These experiments led to understanding of the principles: how charged particles can be trapped by electric and magnetic fields to two or three dimensional motions. Based on operating principle we can outline three ion-traps, which are commonly used as mass analyzers for mass spectrometry: Paul ion trap, Penning ion trap, Kingdom ion trap (Orbitrap).

Paul`s ion traps belong to the family of mass analyzers whose operation is based on ion motion in dynamic electric fields [69]. The stability properties of ion motion can be well described by physics of the dynamic stabilization of ions in two and three dimensional radiofrequency (RF) fields.

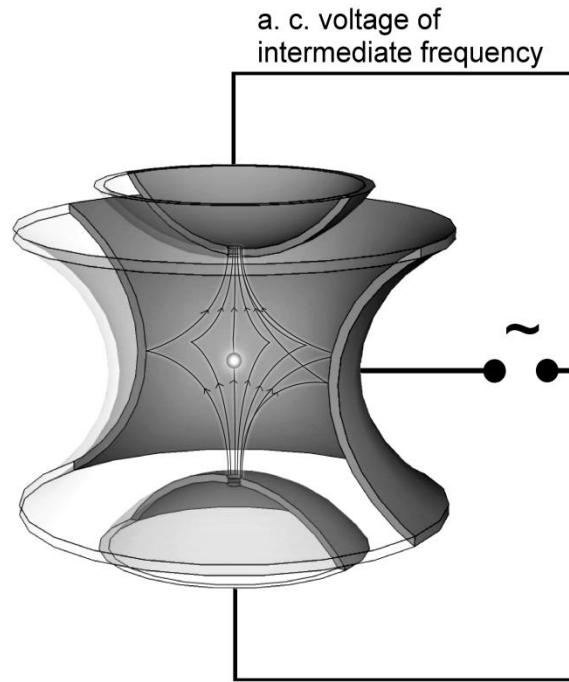


**Figure 1.10.** Principal scheme of Paul's Ion trap.

The Paul's ion trap contains hyperbolic shaped ring and two hyperbolic rotationally symmetric caps, as presented in Figure 1.10. The electric field is a quadratic function in the Cartesian coordinates, where the ions move in parabolic potential [68]. Ions in the trap perform motions in the three dimensional configuration, if the periodic voltage is applied between the caps and the ring electrodes. The motion trajectory is defined by Mathieu equations:

$$a = \frac{4eU}{mr_0^2\omega^2}, \quad q = \frac{2eV}{mr_0^2\omega^2}, \quad \tau = \frac{\omega t}{2}.$$

The solution of the Mathieu equations is the stability diagram which represents stable parabolic motion of the particles in  $x$ ,  $y$  and  $z$  directions.

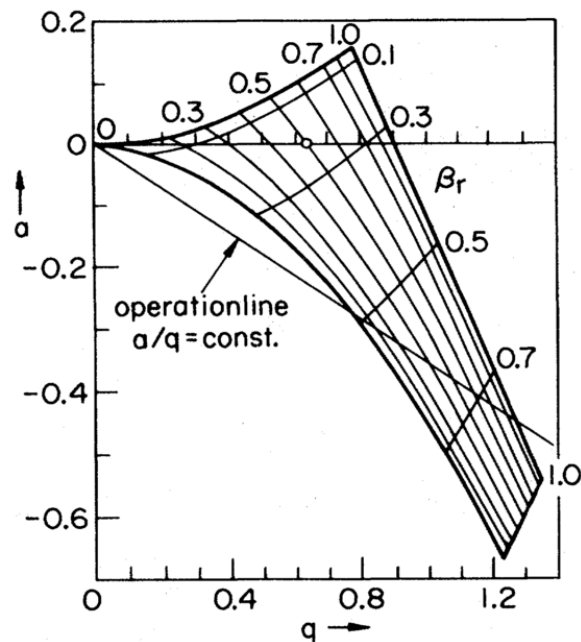


**Figure 1.11.** The region of ion stability in the ion trap [68].

When ion trap mass analyzer operates in MS scan mode the trapped ions can be ejected to the detector from the trap one-by-one by increasing RF voltage at  $q$  direction. The  $q$  is inversely proportional to  $m/z$  value therefore light ions are ejected first and heavy – last. At the tip of the stable region the instrument can trap only “one”  $m/z$  value ions. The other charged species are ejected from the trap or discharged by hitting the electrodes due to unstable motion. The great advantage of the ion traps is that it is possible to perform multiple fragmentation of isolated ions.

The quadrupole mass analyzer has the same operation principles as Paul`s ion trap, but instead of trapping ions in 3D motion, they are guided along the quadrupole [68]. Ion motion is also described by Mathieu equations [70] where ions stability is expressed by parameters  $a$  and  $q$  (Figure 1.13). If you don`t apply DC potential, the parameter  $a$  becomes equal to zero, therefore the quadrupole acts as ion guide. Ramping DC and RF voltages enables the separation of the ions by their  $m/z$  ratio.

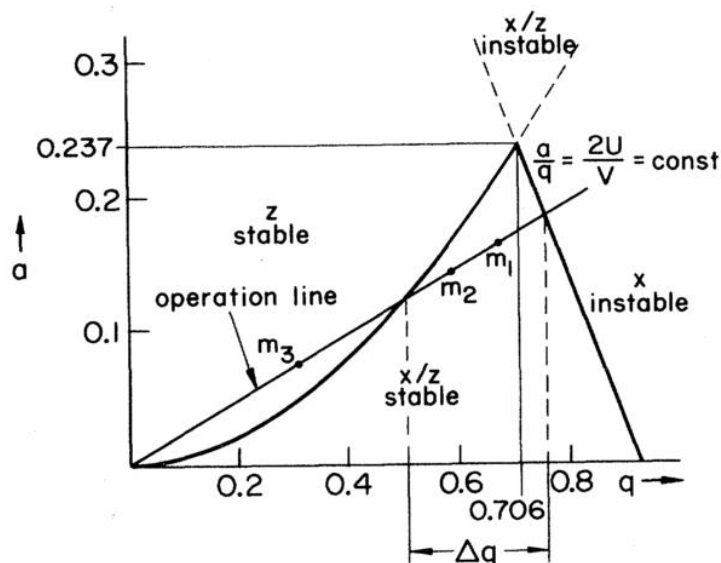


**Figure 1.12.** Ion stability diagram for quadrupole mass analyzer [68].

The resolution and sensitivity is the compromise of the operation line slope. Usually the quadrupole instruments are designed to obtain superior sensitivity with mass resolution up to 0.2 Da FWHM per peak. Quadrupole mass filters are one the most popular mass analyzer due to their simple construction, effective  $m/z$  filtering capacities and easy applications in tandem MS instruments.

A new mass analyzer, named Orbitrap, was introduced in 2005 by Makarov et al.[71]. Immediately after the commercialization Orbitrap became a huge success due to its ability to deliver extremely high resolution. Before Orbitrap the high mass resolution ( $>100,000$ ) could be routinely obtained only by Penning trap and double focusing sector instruments. However, the analysis with Penning trap is costly, due to high magnetic field that is required for this instrument. Magnetic sector instruments are not attractive due to their size and cost. The latest Orbitrap analyzers can achieve up to 450,000 resolution on benchtop instruments and are fully compatible for high mass transition. In addition, Orbitrap has moderately low price, simple design and operates in high mass accuracy with satisfactory robustness (Figure 1.13).



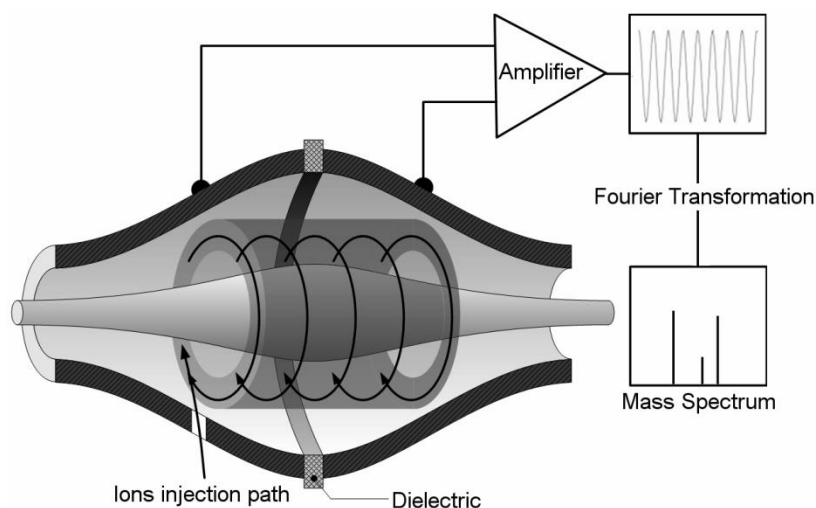


**Figure 1.13.** Orbitrap mass analyzer.

The Orbitrap operates by radially trapping ions in electrostatic field about a central spindle electrode [71,72]. The ion motion frequency is proportional to  $m/z$  value, which is amplified and converted to mass spectrum by operating Fourier transformation. One drawback of the Orbitrap mass analyzer is that it is not possible to perform fragmentation in the analyzer. This drawback is solved by different architecture tandem MS instruments that can contain multiple mass analyzers in one MS instrument.

One of the most popular high resolution mass analyzers is the Time of flight (TOF). Introduced in in the middle of the 20th century TOF remained the attractive instrument for high resolution MS applications. The biggest advantages of this type mass analyzer are the unlimited mass range [58] and extremely high scan rate [73].

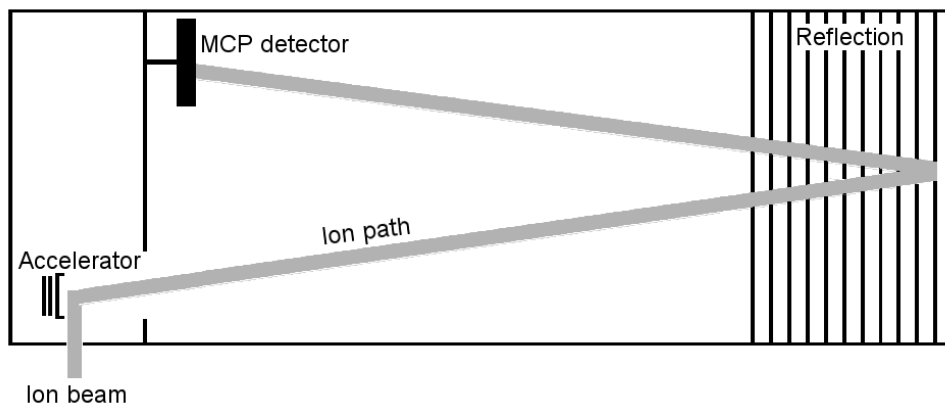


**Figure 1.14.** Time of flight (TOF) mass analyzer.

The principal scheme of TOF analyzer is presented in Figure 1.14. The ions from the ion source or other mass analyzer are accelerated perpendicularly towards the flight tube. Initially equal amount of potential energy is transferred to all ions, whereas the acceleration depends on  $m/z$  ratio. To increase the resolution, flight path is usually increased by the reflection electrodes system. Finally the ions reach the detector creating the signal. The time that the ion spends in the flight tube is proportional to its mass to charge ratio. Modern TOF analyzers are capable of achieving resolution up to 80,000 with mass accuracy of sub 2 ppm.

### 1.4.3. Tandem mass spectrometry (MS/MS)

One of the reasons why mass spectrometry has become such a universal analytical technique is the ability to perform tandem mass analysis. Tandem mass spectrometry (MS/MS) involves more than one-step of mass separation steps and fragmentation is usually induced between them. Based on the instrument construction there are several ways to isolate, fragment and analyze fragment ions. Ion traps, except for Orbitrap, are designed to perform multiple  $MS^n$  fragmentation in one mass analyzer. Other type of MS analyzers, such as quadrupole, TOF and sector instruments, which separate ions in “space” need to have collision cell in ion travel path. Most common commercial tandem mass spectrometers are triple quadrupole (QqQ), linear ion trap combined with quadrupole, quadrupole-TOF, TOF-TOF and hybrid Orbitrap MS instruments

that contain either quadrupole with C-trap, or linear ion trap with C-trap in different architecture.

The fragmentation of ions may occur when fraction of ion's kinetic energy is transformed into internal energy causing bond dissociation [74]. This can be accomplished by collisions with neutral gas molecules or by/together with kinetic excitation of trapped ions. Such fragmentation technique is called collision induced dissociation or collision activated dissociation. Nitrogen and argon are the most common gases used in commercial tandem mass spectrometers with multiple mass analyzers, whereas fragmentation of ions trapped in ion trap mass analyzers is accomplished by increase of kinetic energy and helium pressure [75]. Collision induced dissociation has been known for years [74] and is widely applied in commercial mass spectrometers, although novel fragmentation techniques that provide much "softer" and specific fragmentation pathways have been developed recently. Such fragmentation methods are based on interactions between analyte ions with either free low-energy electrons, or with reagent radical anions possessing an electron available for transfer [76]. When the bond dissociation is induced by low energy electrons, the technique is called electron-capture dissociation [77], whereas when the electron is generated by anion radical – electron transfer dissociation [78]. During recent years, these fragmentation techniques have been mainly involved for protein analysis middle-down and top-down approaches.

Triple quadrupole mass spectrometers are associated with couple tandem MS experiments: product ion monitoring, precursor ion monitoring, single ion monitoring (SIM), multiple reaction monitoring (MRM) and neutral gain/loss modes. Product and precursor ion monitoring experiments are performed during method development stage, whereas other tandem MS techniques are usually involved in quantitative assays.

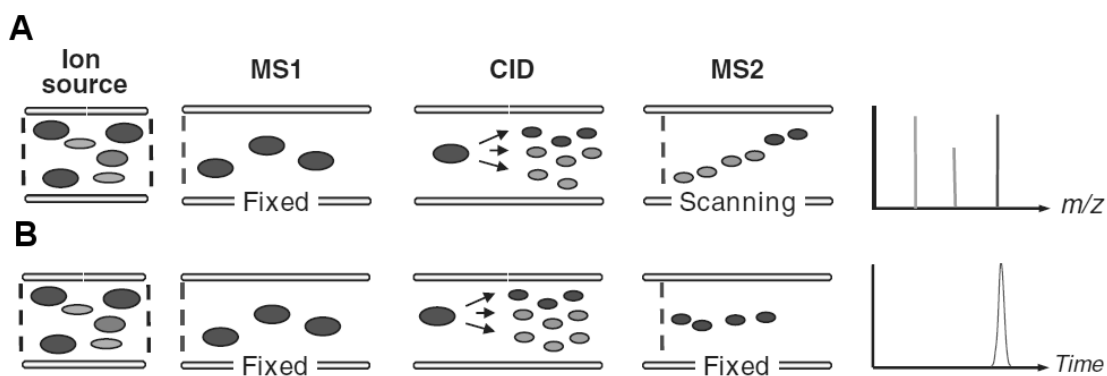


**Figure 1.15.** Schematics of multiple reaction monitoring (MRM) experiment performed on triple quadrupole mass spectrometer. A – product ion scan, B – multi reaction monitoring MRM [79].

In Product ion mode first quadrupole is set to fixed ion transition mode. Selected ion (precursor) is then fragmented in the collision cell and fragments are scanned in the second quadrupole. Product ion mode generates unique fragmentation pattern of the selected precursor (Figure 1.15 A). Multiple reaction monitoring or elsewhere called selected reaction monitoring is the technique when the first quadrupole is used to select a precursor ion, which is fragmented in the collision cell. Then the selected fragment ion is isolated in the second quadrupole and detected (Figure 1.15 B). Usually two specific MRM transitions are monitored for one analyte: the most intense fragment ion is used for quantification, whereas the second one – for identity confirmation. If the signal comes only from the particular analyte, the signal intensity ratios of both MRM transitions should be constant at linear concentration range. Such detection approach not only increases the sensitivity due to significant background noise reduction, but also provides much higher determination specificity.

### 1.5. Hydrolyzed protein fertilizers

Organic farming products are becoming essential part of modern agriculture that is necessarily to meet today's standards in terms of ecology and growth outcome. Classical inorganic fertilizing materials have been rapidly replaced by processed organic materials for eco-friendly farming in most cases. The well-known way

to introduce organic nitrogen to the soil is by adding proteins, peptides or free amino acids [83-85]. Such fertilizers, produced by chemical or enzymatic hydrolysis of the natural origins [80], are known as hydrolyzed protein fertilizers (HPF). Cultivars, such as soybeans and seaweeds are among the most common materials for fertilizers production, since they are a nitrogen-fixing organisms. Besides that, the increase of bio-diesel production from soybeans increases the amount of soybean meal available for HPF manufacturing [83]. Hydrolysis of organic matrices of animal origin is another approach for HPF production.

Amino acids are fundamental ingredients in the protein biosynthesis and have strong influence on plant physiological activity. The use of amino acids during plant growth is a well-known method to increase crop yield and quality. In addition, amino acids may form chelates with trace elements which can kill bacteria and insects and decrease the amount of residual pesticides [84]. Usually, amino acid-based fertilizers are recommended to use during critical growth periods, after transplantation, during flowering period, and at climatic stresses [81]. They are particularly effective when used in combination with microelements as a result of their chelation properties because chelated nutrients are more plant-available.

The content of free amino acids in HPF products usually varies from 5 to 40 % by mass and is an important parameter describing product quality. However, only L-amino acids can be effectively assimilated by plants, whereas D-amino acids are not involved in enzymatic growth processes or might even be toxic in some cases [88-90]. The hydrolytic manufacturing processes are usually conducted at high temperatures in the presence of high concentration of acid or base. Such conditions may result in high degree of racemization of the free amino acids [88]. Therefore the total amount of free amino acids as well as the enantiomeric composition of HPF would provide complete quality profile.

The European Commission provides harmonized legislation guideline for fertilizing materials in EU [89]. Figure 1.16 represents the list of raw materials used as ingredients of fertilizers.

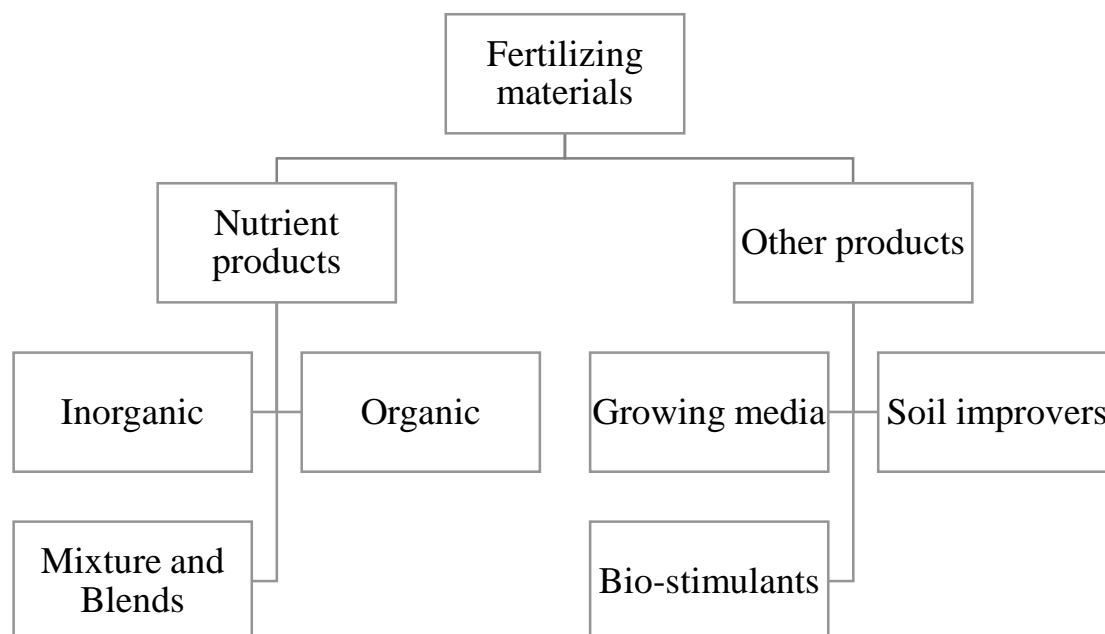


**Figure 1.16.** List of raw materials used as ingredients or additives in fertilizing materials provided by European Commission.

Hydrolyzed protein fertilizers are a part of organic nutrient products, whereas free amino acids can also be constitutes in growing media and bio-stimulant products. Surprisingly, neither control of the total amino acid content, nor control of the enantiomeric purity of amino acids constituting HPF products are required by any current EU directive. Due to rapidly growing demand of fertilizers, manufacturers provide increased number of various HPFs with very different quality. Thus, the need for the fast and effective control of the quality of HPF products will certainly arise in the near future.

### 1.6. Determination of amino acids

Up to date there have been several qualitative and quantitative approaches for amino acid analysis. By far, the most popular ones are chromatographic methods [93-100]. However, most of them include pre- or post-column derivatization due to weak response to conventional detectors and high analyte polarities.

Analysis of amino acids using gas chromatography requires the quantitative conversion of the amino acids to volatile derivatives. The derivatization procedure most commonly employed is silylation, a method through which acidic hydrogens are replaced by an alkylsilyl group [98]. Another derivatization method includes esterification using an alkyl chloroformate and alcohol [99,100]. The main disadvantage of GC seems to be the procedure of derivatization, due to the complexity of reactions and types of reagents used. In most cases the reagent and derivative are sensitive to moisture and relatively unstable. The speed at which derivatization takes place differs from one amino acid to another and strict reproduction of reaction conditions is essential for all samples. Moreover, most of the volatile derivatives of amino acids may be lost during the concentration of the sample.

HPLC with its various separation modes is another and perhaps the most widely employed technique for the analysis of amino acids. General approaches are ion-exchange chromatography and RP-HPLC. By using ion-exchange chromatography the amino acids are separated in their native form and then reacted with ninhydrin in a post-column derivatization system and detected by UV absorbance [99]. A disadvantage of this technique is that non-volatile mobile phases are not compatible with MS detection.

The determination of amino acids by the most popular RP-HPLC is associated with two problems. As already mentioned above, most of the amino acids cannot be detected using conventional UV detector due to lack of chromophore. A more serious problem is that conventional RP stationary phases do not provide sufficient retention of very hydrophilic analytes. Pre-column derivatization is therefore required to improve detectability and to reduce hydrophilicity of the amino acids. For example, Jia et al. [91] suggested the RP-HPLC method for the separation of 23 amino acids and 7 biogenic amines on RP sorbent using pre-column derivatization with dansyl-chloride. In the other RP-HPLC method pre-column derivatization with *o*-phthaldialdehyde followed by fluorescence detection was employed [90]. Although pre-column derivatization approach is

well understood and has been historically well received, it is labour-intensive, time-consuming and susceptible to errors.

The ability to analyze underivatized amino acids provides the advantages of increased convenience, simplicity and repeatability, while still providing the desired sensitivity and separation speed. The elimination of the derivatization step reduces the possibility of side reactions and reagent interference or the possibility of altering the sample through contamination/degradation. One of the approaches to separate underivatized amino acids on conventional RP stationary phases is ion pairing RP-HPLC technique. For the separation of charged analytes in this mode an oppositely charged ion-pairing reagent is added to the mobile phase [92,94]. The purpose of adding an ion pairing reagent to the mobile phase is usually to reduce the charge of the analyte via ion pairing and, consequently, to increase its retention. A complicated mobile phase containing pentafluoroheptanoic, trifluoroacetic and formic acids was applied by Samy et al. [92] to separate 16 amino acids. Alarcon-Flores and co-workers [94] separated 19 underivatized essential amino acids on the RP stationary phase by adding pentadecafluorooctanoic acid to the mobile phase as an ion-pairing reagent. The use of ion-pairing reagents, however, has several disadvantages such as greater complexity of operation and more challenging interpretation of the results, slow column equilibration after changing the mobile phase and incompatibility with MS detection. Although volatile ion-pairing reagents are already available for use with MS, significant reduction in MS response is usually observed compared with response obtained with no ion-pairing reagent.

Hydrophilic interaction chromatography is perhaps the most promising technique for separation of underivatized small polar analytes [100,101]. In HILIC the retention is based on strong hydrophilic interaction between the hydrophilic stationary phase and polar analytes, which makes this separation mode an ideal option for amino acids analysis. Moreover, high organic content in the mobile phase is favoured by an ESI source for better sensitivity [93,95]. However, only few articles have been published to date on the separation of



amino acids in the HILIC mode. Xu and co-workers [95] on the TSK-GEL Amide stationary phase separated 15 amino acids from rat serum. Yao et al. [93] quantified 20 amino acids in *Ginkgo Biloba* leaves employing HILIC system coupled with tandem mass spectrometric detection. Thus, the potential of HILIC technique for the analysis of protein amino acids in various objects has been unexploited.

### **1.7. Enantioselective HPLC determination of amino acids**

For the chiral separation of amino acids HPLC is perhaps the most popular and reliable technique among all chromatographic and electromigration separation methods [102]. There are two main approaches for HPLC separation of enantiomers: indirect, which uses derivatization prior to analysis, and direct, which uses chiral stationary phases or, more rarely, chiral mobile phase additives. For indirect analysis, a large number of the commercial chiral derivatization agents based on carboxylic acids, chloroformates, isothiocyanates, N-haloarylamino acid derivatives, and *o*-phthalaldehydes is available [103,104]. The major type of derivatization reactions for amines and amino acids are mainly formation of amides, carbamides, ureas, and thioureas. The indirect method is an efficient technique, although several points must be taken into account: the molecule must be easy derivatizable, derivatization should be comparatively fast, the process should proceed quantitatively, and no racemization should occur for both enantiomers. Besides that, chiral derivatization agents must be enantiomerically pure, or at least, the purity must be known; otherwise, the formation of stereoisomers leads to inaccuracies.

Another strategy for enantiomers analysis is enantioselective stationary phase. Currently a lot of chiral stationary phases are available for direct separation of chiral compounds in HPLC [18]. By far, the most successful enantioselective separation of amino acids and small peptides was achieved on macrocyclic antibiotic-based chiral selector stationary phases, introduced in 1994 by Armstrong et al. [38]. There is a large number of macrocyclic antibiotics that comprise a big variety of structural types, including polyene polyols, aliphatic-

bridged aromatic ring systems, glycopeptides, peptides, etc. Some of them are used for chiral separation in HPLC, namely, avoparcin, teicoplanin, ristocetin, and vancomycin analogues, which possess several characteristics that allow them to interact with analytes and serve as chiral selectors [39,47,50,105]. The most enantioselective separations of amino acids were carried out on teicoplanin or teicoplanin aglycone chiral stationary phases. The retention occurs when the teicoplanin ammonium group interacts with the carboxylate group of the amino acid or the ammonium group of the amino acid interacts with teicoplanin carboxylate, whereas chiral discrimination results from a complex interaction between analyte and tertiary teicoplanin structure [47]. The retention and chiral resolution can be optimized by changing the concentration and nature of the organic modifier in the mobile phase and enhancing steric conformation of the chiral stationary phase by adjusting pH, ionic strength of the mobile phase, and column temperature [47,50,106,107].

### **1.8. Determination of amino acids in HPF**

Up to date, there are few papers dealing with the determination of amino acids in hydrolyzed protein fertilizers (HPFs) [94,108,109]. Alarcón-Flores and co-workers [94] developed an ion pairing ultrahigh-performance liquid chromatography–tandem mass spectrometry method for the non-chiral determination of 19 underivatized protein amino acids in HPF samples. All amino acids were separated in 8 min by reversed phase with the pentadecafluorooctanoic acid as the ion-pairing reagent. Cavani et al. [108] described the separation of protein amino acids derivatized with dansyl chloride by micellar electrokinetic chromatography and direct UV detection, employing  $\beta$ -cyclodextrin as the chiral selector. However, only one amino acid (dansylated D-/L-alanine) was considered, and its degree of racemization was calculated. More recently, Sánchez-Hernández et al. [109] have proposed a capillary electrophoresis–tandem mass spectrometry technique using cyclodextrins as chiral selectors to determine the degree of racemization of the free amino acids

in HPFs. The enantiomeric separation of up to 14 amino acids was achieved in about 60 min with resolutions above 1.0.

### **1.9. Method validation**

Validation procedure applied for an analytical assay depends on the type of analysis performed [110]. The most common types of the analytical procedures are:

- ❖ Identification test;
- ❖ Quantitative tests for impurities content;
- ❖ Limit tests for the control of impurities;
- ❖ Quantitative tests of the target compounds in the samples.

There are several other types of analytical procedures that may involve physical or chemical characterization of sample properties and each of them may require specific method evaluation/validation protocol. In this part a brief description of validation procedures applied for identification test and for quantitative analysis of target compounds is summarized. The list of validation characteristics required for the validation of both analytical procedures is presented in Table 1.3.

It should be noted that the degree of validation required also depends on the nature of the sample.

**Table 1. 3.**

Most important validation characteristics regarding to analytical procedure

Characteristic	Type of analytical procedure	
	Identification	Quantitation
Specificity	+	+
Accuracy	–	+
Precision	–	+
• Repeatability	–	+
• Intermediate precision	–	+
Detection limit (LOD)	–	+
Quantitation limit (LOQ)	–	+
Linearity	–	+
Range	–	+

Specificity is the ability to assess unequivocally the analyte in the presence of components which may interfere with the signal of the analyte and, consequently, may give false positive or false negative result. Appropriate identification assay should be able to discriminate between the compounds which have closely related structures and are likely to be present in the sample. The use of liquid chromatography combined with tandem mass spectrometry usually provides high degree of specificity due to the unique retention time and specific MRM transitions for individual analyte. Thus, to ensure bias free results, the retention time drift for consecutive injections must be evaluated. In addition, due to identical molecular formulas, some amino acids (leucine/isoleucine and glutamine/lysine) provide the same precursor ions. Therefore fragmentation patterns must be evaluated carefully, and if it is possible, specific ones should be selected.

Accuracy (also sometimes termed as trueness) of the analytical procedure shows the closeness of agreement between the determined value and the conventional

true value. This parameter is difficult to evaluate accurately as the accessibility of certified reference materials (CRM) with certified reference values is usually limited. In absence of reference material, method trueness can be evaluated by spike and recovery experiments. The sample is analyzed both in its original state and after addition (spike) with known analyte amount. The difference between two results is so called surrogate recovery (elsewhere – marginal recovery). Although such approach cannot evaluate extraction performance of the analyte from complicated matrices, this protocol is accepted when CRMs are not available.

Precision of the analytical procedure describes closeness of agreement between a series of results obtained from multiple sampling of the same homogeneous sample using certain method. Precision is expressed in terms of repeatability, intermediate precision and reproducibility. Method repeatability (also called inter-day precision) is evaluated in a short term time interval under the same operating conditions. Intermediate (intra-day) precision expresses within laboratory variations. Analyses are performed in consecutive days, by different analysts or by different equipment. Reproducibility is the precision obtained between different laboratories, usually by collaborative studies or during laboratory standardization.

LOD and LOQ. The detection and quantitation limits represent the lowest amount of analyte that can be detected or quantified with suitable precision and accuracy, respectively.

Linearity of the analytical procedure shows the concentration interval in which the signal response is directly proportional to the concentration of analyte in the sample.

Range of an analytical procedure shows the interval from minimal to maximal concentration of analyte in the sample for which the analytical method has a suitable level of precision, accuracy and linearity.

## **2. EXPERIMENTAL**

### **2.1. Equipment**

Chromatographic separations were performed using an Agilent 1290 Infinity LC system coupled with a triple quadrupole 6410 tandem mass spectrometer equipped with an electrospray ionization (ESI) interface (Agilent Technologies, Santa Clara, CA).

Columns used in current study:

- ❖ Acquity BEH HILIC (100 × 2.1 mm, I.D., 1.7 μm), Waters;
- ❖ Acquity BEH Amide (100 × 2.1 mm, I.D., 1.7 μm), Waters;
- ❖ Atlantis HILIC (100 × 2.1 mm, I.D., 3.0 μm), Waters;
- ❖ Astec CHIROBIOTIC T2 (150 × 2.1 mm I.D., 5.0 μm), Supelco.

The ESI ion source was set for positive ionization at the following setup: capillary voltage, 4 kV; gas temperature, 300 °C; gas flow, 8 L/min; and nebulizer gas pressure, 30 psi. Cell accelerator voltage and dwell time were kept constant for all analytes and were set at 6 eV and 20 ms, respectively.

### **2.2. Materials**

Amino acids L-alanine, L-arginine, L-asparagine, L-aspartic acid, L-cysteine, glycine, L-glutamine, L-glutamic acid, L-histidine, L-leucine, L-isoleucine, L-lysine, L-methionine, L-phenylalanine, L-proline, L-serine, L-threonine, L-tryptophan, L-tyrosine, and L-valine were purchased from Sigma-Aldrich (St. Louis, MO) as the L-amino acid kit. D-amino acids D-alanine, D-arginine, D-asparagine, D-aspartic acid, D-cysteine, D-glutamine, D-glutamic acid, D-histidine, D-leucine, D-lysine, D-methionine, D-phenylalanine, D-proline, D-serine, D-threonine, D-tryptophan, D-tyrosine, and D-valine were purchased separately also from Sigma-Aldrich. Stock standard solution was made at 1 g/L concentration level in 1 mol/L aqueous formic acid solution and kept at 4 °C, in amber glass containers. Working standard solutions were made by appropriate dilution of stock standards in methanol/water solution (50:50, v/v) and kept at 4

°C temperature in amber glass vials prior to analysis. LC-MS grade acetonitrile was purchased from Carl Roth GmbH & Co. (Karlsruhe, Germany), and ammonium acetate, formic acid, acetic acid, ethanol, and methanol (all LC-MS grade) were purchased from Sigma-Aldrich. Purified water was obtained with a Milli-Q apparatus (Millipore, Bedford, MA).

The fertilizer samples were obtained from local supplier. All samples are listed in Table 2.1.

**Table 2.1.**

Samples analyzed by HILIC-MS/MS and Chiral HPLC-MS/MS

Analysis Method		Samples identifiers			
		Different origin soil additives			
HILIC –MS/MS	Aminocat	Razormin™	Zytron™	Canleys™	
	30%™				
		Hydrolyzed protein fertilizers from different vendors			
Chiral HPLC-MS/MS	Aminocat	Terra Sorb	ILSA Drip	Protifert	Rutter™
	30%™	Complex™	Forte™	LMW8™	

### 2.3. Sample preparation

The extraction protocol used for HILIC separations was as follows: 500 mg of crude fertilizers sample was extracted with 10 mL of an aqueous/acetonitrile (1:5, v/v) solution containing 1 mol/L acetic acid in ultrasonic bath for 10 min, then diluted (1:1) with acetonitrile and centrifuged for 2 min at 10000 rpm. 1 mL of supernatant was filtered through a 0.2 µm nylon syringe filter (Carl Roth GmbH & Co., Karlsruhe, Germany) and diluted with initial mobile phase appropriately before the analysis.

For enantioselective separations all samples were prepared according to the procedure suggested by Alarcón-Flores *et al.* [94]. An aliquot of fertilizer was weighed (100 mg), and 10 mL of water solution adjusted to pH 1.5 with heptafluorobutyric acid was added. The mixture was thoroughly vortexed for 1

min and centrifuged for 15 min at 3000 rpm. After centrifugation, supernatant was filtered through a 0.20  $\mu\text{m}$  nylon syringe filter, 20  $\mu\text{L}$  of the filtrate was transferred into the vial, 980  $\mu\text{L}$  of the initial mobile phase was added, and the final solution was taken for enantioselective HPLC-MS/MS analysis. Because of the large amount of glutamic acid in sample A, the quantitation of D-/L-Glu in this sample was performed separately from 10 times extra-diluted extract.

#### **2.4. Method validation**

For HILIC method only the method specificity was controlled by applying tandem mass spectrometric detection in MRM mode, where two specific MRM transitions were monitored for each amino acid (except for alanine and proline). The retention time drifts were also evaluated.

Enantioselective HPLC method was validated in terms of linearity, limit of detection (LOD), limit of quantitation (LOQ), accuracy, and precision, following the ICH harmonized tripartite guideline [110].



### 3. RESULTS AND DISSCUSIONS

#### 3.1. Characterization of amino acids

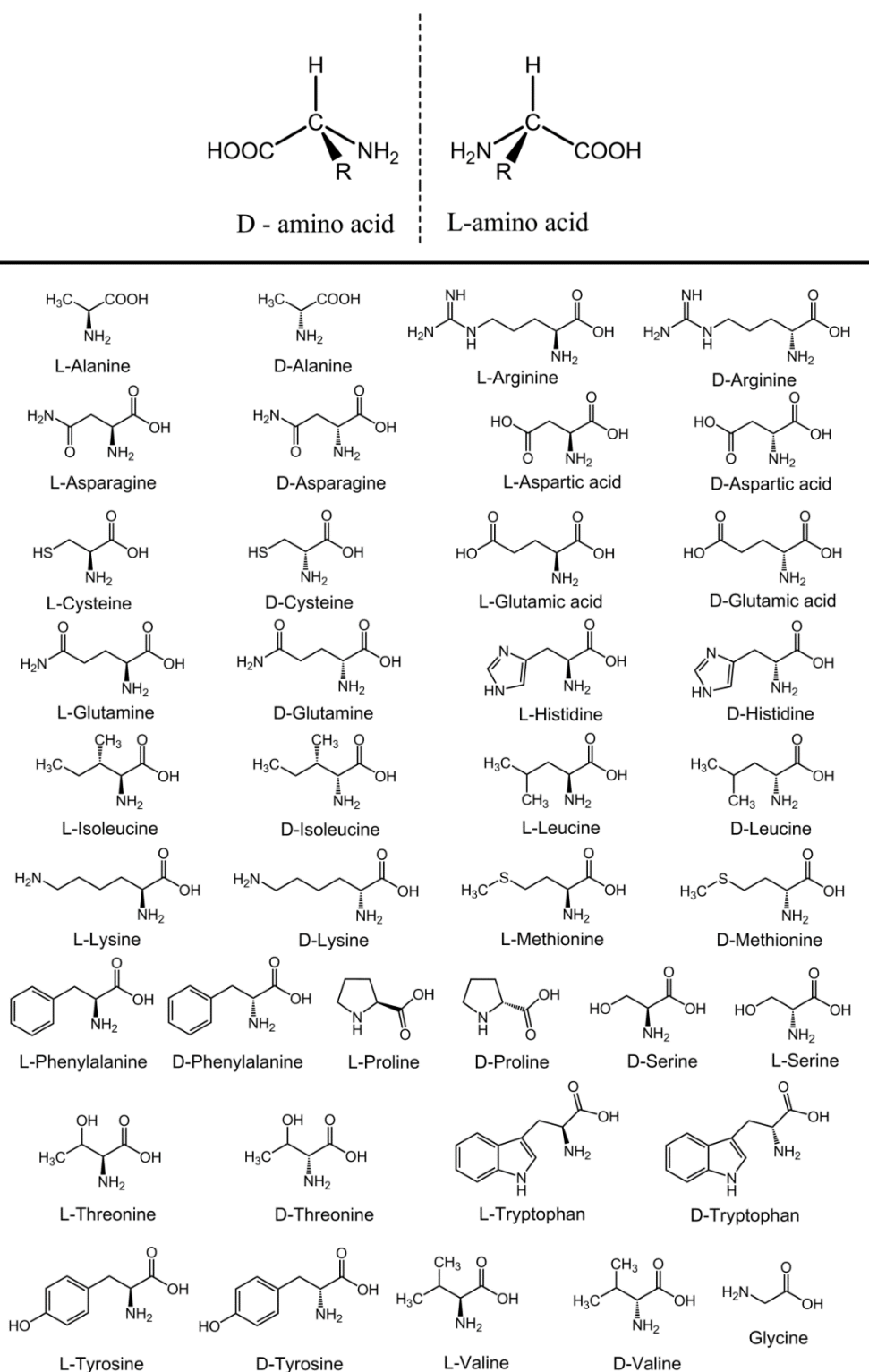


**Figure 3.1.** Chemical structures of protein amino acids.

Chemical structures of protein amino acids investigated in this study are presented in Figure 3.1.

Amino acids are zwitterionic compounds and their acidity is determined by *pI* value. Some physical properties of protein amino acid are listed in Table 3.1. Arginine, histidine and lysine are characterized by basic *pI* values, the rest are slightly acidic, except for aspartic and glutamic acids, which are the strongest acids above listed.

**Table 3.1.**

Some physical properties of protein amino acids.

Name	Abbreviation	- R	M <sub>w</sub>	<i>pI</i>
Alanine	Ala	-CH <sub>3</sub>	89	6.01
Arginine	Arg	-C <sub>4</sub> H <sub>10</sub> N <sub>3</sub>	174	10.76
Asparagine	Asn	-C <sub>2</sub> H <sub>2</sub> NO	133	5.41
Aspartic acid	Asp	-C <sub>2</sub> H <sub>3</sub> O <sub>2</sub>	134	2.85
Cysteine	Cys	-CH <sub>3</sub> S	121	5.05
Glycine	Gly	-H	75	6.06
Glutamine	Gln	-C <sub>3</sub> H <sub>6</sub> NO	146	5.65
Glutamic acid	Glu	-C <sub>3</sub> H <sub>5</sub> O <sub>2</sub>	147	3.15
Histidine	His	-C <sub>4</sub> H <sub>5</sub> N <sub>2</sub>	155	7.60
Hydroxyproline	Hyp	-C <sub>3</sub> H <sub>5</sub>	131	-
Isoleucine	Iso	-C <sub>4</sub> H <sub>9</sub>	131	6.05
Leucine	Leu	-C <sub>4</sub> H <sub>9</sub>	131	6.01
Lysine	Lys	-C <sub>4</sub> H <sub>10</sub> N	146	9.60
Methionine	Met	-C <sub>3</sub> H <sub>7</sub> S	149	5.74
Phenylalanine	Phe	-C <sub>7</sub> H <sub>7</sub>	165	5.49
Proline	Pro	-C <sub>3</sub> H <sub>5</sub>	115	6.30
Serine	Ser	-CH <sub>3</sub> O	105	5.68
Threonine	Thr	-C <sub>2</sub> H <sub>5</sub> O	119	5.60
Tryptophan	Trp	-C <sub>9</sub> H <sub>8</sub> N	204	5.89
Tyrosine	Tyr	-C <sub>7</sub> H <sub>7</sub> O	181	5.64
Valine	Val	-C <sub>3</sub> H <sub>7</sub>	117	6.00

### 3.2. Tandem mass spectrometry parameters

Due to the zwitterionic nature of amino acids both positive and negative electrospray ionization modes could be employed for their mass spectrometric detection. However, initial experiments and literature studies suggested that the positive ESI is by far more sensitive than negative ESI mode.

Ion source (IS) parameters such as capillary voltage, gas temperature and flow rate together with nebulizer gas pressure highly depend on analytes origin and mobile phase composition/flow rate. Therefore IS parameters were tuned for the best signal response. The IS parameters were evaluated by monitoring protonated ion intensity via direct injection of acidic (Glu) moderately neutral (Pro) and basic (His) amino acids in initial mobile phase composition. The IS parameters optimized for HILIC and for chiral HPLC are presented in Table 3.2. Slightly higher capillary voltage and gas flow rate values were required for chiral HPLC most likely due to higher water content used in the mobile phase in this separation mode

**Table 3.2.**

Ion source parameter set up for HILIC and Chiral LC separation methods

Parameter	HILIC	Chiral LC
Capillary voltage, kV	3	4
Gas (N <sub>2</sub> ) temperature, °C	300	300
Gas (N <sub>2</sub> ) flow, L/min	7	8
Nebulizer gas (N <sub>2</sub> ) pressure, psi	30	30

Mass analyzer parameters were optimized manually via direct infusion of a standard solution of 100 µg/L of each amino acid at 3 µL/min flow rate. The standard solutions were prepared in water/MeOH (50:50, v/v) containing 10 mmol/L formic acid. Full scan MS spectra obtained in positive ESI mode showed the most abundant protonated [M+H]<sup>+</sup> molecular ion for all amino acids. First quadrupole was set to single ion monitoring mode for the selected

protonated precursor ion, and the fragmentor voltages (from 50 to 150 V) were tuned individually to each amino acid. Then the product ion MS spectra were acquired and from the collision-induced dissociation experiments, the most abundant product ions were selected. Only one transition was observed for alanine and proline because of their low molecular weights (Figure 3.2.). The rest of the amino acids produced at least two MRM transitions each. The most intense transition was used for quantification, whereas the second one was used to complete the identification. Product ion scan mass spectra of the representative amino acids are given in Figure 3.3. Most of the amino acids gave quantitative MRM transition corresponding to the loss of formic acid  $[M-HCOOH+H]^+$  or loss of formic acid and ammonia  $[M-HCOOH-NH_3+H]^+$ , whereas Arg and Trp led to the formation of  $[M-104+H]^+$  and  $[M-NH_3+H]^+$  ions, respectively.

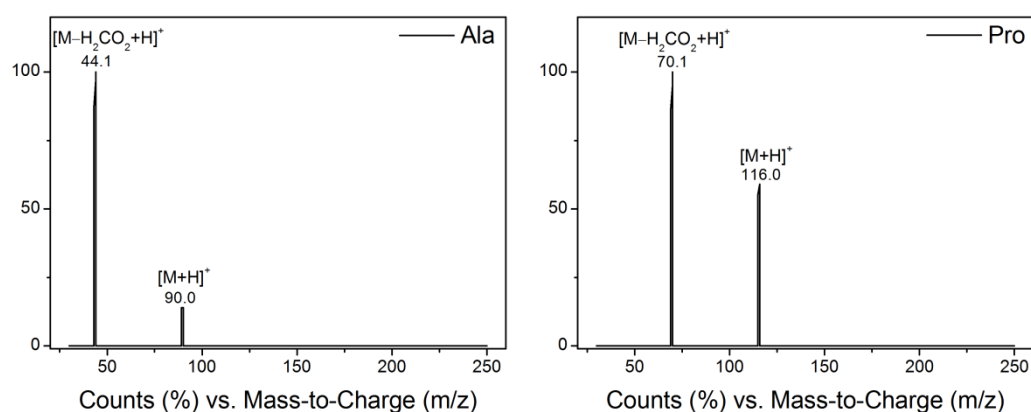


**Figure 3.2.** Product ion scan mass spectra of alanine and proline (100  $\mu\text{g/L}$ ) obtained by direct infusion.

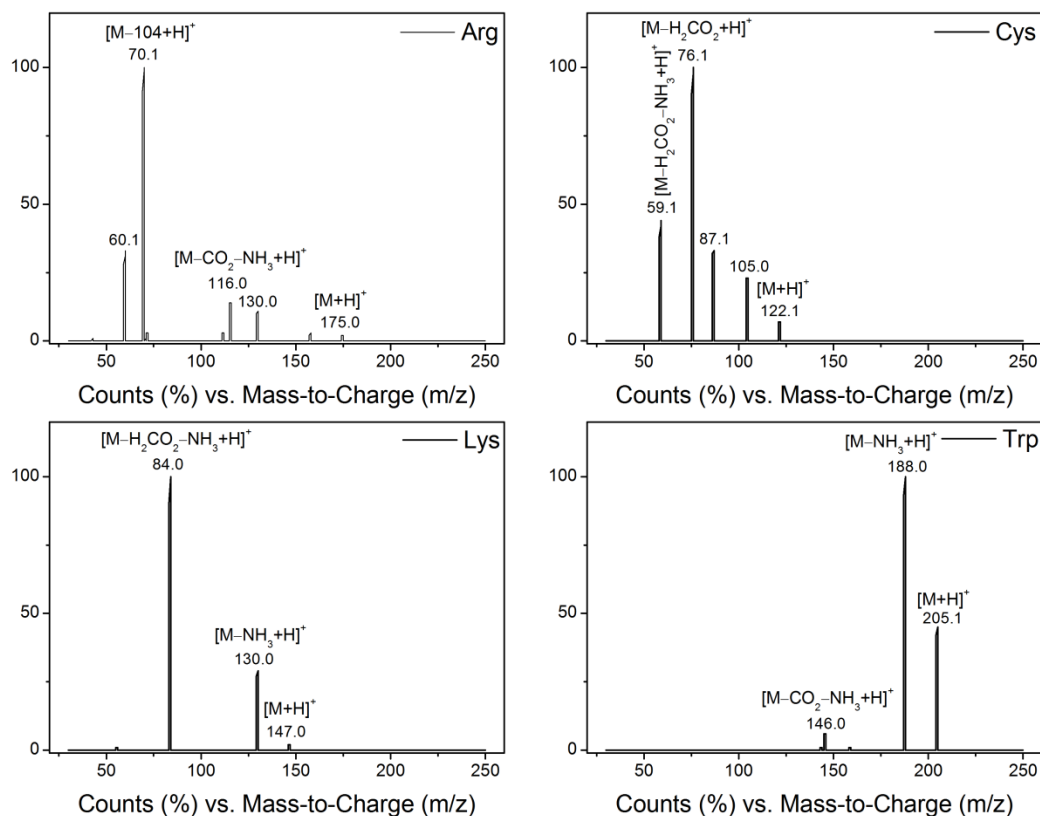


**Figure 3.3.** Product ion scan mass spectra of representative amino acids (100 µg/L) obtained by direct infusion.

The CID collision energies were also tuned manually by monitoring product ion intensity in the range from 2 to 30 eV. All selected MRM transitions as well as optimized fragmentor voltages and the collision energies for investigated amino acids are presented in Table 3.3. The selected quantification transitions are in bold.

**Table 3.3.**

Optimized MRM transition parameters for studied amino acids

Amino acid	Precursor ion	MRM transition <sup>a</sup>	Fragmentor voltage, V	Collision energy, eV
<b>Ala</b>	90	<b>90 → 44</b>	70	10
<b>Arg</b>	175	<b>175 → 70</b>	90	25
		175 → 116		11
<b>Asn</b>	133	<b>133 → 74</b>	70	13
		133 → 87		4

<b>Asp</b>	134	<b>134 → 74</b>	70	12
		134 → 88		5
<b>Cys</b>	122	<b>122 → 76</b>	70	11
		122 → 59		9
<b>Glu</b>	148	<b>148 → 84</b>	70	14
		148 → 130		4
<b>Gln</b>	147	<b>147 → 84</b>	70	16
		147 → 130		5
<b>Gly</b>	76	<b>76 → 30</b>	70	4
		76 → 48		3
<b>His</b>	156	<b>156 → 110</b>	100	12
		156 → 95		15
<b>Iso</b>	132	<b>132 → 69</b>	90	16
		132 → 86		5
<b>Leu</b>	132	<b>132 → 86</b>	90	6
		132 → 69		18
<b>Lys</b>	147	<b>147 → 84</b>	90	16
		147 → 130		5
<b>Met</b>	150	<b>150 → 104</b>	80	6
		150 → 133		4
<b>Phe</b>	166	<b>166 → 120</b>	90	10
		166 → 103		22
<b>Pro</b>	116	<b>116 → 70</b>	60	14
<b>Ser</b>	106	<b>106 → 60</b>	70	8
		106 → 42		18
<b>Thr</b>	120	<b>120 → 74</b>	70	7
		120 → 102		3
<b>Trp</b>	205	<b>205 → 188</b>	75	2
		205 → 146		2
<b>Tyr</b>	182	<b>182 → 136</b>	60	8
		182 → 165		3
<b>Val</b>	118	<b>118 → 72</b>	50	7
		118 → 55		23

Constant sampling time across chromatographic peaks provides equal data points for each analyte. This parameter is controlled by dwell time, where the physical meaning of this parameter is the time, that the instrument spends monitoring individual transition. The number of MRM transitions increases together with increase of target compounds. Therefore the data points for each

MRM chromatogram is significantly reduced if large number of compounds is analyzed at once. Consequently, it is necessary either to reduce the dwell times for these transitions or to increase the cycle time for each MS scan. One way to overcome this drawback is the time segmentation: method with multiple predefined time segments and the triple quad MS is programmed to perform MRM transitions for only those analytes that elute during each time segment. However, due to high number of closely eluting analytes the time segmentation in the present study was not employed. Reducing the dwell time might compromise MS data due to insufficient collision cell clearing before sequential transition. In addition, decreasing the dwell time results in less time spend on each transition and, consequently, in decreased sensitivity. The detection sensitivity was not the primary object in this assay and the collision cell cross-contamination was evaluated by precision experiments. Therefore the 20 ms dwell time for each MRM transition was appropriate in terms of method sensitivity and chromatographic peak quality.

### 3.3. HILIC separation

Three HILIC stationary phases, namely Atlantis HILIC, Acquity BEH HILIC and Acquity BEH Amide, were employed for amino acids separation (Figure 3.4).

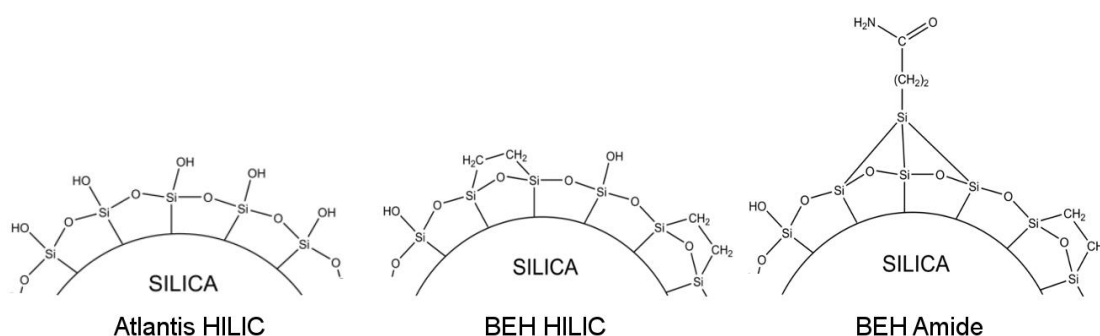


**Figure 3.4.** Structures of the stationary phases employed for HILIC.

Initial separation was performed in isocratic elution mode (flow rate 0.5 mL/min) using a mixture of acetonitrile and water (80:20, v/v) with

20 mmol/L formic acid as the mobile phase. As expected, the Atlantis HILIC bare silica stationary phase showed the strongest retention and the lowest peak efficiency for the majority of amino acids. Such results can be attributed to higher number of silanol groups on Atlantis stationary phase surface and bigger particle size (3  $\mu\text{m}$ ). Considerably better overall separation of amino acids was observed on Acquity BEH HILIC and Acquity BEH Amide stationary phases. Waters Acquity BEH type columns contain smaller (1.7  $\mu\text{m}$ ) particles which provide higher efficiencies. In addition, in this type of stationary phases bridging ethylene groups are embedded into silica matrix and nearly one third of free silanol groups are removed [111]. Furthermore, in BEH Amide stationary phase about half of surface silanols are coated with amide ligands. Lower density of free silanols leads to reduced secondary ion exchange interactions between protonated amino groups of the analytes and dissociated silanols. The effect of secondary ionic interactions was much more pronounced for basic analytes. Arginine ( $pI = 10.76$ ), histidine ( $pI = 7.60$ ) and lysine ( $pI = 9.60$ ) were most strongly retained on all three stationary phases. Arg and His did not elute on Atlantis HILIC and Lys did not elute on Atlantis HILIC and BEH Amide columns within 20 min. analysis run (Figure 3.5).



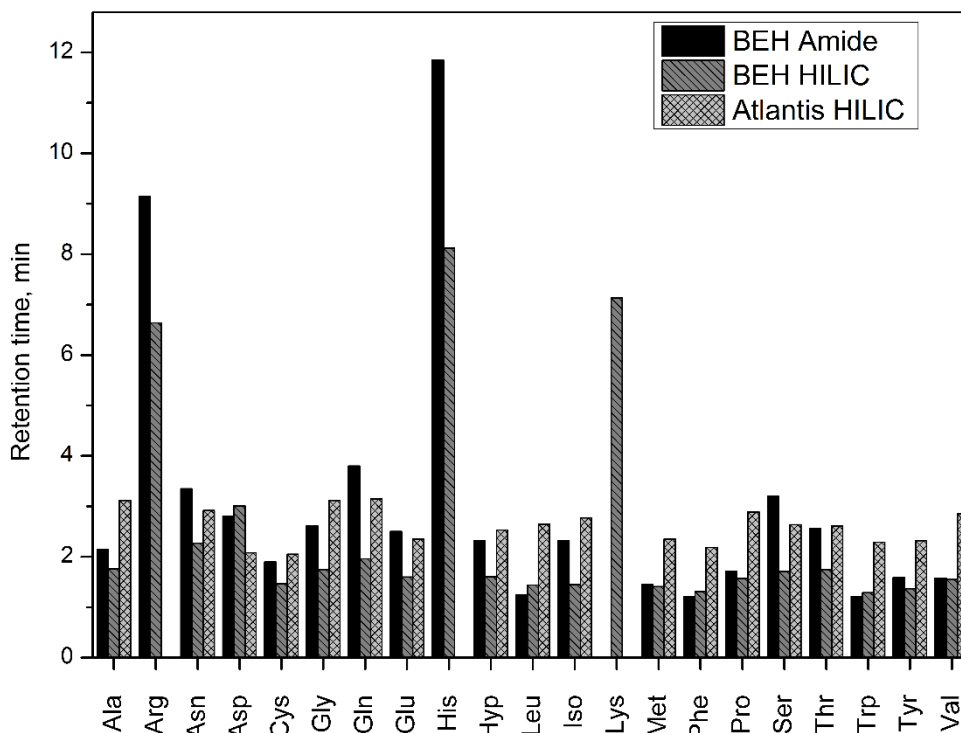


**Figure 3.5.** Retention of amino acids on three stationary phases. Mobile phase: A – aqueous 20 mmol/L HCOOH, B – CH<sub>3</sub>CN (20/80, v/v). Isocratic elution, flow rate – 0.5 mL/min.

As an example, the extracted ion chromatograms of selected amino acids obtained on three stationary phases are compared in Figure 3.6. Although for basic amino acids the better peak shapes were obtained on the BEH HILIC stationary phase, stronger retention and much better peak efficiency for the rest analytes was observed on BEH Amide stationary phase. Thus, the best overall performance with respect to peak shape and retention was obtained on the BEH Amide stationary phase. Given the facts above, BEH Amide column was chosen for further optimization.

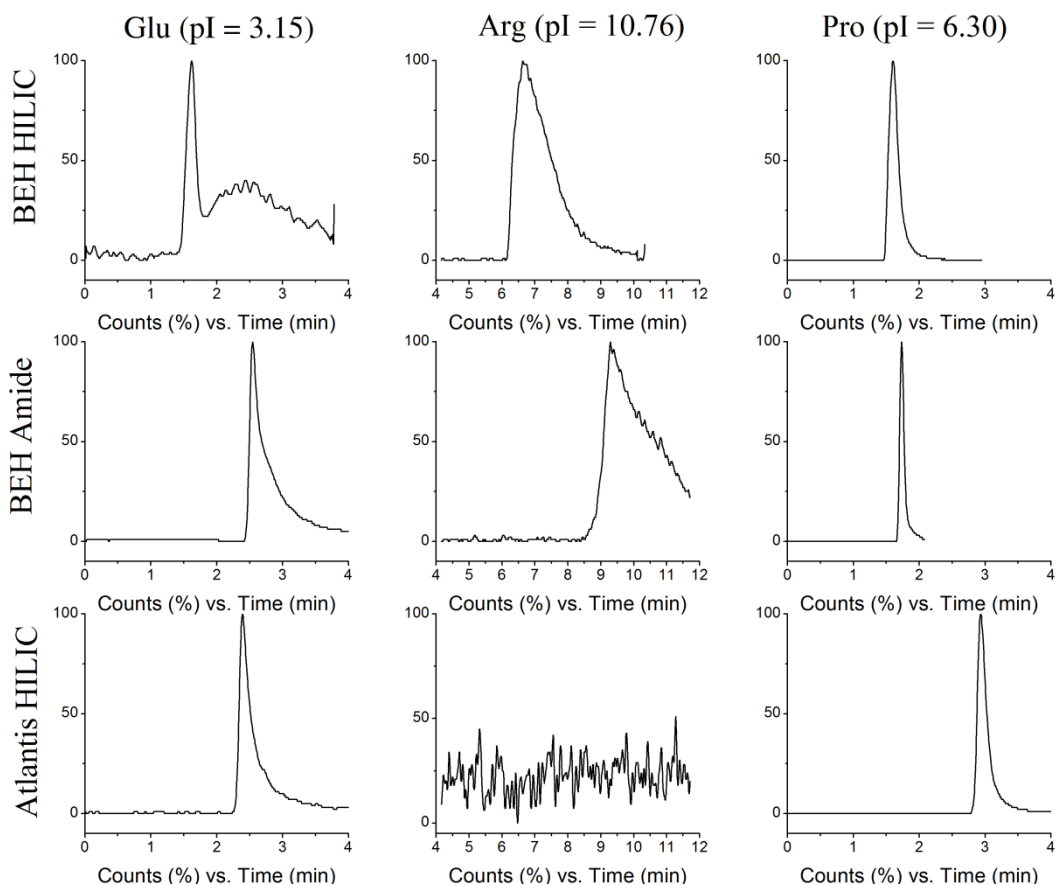


**Figure 3.6.** Extracted ion chromatograms of glutamic acid, arginine and proline on BEH HILIC, BEH Amide and Atlantis HILIC stationary phases.

Next, various mobile phase additives, namely acetic and formic acids, ammonium acetate and ammonium formate, were tested in terms of retention, resolution and MS signal response. The obtained results showed that none of the individual mobile phase additive can provide acceptable resolution of all amino acids. The best peak shapes and resolution was achieved only by using acidified mixture of ammonium formate and ammonium acetate salts as mobile phase additive in conjunction with gradient elution. This is clearly illustrated by the separation of isobaric (leucine, isoleucine and hydroxyproline) amino acids using different mobile phase additives (Figure 3.7.).

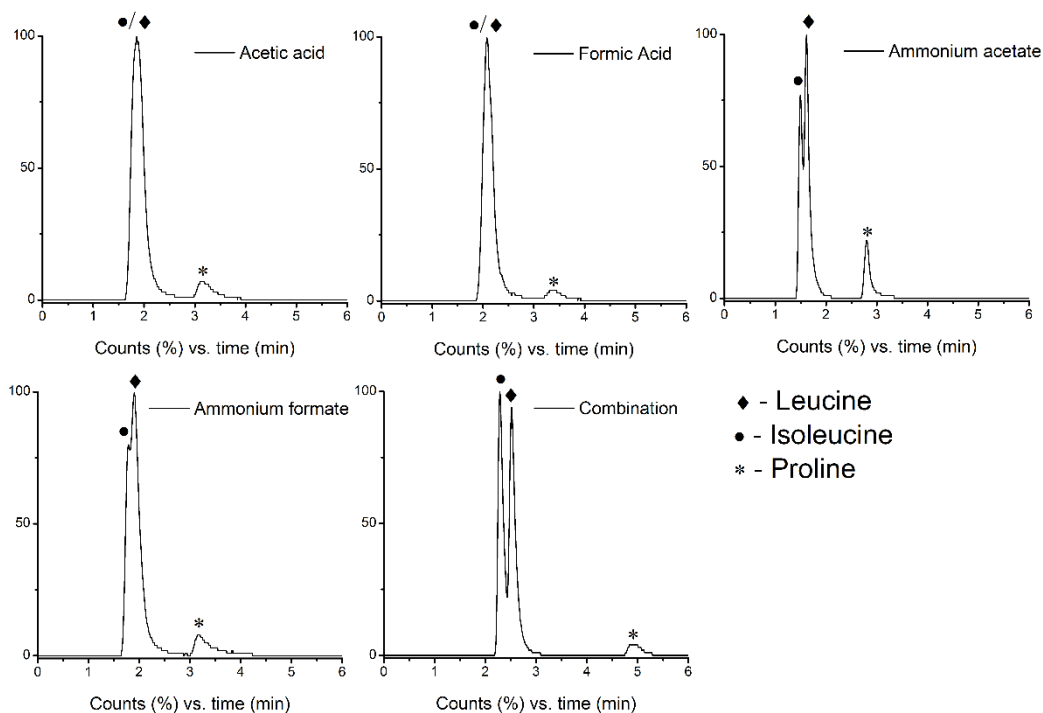


**Figure 3.7.** Influence of mobile phase modifier nature on the resolution of isobaric amino acids.

Figure 3.7 represents isocratic elution of Leu, Iso and Hyp on BEH Amide stationary phase with different mobile phases containing 10 mmol/L of appropriate modifier in 1:4 (v/v) H<sub>2</sub>O/CH<sub>3</sub>CN solution. Leu and Iso completely overlap when acetic or formic acid was used as mobile phase modifier. Slightly better resolution was obtained using ammonium acetate or ammonium formate additive. Finally, the use of 5 mmol/L ammonium formate and 5 mmol/L ammonium acetate mixture acidified by 0.15 % (by volume) formic acid in combination with linear gradient elution (from 0 to 6 min the water content increased from 15 to 20%) gave much better resolution of Leu/Iso pair and slightly improved peak shapes.

It is well known that the concentration of mobile phase additives considerably influences the ionization efficiency and the MS signal response of analytes. The concentration of mobile phase modifiers was therefore optimized in order to obtain higher signal responses. Obtained results are summarized in Figure 3.8.

As can be observed, the highest signal intensity for the most of the amino acids was observed when formic acid, ammonium formate and ammonium acetate concentrations in the final mobile phase were 10 mmol/L.

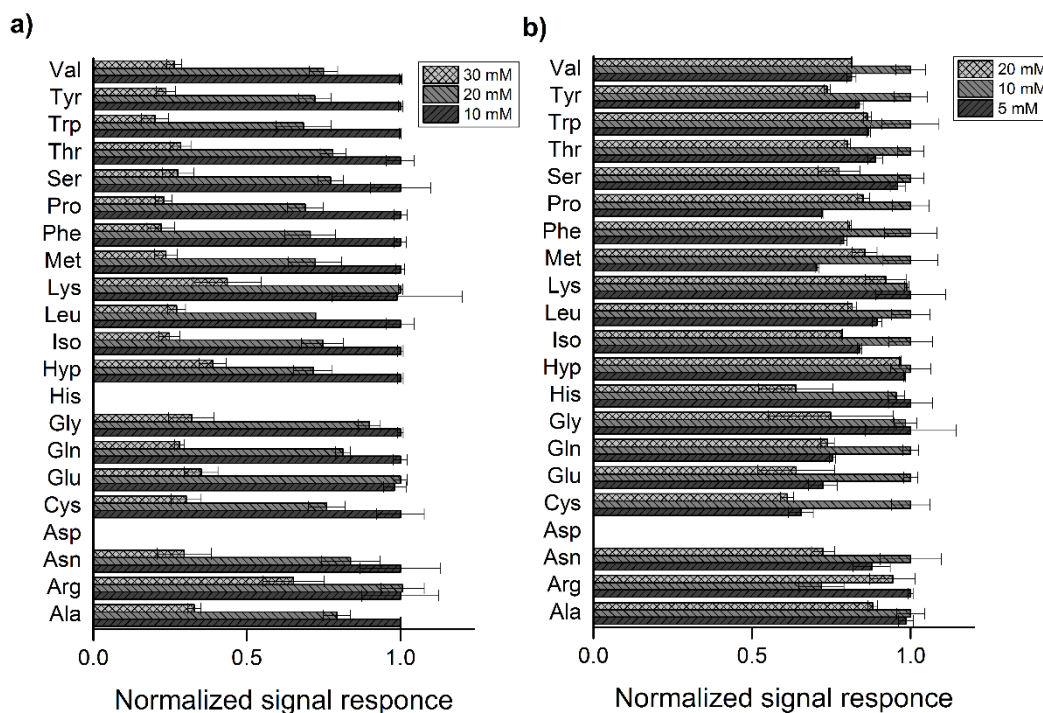


**Figure 3.8.** Effect of the concentration of mobile phase additives on MS signal response for amino acids. a) 10-30 mmol/L HCOOH + 5 mmol/L CH<sub>3</sub>COONH<sub>4</sub> and 5 mmol/L HCOONH<sub>4</sub>; b) 10 mmol/L HCOOH + 5-20 mmol/L CH<sub>3</sub>COONH<sub>4</sub> and HCOONH<sub>4</sub>.

For ionizable analytes, such as amino acids, increasing the salt concentration in the mobile phase decreases the retention if ion exchange mechanism is dominant. The opposite effect may occur if the analytes retention is promoted in the absence of ion exchange [10]. Obtained results showed that the increase in ionic strength did not influence noticeably the retention of acidic ( $pI < 5.0$ ) and moderately acidic amino acids ( $pI 5.0-6.3$ ), whereas the retention of basic amino acids slightly increased with increase of salt concentration in the mobile phase. This is illustrated (Figure 3.9.) by the extracted ion chromatograms ( $m/z = 147$ ) measured for two isobaric amino acids Gln ( $pI = 5.65$ ) and Lys ( $pI = 9.60$ ) at

three different salt concentrations. The retention time of Gln does not change by increasing of salt concentration in the mobile phase, whereas Lys did slightly stronger retained at higher ammonium acetate and ammonium formate concentrations. These data suggest that the impact of ion exchange interactions on the retention of amino acids is negligible. This is not surprising, given the fact that in BEH Amide stationary phase most of prone to ionization surface silanols are “neutralized” with amide ligands.

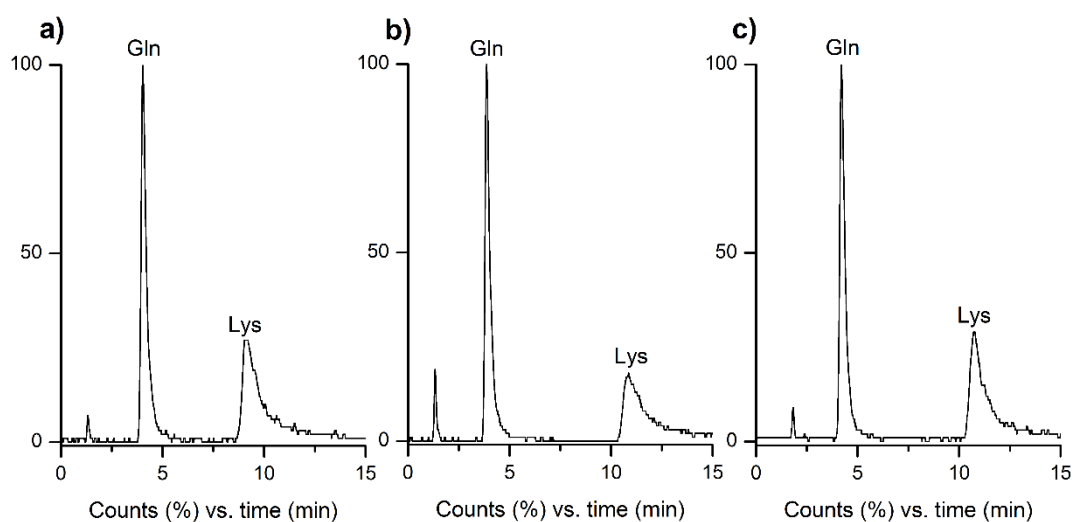


**Figure 3.9.** Extracted ion chromatograms of glutamine and lysine. Isocratic elution. Mobile phase: 90 % of ACN with aqueous 20 mmol/L HCOOH solution containing a) 5 mmol/L  $\text{CH}_3\text{COONH}_4$  + 5 mmol/L  $\text{HCOONH}_4$ ; b) 10 mmol/L  $\text{CH}_3\text{COONH}_4$  + 10 mmol/L  $\text{HCOONH}_4$ ; c) 10 mmol/L  $\text{CH}_3\text{COONH}_4$  + 20 mmol/L  $\text{HCOONH}_4$ .

Although HILIC is used extensively in the last two decades, the exact mechanism of HILIC separation is still under debate. The mechanism and theoretical description of analyte retention in HILIC has been the subject of many articles. There are essentially two possible ways to model the separation mechanism [6]. The first assumes the preferential adsorption of the water from the mobile phase onto the stationary phase surface followed by the partitioning of the analyte between the adsorbed aqueous layer and acetonitrile rich bulk

mobile phase. The second is the conventional adsorption of the analyte onto the surface of the stationary phase.

In the present work, partition and adsorption models were applied for binary mobile phase composition to describe amino acids retention on Amide stationary phase. The relationship for partition mechanism is well described in RP mode and can be expressed by following equation [112]:

$$\log k = \log k_w - S\varphi \quad (3.1.)$$

where  $k$  is analyte retention factor for the binary mobile phase;  $k_w$  is analyte retention factor for the weaker mobile phase component (acetonitrile) as mobile phase;  $\varphi$  is the volume fraction of the stronger member (water) of the binary mobile phase mixture; and  $S$  is the slope of  $\log k$  vs  $\varphi$  when linear regression model is fitted.

Adsorption mechanism is well expressed for conventional NP chromatographic system, where the retention of analytes is based on surface adsorption. The relationship between retention and volume fraction of the stronger solvent (water) in the mobile phase is expressed as follows [112]:

$$\log k = \log k_B - \frac{A_s}{n_b} \log \varphi \quad (3.2.)$$

where  $k$  is analyte retention factor for the binary mobile phase;  $k_B$  – analyte retention factor with pure stronger solvent (water) as eluent;  $\varphi$  is the volume fraction of the stronger member (water) of the binary mobile phase mixture;  $A_s$  and  $n_b$  are the cross-sectional areas occupied by the analyte and stronger solvent molecules, respectively.

Linear function of  $\log k$  versus volume fraction  $\varphi$  of stronger mobile phase solvent would indicate that partition mechanism is dominant in retention, whereas adsorption mechanism would give linear dependence by plotting  $\log k$  versus  $\log \varphi$  [5,112]. The lack of fit of experimental data to both equations can be attributed to mixed-mode retention mechanism.

Retention factors were measured with water fraction in mobile phase ranging from 14.5 % to 33.5 % (by volume) for all analyzed amino acids except for Asn, Asp, His and Lys, which were retained very strongly when water content exceeded 24 % (by volume). The data are shown in Figures 3.10 and 3.11.

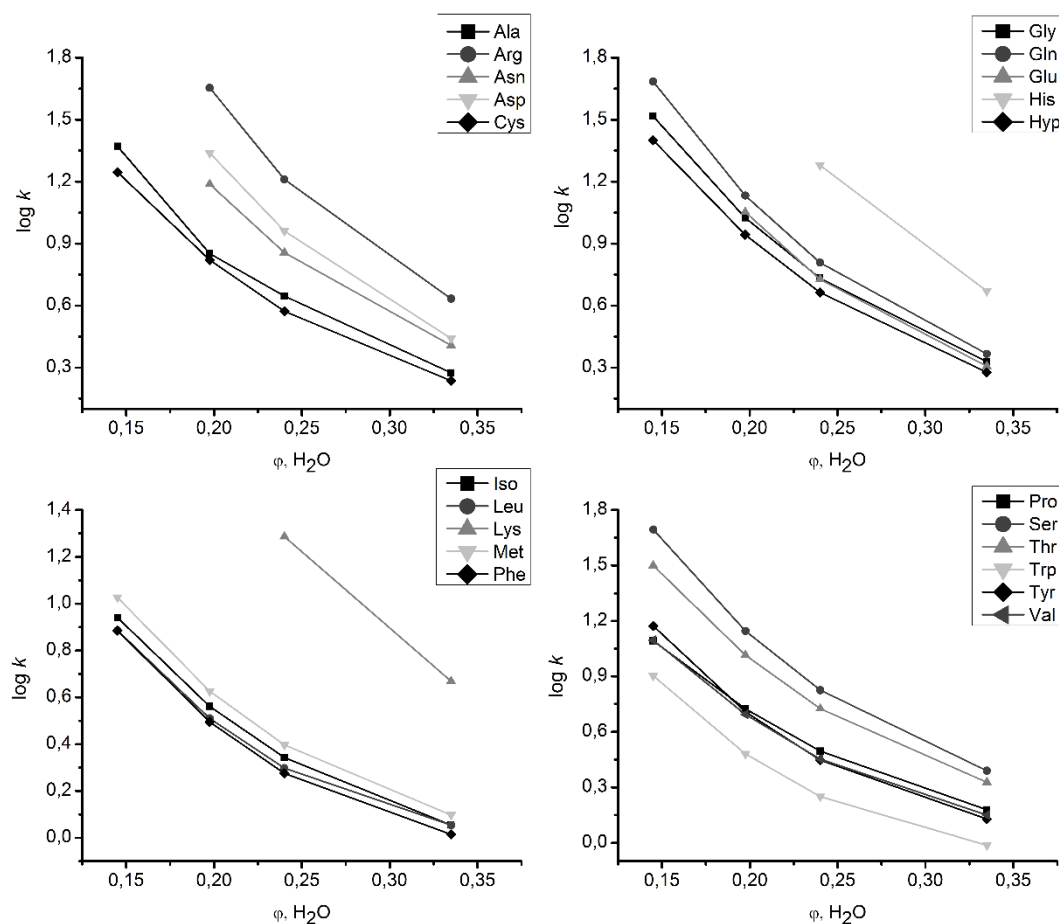


**Figure 3.10.** Dependencies of  $\log k$  versus volume fraction  $\phi$  of water in the binary mobile phase.

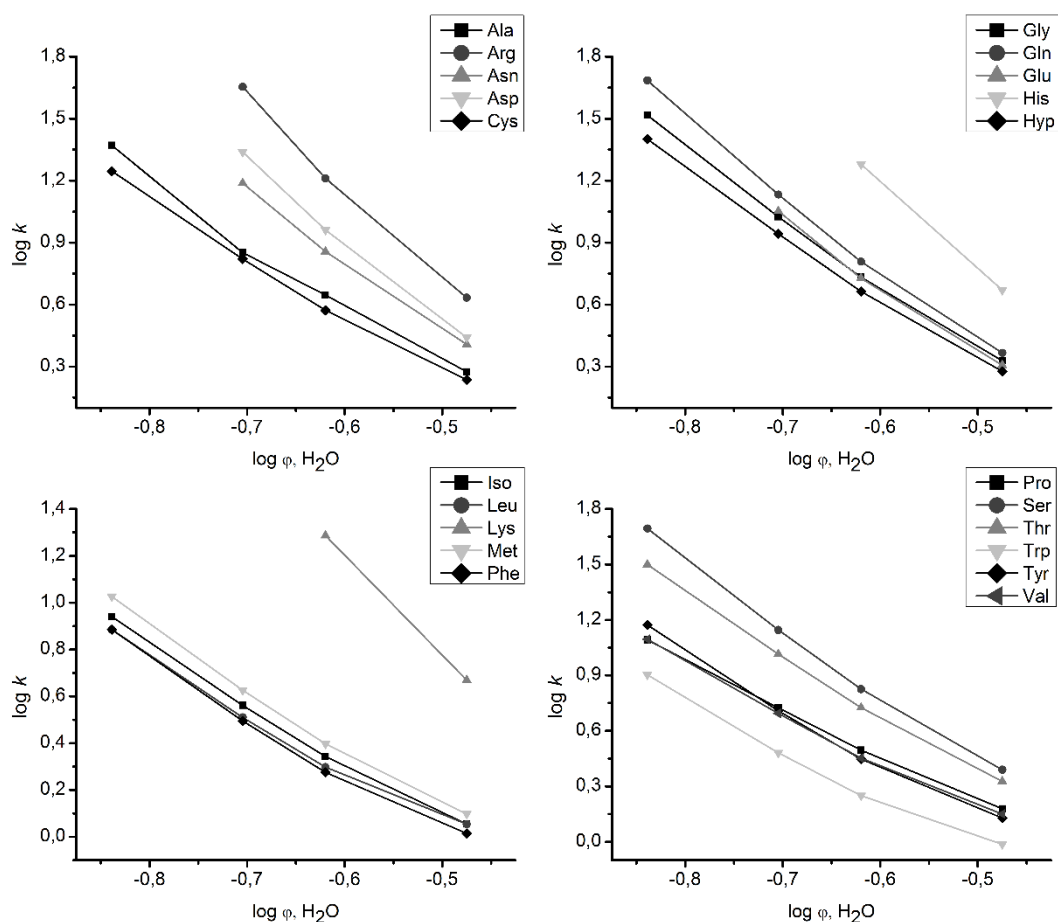


**Figure 3.11.** Dependencies of  $\log k$  versus  $\log \varphi$  of water in the binary mobile phase.

The correlation coefficients for plots obtained by partition mechanism varied from 0.962 to 0.992, whereas for adsorption from 0.990 to 0.998. Based on these results the assumption can be made that most likely under HILIC conditions amino acids are retained by the mixed partition/adsorption retention mechanism in which the impact of adsorption is slightly higher.

Liang and co-workers [113] proposed HILIC retention model which relates molecular volume of analyte and the interaction energy of analyte with the stationary phase and the mobile phase. This model not only considers the interaction of analyte and mobile phase with the stationary phase, but also the interaction between analyte and mobile phase. The retention behavior is expressed as follows:



$$\ln k = a + b \ln \varphi + c\varphi \quad (3.3)$$

where  $k$  is analyte retention factor;  $\varphi$  is the volume fraction of the stronger solvent of the binary mobile phase mixture;  $a$  – constant that relates molecular volume of the analyte;  $b$  – coefficient that relates direct analyte-stationary phase interaction,  $c$  – coefficient that is related to the interaction energy between analyte and solvents.

The dependencies of  $\ln k$  versus  $\varphi$  of water in the binary mobile phase approximated by Equation 3.3 are shown in Figure 3.12.

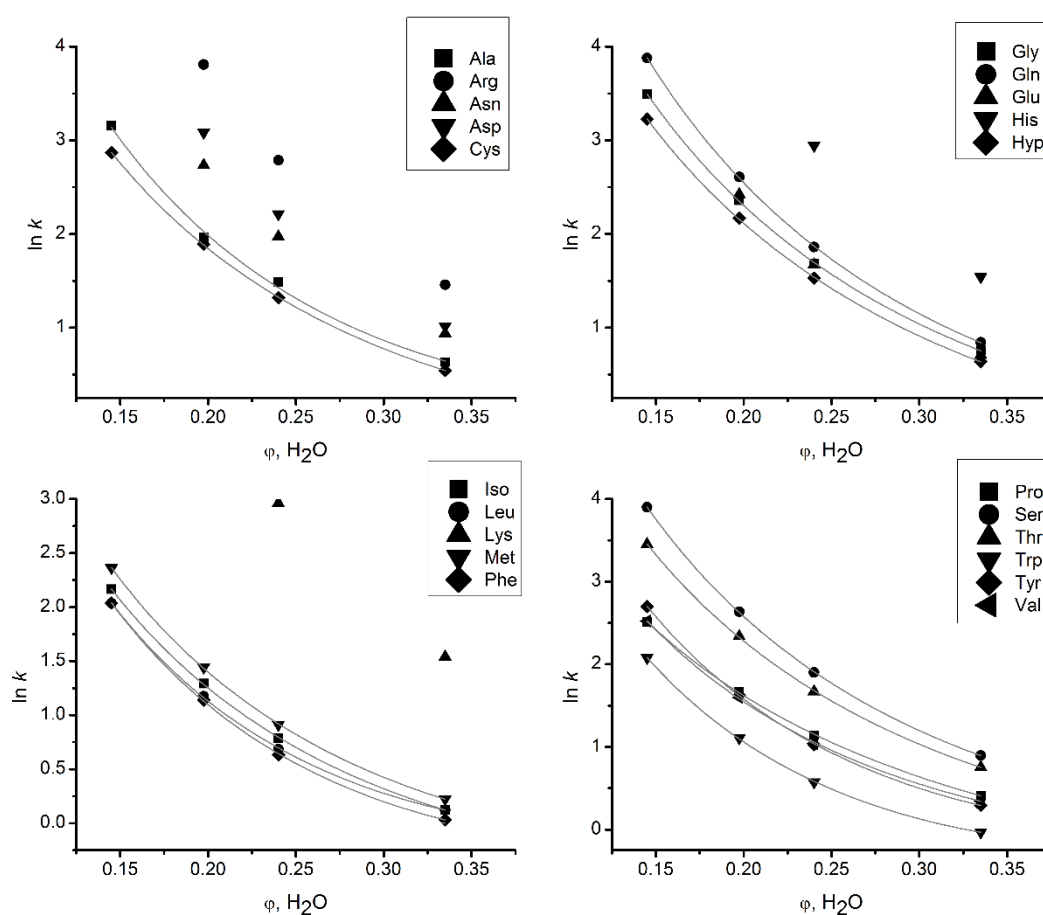


**Figure 3.12.** Dependencies of  $\ln k$  versus  $\varphi$  of water in the binary mobile phase.

The regression results based on equation 3.3 gave very good correlation with correlation coefficients exceeding 0.999, except for alanine ( $R^2 = 0.9926$ ). The

summarized regression data for all three mathematical retention models are listed in Table 3.4.

**Table 3.4.**

Correlation parameters for partition, adsorption and HILIC models.

Analyte	Partition model	Adsorption	HILIC model
	Eq. (3.1.)	model	Eq. (3.3.)
	$R^2$	Eq. (3.2.)	$R^2$
	$R^2$	$R^2$	$R^2$
Ala	0.9692	0.9926	0.9926
Arg <sup>1</sup>	0.9900	0.9972	–
Asn <sup>1</sup>	0.9916	0.9980	–
Asp <sup>1</sup>	0.9921	0.9983	–
Cys	0.9771	0.9967	0.9998
Gly	0.9896	0.9970	0.9998
Gln	0.9778	0.9969	0.9998
Glu <sup>1</sup>	0.9791	0.9974	–
His <sup>1</sup>	–	–	–
Hyp	0.9803	0.9978	0.9997
Iso	0.9750	0.9959	0.9999
Leu	0.9658	0.9916	0.9994
Lys <sup>1</sup>	–	–	–
Met	0.9739	0.9954	0.9998
Phe	0.9675	0.9925	0.9997
Pro	0.9817	0.9982	0.9995
Ser	0.9773	0.9968	0.9999
Thr	0.9791	0.9974	0.9998
Trp	0.9629	0.9902	0.9997
Tyr	0.9690	0.9932	0.9998
Val	0.9746	0.9956	0.9993

<sup>1</sup> – Not enough data points (due to strong retention) to calculate regression parameters.

The results suggest that amino acids on the HILIC stationary phase are retained by the mixed mechanism, and that the analytes retention can be best expressed by model developed by Liang *et al.* [113].

The effect of the column temperature was investigated in the range of 15–55 °C. All the analytes showed so called “normal behavior”, that is, decrease in retention as the column temperature increases. However, no significant improvement in resolution was observed at higher temperatures. Van`'t Hoff plots ( $\ln k$  vs.  $1/T$ ) showed linear relationship for majority of analyzed amino acids. Effect of column temperature on the retention of selected amino acids is demonstrated in Figure 3.13. Only glutamic and aspartic acids gave nonlinear dependencies, which indicates that for these amino acids electrostatic and adsorptive forces are responsible for analytes retention [101]. For both acids the  $pK_a$  values of their second carboxylic group (3.65 and 4.25 for Asp and Glu, respectively) are near the mobile phase pH. Most likely nonlinear dependences could be attributed to the changes in their effective charge caused by the reduction in their  $pK_a$  that occur as column temperature is raised [114]. Consequently, in this case the contribution of electrostatic interaction between acid and stationary phase may change with column temperature. In contrast, the other amino acids studied contain one carboxylic group with much lower  $pK_a$  values (1.82-2.36) and, most likely, remain unchanged under conditions of the experiment.

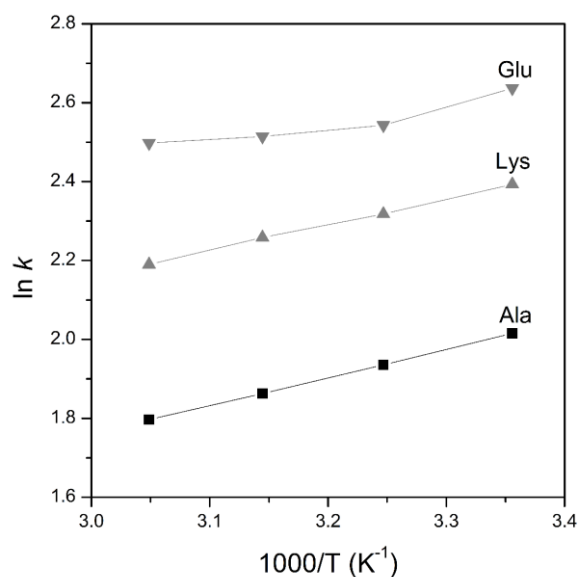


**Figure 3.13.** Effect of column temperature on the retention of selected amino acids on BEH Amide stationary phase.

Finally, series of experiments were conducted to optimize gradient elution conditions. Optimization was done using binary mobile phase: A – aqueous solution containing 20 mmol/L HCOOH, 3 mmol/L HCOONH<sub>4</sub> and 3 mmol/L CH<sub>3</sub>COONH<sub>4</sub>; B – 20 mmol/L HCOOH, 3 mmol/L HCOONH<sub>4</sub> and 3 mmol/L CH<sub>3</sub>COONH<sub>4</sub> in H<sub>2</sub>O with 90% of CH<sub>3</sub>CN (v/v). Final gradient elution program was set as follows: 0–7 min from 95% B to 90% B; 7–15 min from 90% B to 70% B; within the next minute returns to the initial mobile phase composition and equilibrates for 4 min prior to next injection.

The representative chromatogram of all 21 amino acids is shown in Figure 3.14. Despite the fact that even under optimized conditions some acids (e.g., Asp and His) exhibit broad and tailing peaks, the obtained overall performance is adequate for identification purposes.

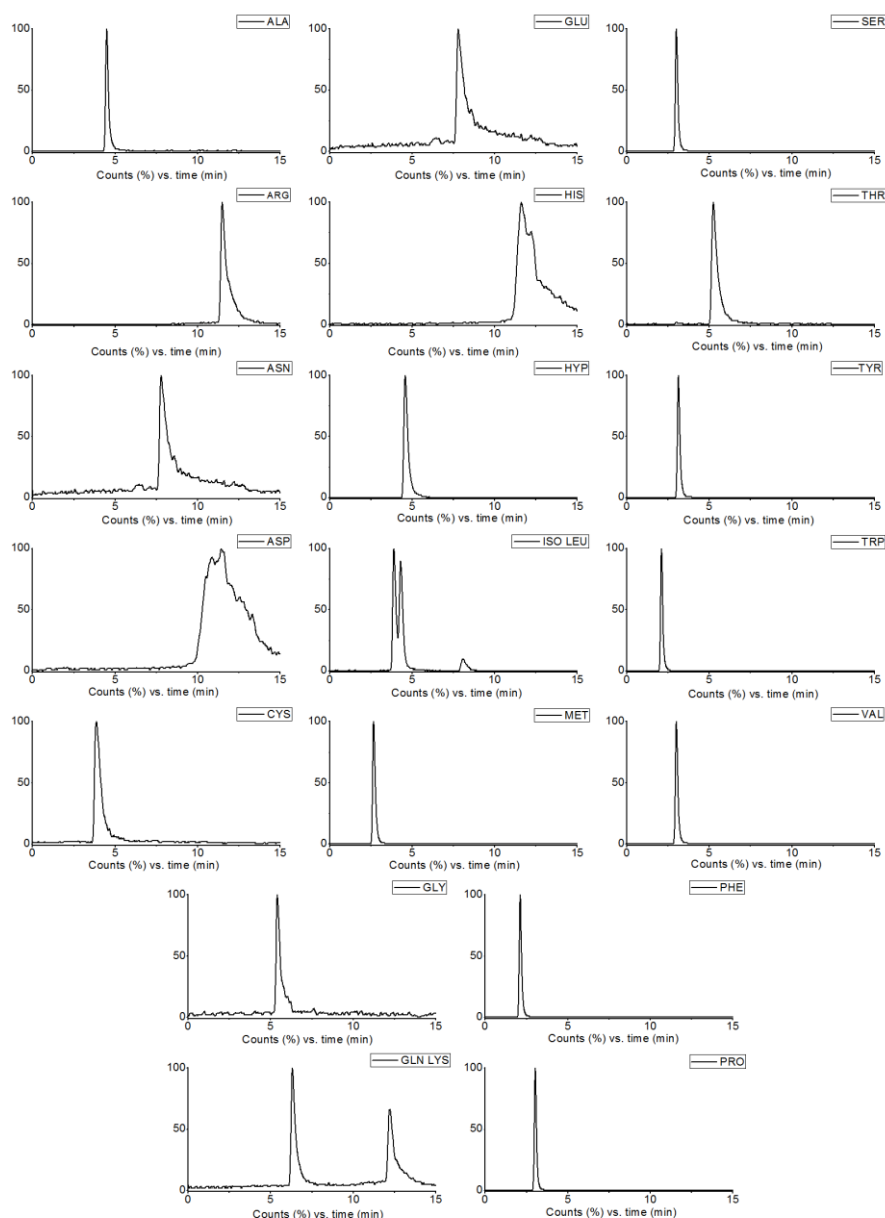


**Figure 3.14.** Optimized HILIC-MS/MS MRM chromatograms of 21  $\alpha$ -amino acids on the BEH Amide stationary phase.

### 3.4. Enantioselective HPLC separation

The existence of enantiomers has been known for many years and the importance of chirality with respect to biological activity has been shown in 19<sup>th</sup> century by Pasteur [104]. Except of glycine, all amino acids have at least one chiral center which is located on  $\alpha$ -carbon atom.

Macrocyclic antibiotic stationary phases are one type of the chiral stationary phases that are employed for enantioselective analysis of small polar compounds. The Chirobiotic T and T2 columns are commercially available teicoplanin based stationary phases that are compatible to perform chiral separations in normal-phase, reversed-phase and polar-organic separation modes [39,114]. However, amino acids are ionic compounds that possess very poor solubility in apolar normal-phase mobile phases. In addition, normal-phase mobile phases are not compatible with the ESI ion source. Much better enantioseparation performance of small polar compounds is usually achieved in reversed-phase or polar-organic separation modes. The major type of molecular interactions taking place between analyte and stationary phase in reversed-phase is electrostatic interactions and hydrophobic driven “pocketing” by analyte and macrocyclic teicoplanin rings. Additional interactions, such as steric effects, H-bonding and  $\pi$ - $\pi$  interaction are virtually nonexistent in reversed-phase mode [47], whereas the major type of interactions in polar-organic mode believed to be H-bonding. Moreover, secondary type interactions such as electrostatic attraction and steric forces probably are also involved in retention and chiral resolution [39,47,115].

Chirobiotic T2 chiral stationary phase was selected for method development and validation. As already mentioned above, macrocyclic antibiotic based chiral stationary phases are compatible with both organic and aqueous mobile phases. This makes Chirobiotic T2 the ideal stationary phase for resolving polar compounds, such as amino acids. Several parameters, such as nature and content of the organic modifier in the mobile phase, mobile phase pH, and column temperature, were tested to find the optimum conditions allowing for the highest enantiomeric resolution of the analytes.

Typically, the resolution of amino acids is strongly influenced by the nature of organic modifier [106,116]. Two common organic modifiers, namely acetonitrile and methanol, were tested in the initial experiments. Acetonitrile provided the best resolution for isobaric L-Leu/L-Iso pair, but the separation of

D-/L-Leu enantiomers was reduced (Figure 3.15). Moreover, the enantiomeric resolution of the rest of the D-/L-amino acids was also reduced at some extent using acetonitrile.

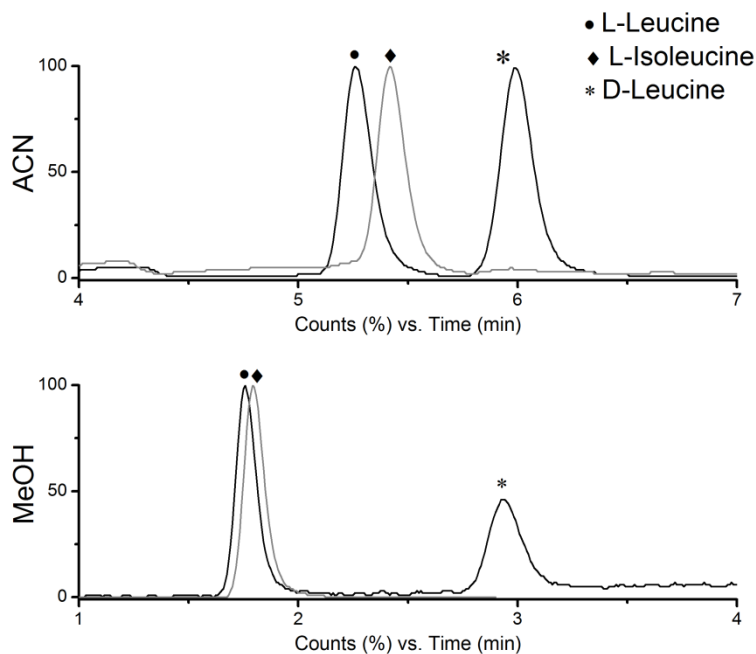


**Figure 3.15.** Resolution of isobaric D-Leu and L-Leu/L-Iso amino acids with ACN and MeOH as organic modifiers in mobile phase. Mobile phase: A – aqueous 10 mmol/L  $\text{CH}_3\text{COONH}_4$  (pH 4.2); B – 10 mmol/L  $\text{CH}_3\text{COONH}_4$  (pH 4.2) in  $\text{H}_2\text{O}$ /organic solvent (5:95, v/v). Gradient elution: 0–5 min, 95% B; 5–15 min, from 95% B to 55% B; 15–20 min, 55% B. Flow rate 0.3 mL/min.

It was shown that the enantiomeric resolution of amino acids can be improved with the increase of the organic modifier chain length [107,115]. The resolution factor can be increased dramatically by changing from methanol to 2-propanol for some analytes [115]. However, the mobile phase viscosity and, consequently, the system back pressure also increase with the alcohol side chain length. In the present study pure ethanol and its mixture with methanol were additionally tested for enantioseparation performance. Enantioselective separation of four selected D-/L-amino acid pairs with different organic mobile phase modifiers is compared in Figure 3.16.

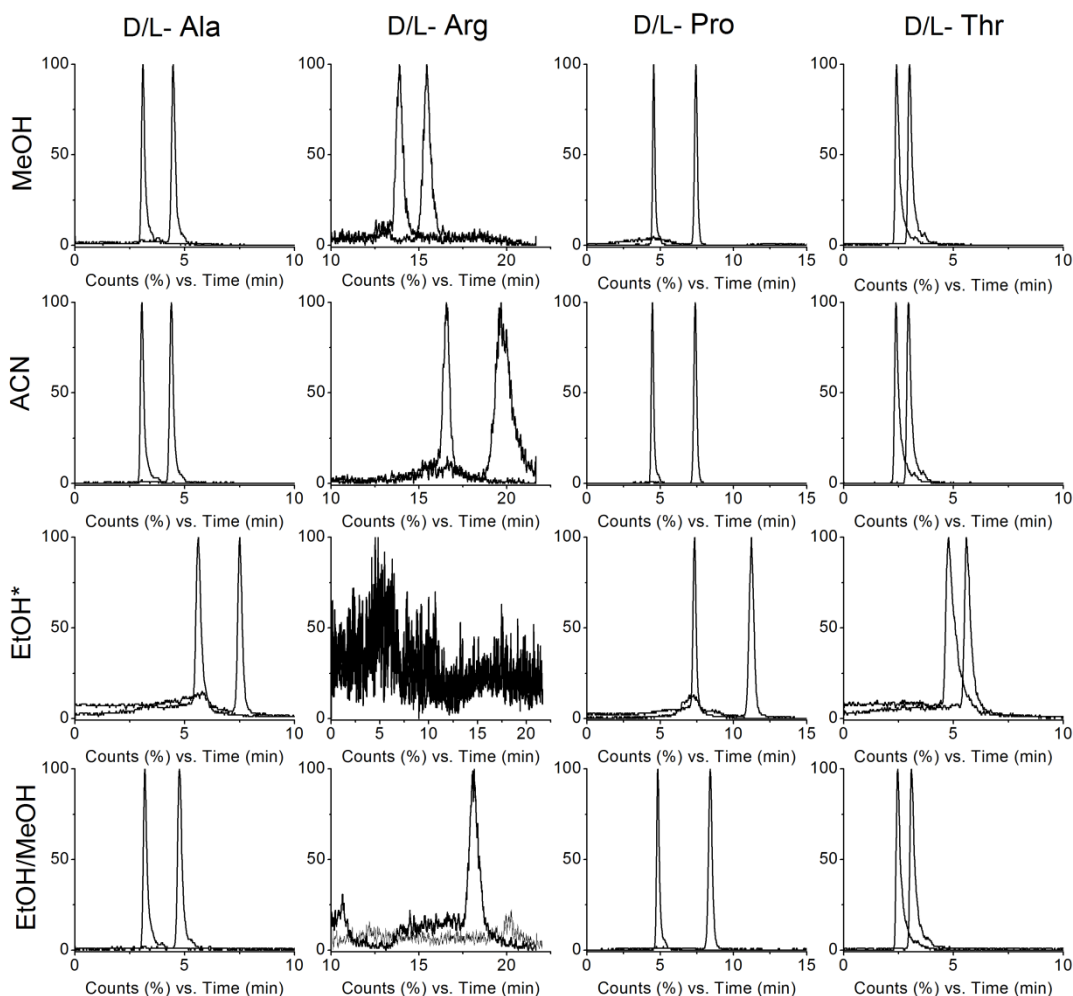


**Figure 3.16.** Enantioselective separation of D-/L-alanine, D-/L-arginine, D-/L-proline and D-/L-threonine with different organic mobile phase modifiers.

Mobile phase (pH 4.0): A – aqueous 10 mmol/L  $\text{CH}_3\text{COONH}_4$ ; B – 10 mmol/L  $\text{CH}_3\text{COONH}_4$  in  $\text{H}_2\text{O}$ /organic solvent (5:95, v/v). Gradient elution: 0–5 min, 95% B; 5–15 min, from 95% B to 55% B; 15–20 min, 55% B. Flow rate 0.3 mL/min. \*Flow rate 0.2 mL/min. Mobile phase for EtOH/MeOH mixture (pH 4.0): A – 10 mmol/L  $\text{CH}_3\text{COONH}_4$  in  $\text{H}_2\text{O}$ /EtOH (75:25, v/v); B – 10 mmol/L  $\text{CH}_3\text{COONH}_4$  in  $\text{H}_2\text{O}$ /MeOH (5:95, v/v).

The use of ethanol as the organic modifier increased system back pressure, therefore lower mobile phase flow rate was employed in this case. However, enantiomeric resolution of amino acids was not improved neither with ethanol/methanol mixture nor with pure ethanol. In addition, the decrease in



peak efficiency was observed with ethanol due to slower mass transfer in high-viscosity mobile phase. Furthermore, stronger retained analytes, such as D-/L-Arg, D-/L-His and D-/L-Lys were not eluted within 25 min. Based on the obtained results methanol was chosen for further optimization. For some analytes in reversed-phase separation mode, macrocyclic glycopeptide-based stationary phases exhibit U-shaped retention versus mobile phase composition plots with a minimum of retention at about 30-50% of organic solvent in the aqueous mobile phase [114,117,118]. The increase in retention with decreasing the MeOH concentration at water-rich mobile phase compositions is usually observed when hydrophobic interactions between analytes and stationary phase are dominant. At organic-rich mobile phase compositions an opposite trend is observed, which can be attributed to the lower solubility of the polar analytes in less polar mobile phases.

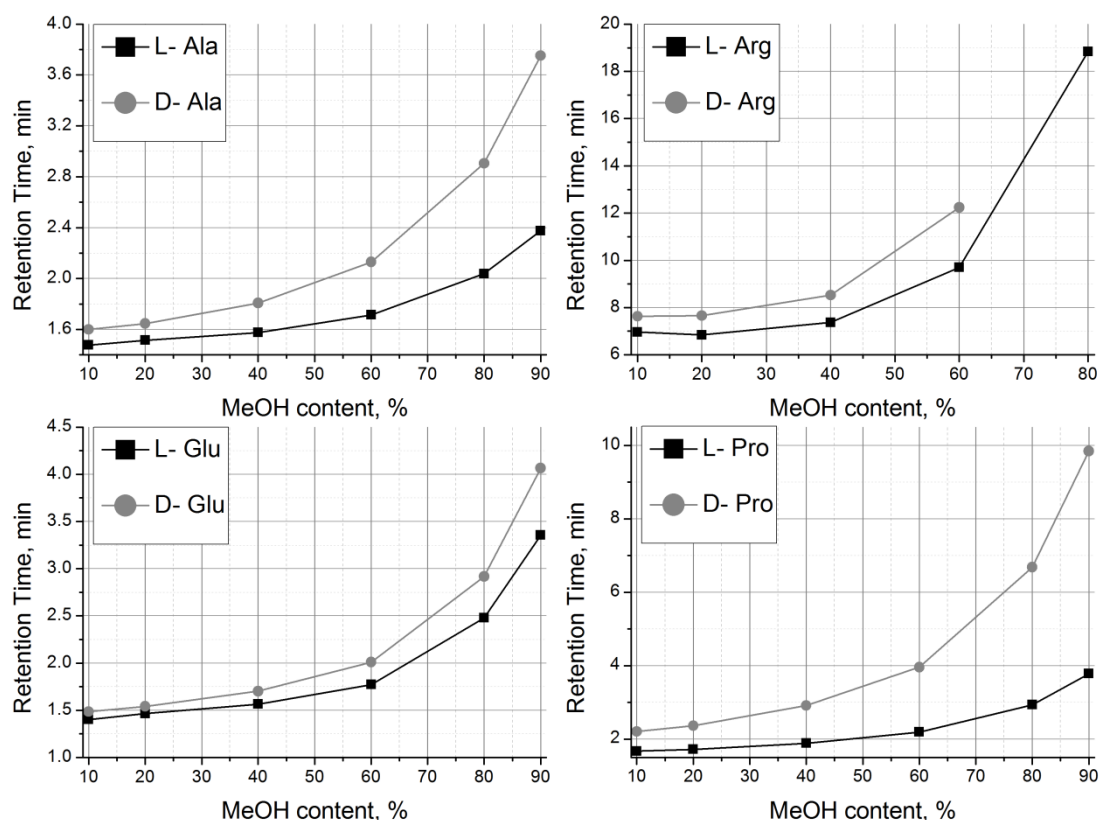


**Figure 3.17.** Effect of the methanol content in the mobile phase on the retention times of D-/L-Ala, D-/L-Arg, D-/L-Glu and D-/L-Pro enantiomers.

The analytes therefore favored the stationary phase, which resulted in a stronger retention at a higher MeOH amount in the mobile phase [118]. Figure 3.17 shows the plots of the retention times for four representative enantiomer pairs as a function of the MeOH concentration in the mobile phase. As can be observed, all four enantiomer pairs do not show U-shaped retention profile. This is also true for the other amino acids (data not shown). The retention times are substantially unaffected by changes in mobile phase composition for MeOH concentrations lower than 30% (v/v). This suggests that for very hydrophilic compounds, such as amino acids, hydrophobic interactions are not the driven retention forces even at water-rich mobile phases. The best enantiomeric resolution was observed in MeOH-rich mobile phases. At higher MeOH concentrations amino acids show typical HILIC retention behavior of increasing retention with increasing MeOH content. Partition, adsorption and HILIC models have been applied to determine the correlation retention mechanism. Obtained plots for D-/L-Ala enantiomers are presented Figure 3.18. The summarized regression data for all amino acids are compared in Table 3.5.

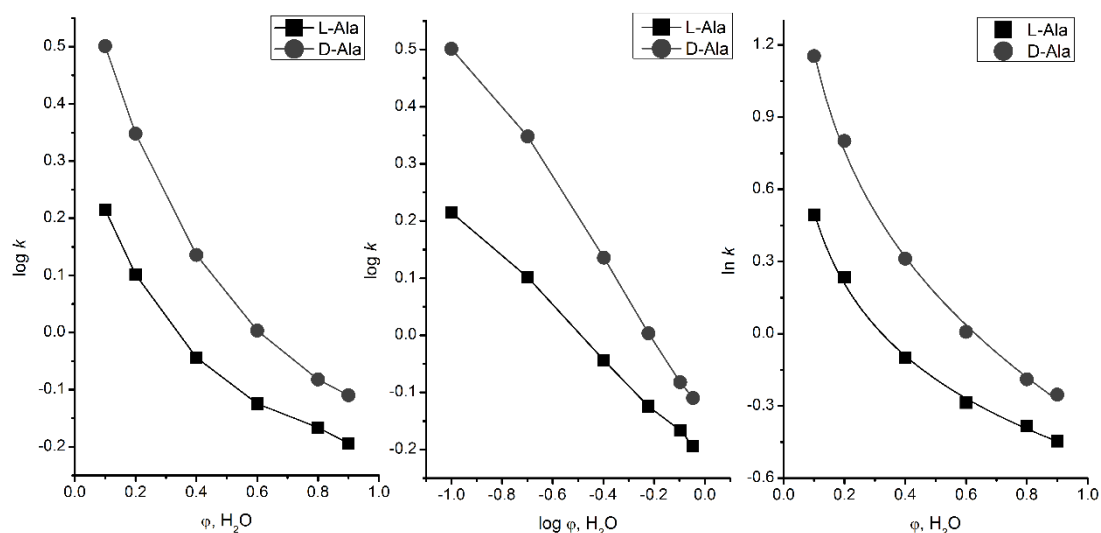


**Figure 3.18.** D-/L-Ala retention factor ( $\log k$  and  $\ln k$ ) plots against stronger solvent fraction in the mobile phase ( $\phi$  and  $\log \phi$  of  $\text{H}_2\text{O}$ ).

No linear correlation was obtained for most of the amino acids when partition model was applied. The adsorption model seems to fit better because significantly higher correlation was observed for most of the analytes. Such dependence suggests that analytes retention, but not the enantiomeric resolution is mainly driven by amino acids adsorption on the stationary phase. The results showed that HILIC retention model suggested by Liang *et al.* [113] best describes the retention of amino acids with correlation coefficients exceeding 0.99 for the majority of analytes. From the data obtained we can conclude that the retention of amino acids on Teicoplanin stationary phase is similar to HILIC mechanism, where analytes adsorption on hydrophilic stationary phase surface predominates over partition.

**Table 3.5.**

Correlation parameters of partition, adsorption values of retention models of D-  
/L-amino acids on Teicoplanin CSP.

Analyte	Partition model Eq.	Adsorption model	HILIC model
	(3.1)	Eq. (3.2)	Eq. (3.3)
	$R^2$	$R^2$	$R^2$
L-Ala	0.9090	0.9976	0.9968
D-Ala	0.9329	0.9948	0.9964
L-Arg	0.7556	0.9268	0.9982
D-Arg	0.7986	0.8961	0.9999
L-Asn	0.8800	0.9965	0.9979
D-Asn	0.8926	0.9973	0.9971
L-Asp	0.9074	0.9910	0.9919
D-Asp	0.9440	0.9967	0.9952
L-Cys	0.9082	0.9991	0.9988
D-Cys	0.9421	0.9936	0.9975
L-Gln	0.8603	0.9929	0.9975
D-Gln	0.8748	0.9953	0.9971
Gly	-	-	-
L-His	0.8850	0.9870	0.9959
D-His	0.8818	0.9861	0.9961
L-Iso/Leu	0.9457	0.9927	0.9978

D-Iso/Leu	0.9698	0.9809	0.9986
L-Lys	0.7910	0.9463	0.9973
D-Lys	0.8528	0.9347	0.9984
L-Met	0.9194	0.9463	0.9998
D-Met	0.9673	0.9347	0.9997
L-Phe	0.4462	0.7465	0.9542
D-Phe	0.8714	0.9930	0.9944
L-Pro	0.9255	0.9968	0.9973
D-Pro	0.9557	0.9887	0.9978
L-Ser	0.8558	0.9921	0.9978
D-Ser	0.8828	0.9965	0.9973
L-Thr	0.8493	0.9893	0.9956
D-Thr	0.8909	0.9975	0.9976
L-Trp	-	-	-
D-Trp	-	-	-
L-Tyr	-	-	-
D-Tyr	-	-	-
L-Val	0.9347	0.9965	0.9987
D-Val	0.9443	0.9930	0.9976

It was reported earlier [107,115,119,120] that the discrimination of D-/L-amino acid enantiomers is influenced by teicoplanin conformation, which can be affected by mobile phase pH and temperature. Figure 3.19 illustrates the geometry of teicoplanin obtained by molecular dynamic simulation. Teicoplanin contains a single primary amine ( $pK_a \approx 9.2$ ) and a single carboxylic ( $pK_a \approx 2.5$ ) groups, which are mainly responsible for chiral recognition [115]. It is important to note that dual electrostatic interactions between teicoplanin amino/carboxylic groups and corresponding amino acids groups is not possible [47]. The distance between the primary amine and the carboxylic group ( $\sim 12 \text{ \AA}$ ) and their relative positions on the aglycone would prevent the simultaneous interactions. Therefore the chiral compounds having acidic group would interact with teicoplanin primary amine, whereas amino group containing analytes would interact with carboxylic teicoplanin site. Zwitterion compounds such as amino acids would probably possess combined docking sites, which would depend on mobile phase pH and analytes  $pI$  value.

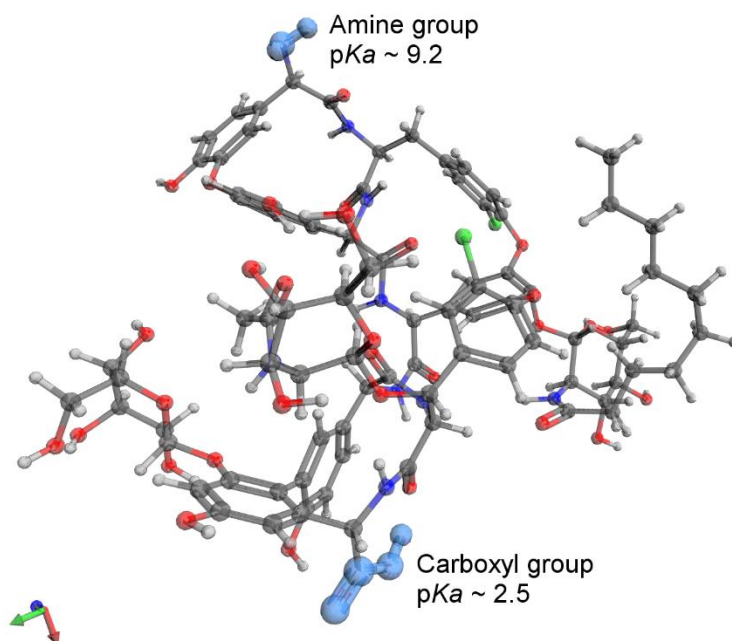


**Figure 3.19.** Optimized geometry of teicoplanin using molecular dynamic simulation software Avogadro 1.1.1.

The effect of mobile phase pH on the enantiomeric resolution was also briefly investigated. Ammonium acetate, which exhibits adequate buffering capacity over the working pH range (3.8-6.8) of the stationary phase, was employed for mobile phase pH adjustment. No significant effect on enantioselectivity within the pH range of 4–6 was observed, and only slightly better resolution was achieved at lower pH values. The variation of the pH between 4 and 6 does not change the charge state of the amino group and only slightly (at pH < 4.5) affects the charge state of the carboxylic group on the stationary phase surface. However, amino acids with *pI* values lower than 4, namely, D-/L-aspartic acid (*pI* = 2.98) and D-/L-glutamic acid (*pI* = 3.08) were only partially resolved under these conditions. Because of the limited stationary-phase pH working range, it was impossible to try to resolve them in their fully protonated form. On the basis of the obtained results, mobile phase with pH 4.2 was chosen for further experiments. It should be noted that more acidic mobile phase is favored for positive ESI ionization mode due to better signal response.

Early observations showed that temperature plays an important role in chiral separation of enantiomers on macrocyclic glycopeptide CSP [120]. Considering the analytes mass transfer from mobile to stationary phases the Gibbs free energy change ( $\Delta G^\circ$ ) of the analytes phase transfer is expressed as follows:

$$\Delta G^\circ = -RT \ln \left( \frac{k}{\varphi} \right) \quad (3.4.)$$

where  $k$  is analyte retention factor and  $\varphi$  is column phase ratio (i.e., the ratio of the volume of the stationary phase to that of the mobile phase in a column). Expressing the Gibbs energy to temperature depended equation, gives the according equation:

$$\ln k = -\frac{\Delta H^\circ}{RT} + \frac{\Delta S^\circ}{R} + \ln \varphi \quad (3.5.)$$

where the  $\Delta H^\circ$  and  $\Delta S^\circ$  are the enthalpy and entropy changes, respectively. Dependences of  $\ln k$  vs.  $1/T$  will give the Van't Hoff plots, where the slopes and the intercepts will represent the thermodynamic parameters of the analytes overall phase transfer from the mobile to the stationary phase. Enantioselectivity factor  $\alpha$  is important parameter for chiral separations, that measures relative retention difference between enantiomers. Combining Equations 3.4 and 3.5 would produce the  $\Delta(\Delta G^\circ)$  expression which shows that enantioselectivity factor  $\alpha$  can be affected by temperature changes, especially if entropy-dominated process encounters chiral separations:

$$\Delta(\Delta G^\circ) = -RT \ln \alpha = \Delta(\Delta H^\circ) - T \Delta(\Delta S^\circ) \quad (3.6.)$$

From the temperature dependence obtained in gradient elution mode, it was observed that for most amino acids the resolution of enantiomers increases as the column temperature decreases (Figure 3.20.).

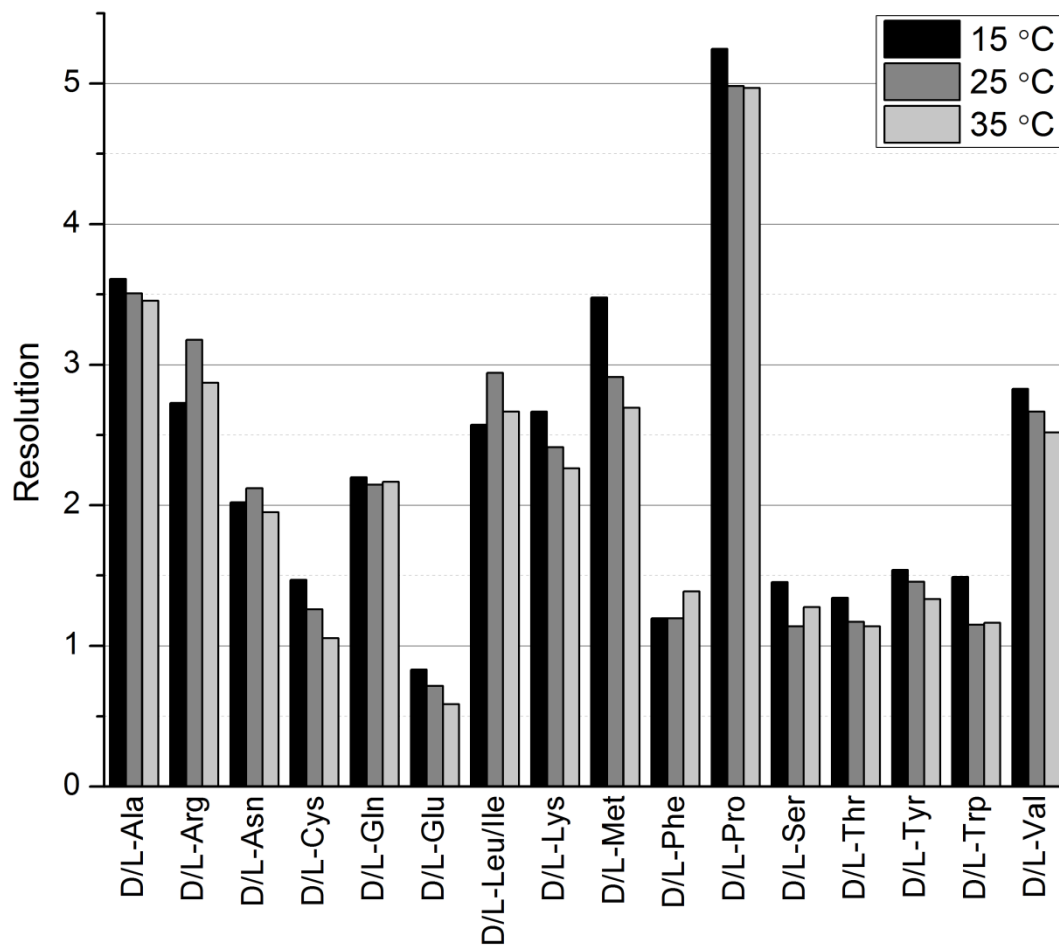


**Figure 3.20.** Effect of temperature on the enantiomeric resolution of amino acids obtained in gradient elution mode ( $n = 2$ ).

A lower temperature generally results in better enantioselectivity ( $\alpha$ ) on most macrocyclic glycopeptide-based chiral stationary phases employed in reversed-phase mode because of the negative enthalpy difference  $\Delta(\Delta H^\circ)$  for the transfer of enantiomers from the mobile phase to the stationary phase [117,118]. All investigated amino acid enantiomers, except for D-/L-Asn, gave negative  $\Delta(\Delta H^\circ)$  values, with correlation coefficients higher than 0.93 (Table 3.6).

**Table 3.6.**

Thermodynamic parameters of D-/L-amino acids separated on Teicoplanin  
CSP.

Enantiomers	$\Delta(\Delta G^\circ) = -RT \ln\alpha = \Delta(\Delta H^\circ) - T\Delta(\Delta S^\circ)$		
	$\Delta(\Delta H^\circ)$	$\Delta(\Delta S^\circ)$	$R^2$
D-/L-Ala	-1.177	0.021	0.9989
D-/L-Arg	-2.215	-0.666	0.9583
D-/L-Asn	0.463	0.474	0.9706
D-/L-Asp	-2.397	-0.842	0.9310
D-/L-Cys	-2.052	-0.422	0.9817
D-/L-Gln	-1.131	-0.122	0.9996
D-/L-Glu	-1.592	-0.474	0.9983
D-/L-Leu/Ile	-2.889	-0.459	0.9930
D-/L-Lys	-2.374	-0.731	0.9995
D-/L-Met	-3.869	-0.886	0.9999
D-/L-Phe	-0.188	0.195	0.9283
D-/L-Pro	-1.327	0.061	0.9970
D-/L-Ser	-1.128	-0.218	0.9941
D-/L-Thr	-1.765	-0.398	0.9959
D-/L-Tyr	-1.297	-0.228	0.9965
D-/L-Trp	-2.269	-0.616	0.9863
D-/L-Val	-2.585	-0.433	0.9984

However, resolution does not always follow the same trend of selectivity. As observed from Figure 3.20, some D-/L-amino acid pairs exhibited slight resolution improvement with increase of the temperature. Raising the temperature most often is associated with an increase in peak efficiency. Thus, because the resolution factor combines both retention differences and efficiency, the higher contribution to the resolution for these acids most likely came from the increase in efficiency.

Several other parameters, such as buffer concentration, mobile phase flow rate, and sample volume, were also briefly tested to improve chromatographic performance, but no obvious improvement in the enantiomeric resolution was observed. The elution sequence of D- and L-enantiomers (L-< D-) of protein



amino acids followed the same order at all cases. The stronger retention of D-enantiomer versus L-enantiomer was also obtained by other studies for  $\alpha$ -amino acids [115] and short peptides [121] on macrocyclic glycopeptide stationary phases.

MRM chromatograms (only transitions used for quantification) of the amino acid standard mixture at the 50  $\mu\text{g}/\text{mL}$  concentration level obtained under optimized HPLC-MS/MS conditions are presented in Figure 3.21. As can be observed, complete enantiomeric separation of 15 amino acids was achieved in about 15 min. D-/L-Glu and D-/L-Asp pairs were partially resolved, and only D-/L-His enantiomers were not resolved.

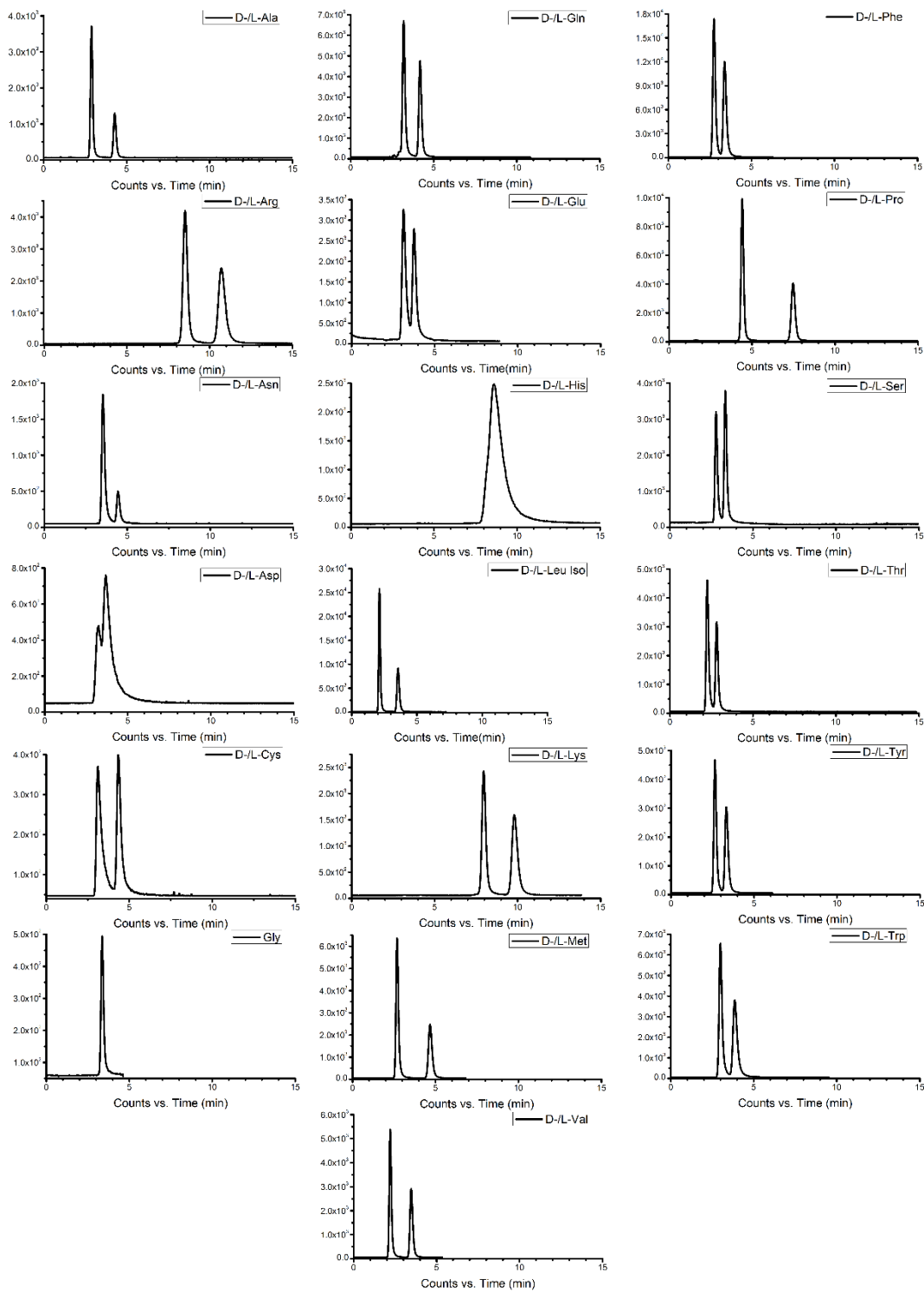


**Figure 3.21.** MRM chromatograms (only transitions used for quantitation) of the amino acid standard mixture at the 50  $\mu\text{g}/\text{mL}$  concentration level obtained under optimized HPLC-MS/MS conditions.

### **3.5. Validation of the methods**

#### **3.5.1. HILIC-MS/MS**

The optimized HILIC-MS/MS method was validated only for the identification of amino acids. One way to detect target compounds selectively is high resolution mass spectrometry. However, employed in this study triple quadrupole mass spectrometer does not provide enough resolution. Therefore the other approach based on specific fragmentation of monitored analyte ions was adopted [122]. Each amino acid was monitored for two specific fragmentation pathways, except for alanine and proline, which, as previously discussed, provided only one fragment ion each. The analyte`s standard solutions at concentration levels of about 100 µg/L were injected into liquid chromatographic system, separated and detected under optimized HILIC-MS/MS conditions. The peaks of the two MRM transitions employed for identification of the amino acids are presented in Figure 3.22. The second transition ion intensity for glycine, histidine, isoleucine, leucine, phenylalanine and tryptophan was considerably lower when compared to major ones. Nonetheless, the intensity of the second MRM ion was sufficient enough for confirmation purposes.

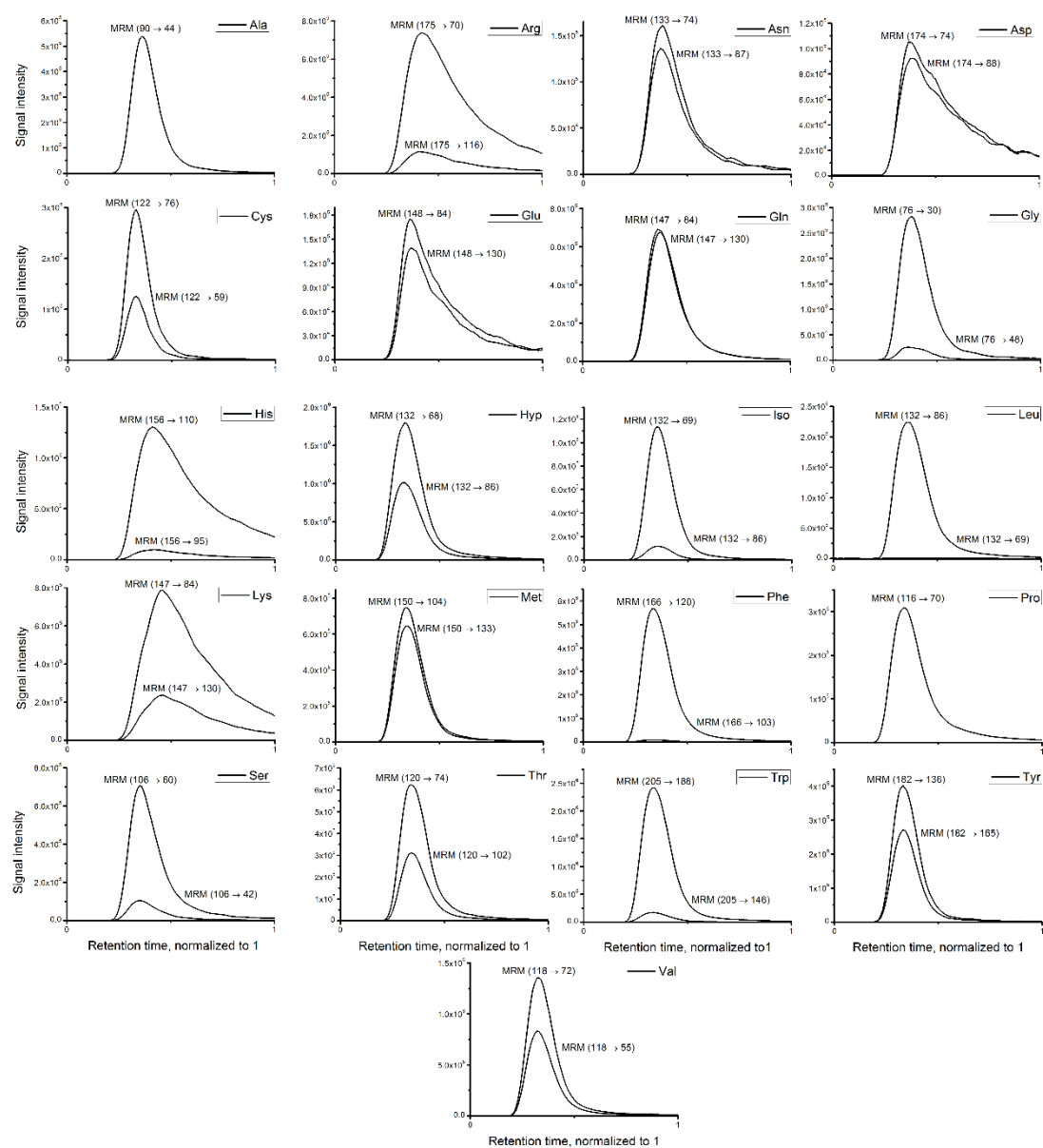


**Figure 3.22.** Peaks of MRM transitions obtained for amino acids by HILIC-MS/MS.

The identification performance was also evaluated for retention time reproducibility in real samples. Four biological fertilizers of different natural origin matrices, namely HPFs from seaweeds, extracts of cinnamon tree and citrus fruits, were used for analysis. Table 3.7 represents the relative standard deviations (RSD) of the retention times obtained for amino acids spiked in fertilizer samples. The RSD values do not exceed 1%, except for histidine, probably due to its poor chromatographic peak shape.

**Table 3.7.**

Retention time reproducibility of amino acids in spiked fertilizer samples.

Analyte	Retention time, min				RSD, %
	Aminocat30 <sup>TM</sup> (Sample 1)	Razormin <sup>TM</sup> (Sample 2)	Zytron <sup>TM</sup> (Sample 3)	Canelys <sup>TM</sup> (Sample 4)	
ALA	3.71	3.71	3.68	3.70	0.38
ARG	9.83	9.78	9.64	9.75	0.82
ASN	5.85	5.77	5.74	5.82	0.85
ASP	10.34	10.30	10.40	10.38	0.43
CYS	3.67	3.64	3.65	3.67	0.41
GLY	4.47	4.47	4.45	4.46	0.21
GLN	2.03	2.03	2.02	2.03	0.25
GLU	5.65	5.62	5.64	5.60	0.39
HIS	12.59	12.09	12.34	12.34	1.64
HYP	3.79	3.78	3.80	3.79	0.22
ILE	1.80	1.80	1.79	1.78	0.53
LEU	1.97	1.96	1.96	1.95	0.42
LYS	10.46	10.47	10.48	10.40	0.34
MET	2.22	2.21	2.20	2.22	0.43
PHE	1.74	1.75	1.75	1.74	0.33
PRO	2.50	2.50	2.48	2.49	0.38
SER	5.38	5.38	5.37	5.37	0.11
THR	4.35	4.33	4.36	4.34	0.30
TYR	2.57	2.55	2.57	2.56	0.37
TRP	1.74	1.74	1.73	1.72	0.55
VAL	2.46	2.47	2.46	2.46	0.20

From the data obtained we can conclude that developed HILIC-MS/MS method exhibits sufficient specificity for the identification of amino acids in complex biological matrices.

### 3.5.1. Chiral LC-MS/MS

The optimized chiral HPLC-MS/MS technique was employed not only for the identification of particular enantiomers but also for their quantification.

Therefore this method was validated in terms of linearity, limit of detection (LOD), limit of quantitation (LOQ), accuracy, and precision, following the ICH harmonized tripartite guideline [123,124]. All HPF samples from the point of composition (provided by the manufacturer) and brief visual evaluation looked similar, but preliminary investigations showed that sample A contains the highest total amount of free amino acids. Consequently, this sample was chosen as the model matrix for validation.

One significant drawback of ESI-MS is that the ionization process is greatly affected by the co-eluting matrix compounds [125]. The matrix effect typically results in the suppression or, less frequently, enhancement of the analyte signal [126,127]. Isotopically labeled internal standards or matrix-matched calibration are the two common approaches that have been widely used to eliminate or correct matrix effects in HPLC-MS/MS analyses. However, neither the blank matrix of analyzed fertilizers nor isotopically labeled standards for all investigated amino acids are unavailable. Therefore, in this study, matrix effects were evaluated by the standard addition method. The signal suppression/enhancement observed with each analyte was calculated as the percentage difference in signal intensity measured in the sample extract versus that measured in the pure solvent:

$$\text{Difference (\%)} = (A_{\text{spiked}} - A_{\text{unspiked}})/A_{\text{solv}} \times 100 \% \quad (3.7.)$$

where  $A_{\text{spiked}}$  is the analyte peak area in the spiked sample,  $A_{\text{unspiked}}$  is the peak area without spiking, and  $A_{\text{solv}}$  is the peak area in pure solvent.

A value of 100% is indicative if no signal suppression/enhancement is observed. The aliquots of 10  $\mu\text{L}$  sample extracts were spiked at two concentration levels (100 and 500  $\mu\text{g/mL}$ ), diluted by a factor of 100, and analyzed. Because of high dilution factor of the extracts, signal suppression was not crucial and was in the range of 92.0–112.6%. Nonetheless, to ensure bias-free results, the standard addition protocol was employed for quantification.

LODs and LOQs were determined from standard addition experiments (for sample A) based on the standard deviation of the response and the slope, expressed as follows:

$$\text{LOD} = 3.3 \sigma/S \quad (3.8.) \quad \text{and} \quad \text{LOQ} = 10 \sigma/S \quad (3.9.)$$

where  $\sigma$  is the standard deviation of  $y$  intercepts of regression lines and  $S$  is the slope estimated from the regression curve. Method performance in terms of regression parameters, signal suppression and LOD, LOQ values is presented in Table 3.8.

**Table 3.8.**

Method performance in terms of regression parameters, limits of detection, limits of quantitation and signal suppression (n = 3).

Analyte	Enantiomer	Regression equation	Correlation coefficient, $R^2$	LOD, $\mu\text{g/mL}$	LOQ, $\mu\text{g/mL}$	Signal suppression, %
ALA	L-	$y = 2916.5x + 9066.3$	0.9990	0.21	0.72	100.5
	D-	$y = 2800.5x + 256$	0.9997	0.08	0.26	99.1
ARG	L-	$y = 2599.8x + 6724.8$	0.9999	0.24	0.79	98.3
	D-	$y = 3414.4x - 85.1$	0.9999	0.13	0.43	100.9
ASN	L-	$y = 1254.2 + 745.7$	0.9999	0.17	0.56	92.0
	D-	$y = 1298.3x + 504.9$	0.9998	0.11	0.37	102.5
ASP	D/L-	$y = 1902.2x + 5913.6$	0.9998	0.13	0.44	96.6
CYS	L-	$y = 209.9 + 236.8$	0.9996	0.05	0.17	92.6
	D-	$y = 281.1x + 358.5$	0.9991	0.08	0.23	99.2
GLY	-	$y = 664.7 + 2797.3$	0.9995	0.12	0.42	100.3
GLN	L-	$y = 2427.9x + 2749$	0.9998	0.13	0.45	111.2
	D-	$y = 1752.1x + 191.37$	0.9999	0.13	0.44	102.0
GLU	D/L-	$y = 2285.7x + 79245$	0.9981	0.08	0.30	112.6
HIS	D/L-	$y = 1318.5x + 1951.1$	0.9993	0.08	0.27	97.1
	L-	$y = 8807.1x + 15376$	0.9991	0.11	0.36	98.7
LEU	D-	$y = 8651.7x + 710.4$	0.9998	0.11	0.35	100.8
	L-	$y = 4284.1x + 15702$	0.9997	0.19	0.64	95.9
LYS	D-	$y = 5030.3x - 616.7$	0.9999	0.15	0.48	99.7
	L-	$y = 2046.8x + 545.5$	0.9997	0.04	0.13	99.3
MET	D-	$y = 2768.9x + 465.7$	0.9999	0.15	0.50	100.2
	L-	$y = 8735.2x + 11981$	0.9993	0.09	0.31	99.9
PHE	D-	$y = 9126.9x + 614.7$	0.9999	0.05	0.16	100.9
	L-	$y = 6556.2x + 12410$	0.9998	0.14	0.46	99.9
PRO	D-	$y = 6956.1x + 3040$	0.9998	0.10	0.34	98.6
	L-	$y = 2243.7x + 6410$	0.9988	0.20	0.67	96.2
SER	D-	$y = 2411.4x + 2279$	0.9996	0.08	0.25	100.4
	L-	$y = 2257.7x + 5372.4$	0.9990	0.12	0.39	102.1
THR	D-	$y = 2226.8x + 213.6$	0.9996	0.16	0.53	99.7

TYR	L-	$y = 1712.6x + 1122.6$	0.9997	0.08	0.27	98.7
	D-	$y = 1677.3x - 9.7$	0.9999	0.11	0.36	99.1
TRP	L-	$y = 6235x + 1188.5$	0.9999	0.07	0.24	112.5
	D-	$y = 6139.9x + 233.0$	0.9999	0.04	0.13	97.8
VAL	L-	$y = 6187x + 16434$	0.9989	0.17	0.58	99.7
	D-	$y = 6926.4x + 138.2$	0.9994	0.15	0.51	99.5

Because of the high number of closely eluting analytes, the time segmentation for MRM analysis was not employed and the dwell time for each MRM transition was set to 20 ms. Although this led to reduced detectability and narrower linear ranges, obtained sensitivity was still acceptable for HPF samples. Because of the absence of reference materials, method trueness was evaluated by spiking/recovery experiments. Fertilizer aliquots (100 mg) were spiked with an approximately 50 µg/mL standard of L- and D-amino acids, and the sample preparation procedure was applied. The recovery values ranged from 73.4% for D-threonine to 115.3% for D-asparagine, with relative standard deviations (RSDs) lower than 20%, except for L-methionine (21.7%) and D-tyrosine (21.9%). Precision was evaluated in terms of repeatability and reproducibility. Interday repeatability was evaluated for the sample without spiking and spiked at two concentration levels: 0.5 and 5.0 µg/mL. This procedure was also performed for interday precision experiments within 4 sequential days. Recovery and precision data are summarized in Table 3.9. Obtained results indicate that the proposed method has an acceptable precision and accuracy for the determination of amino acids in fertilizers.

**Table 3.9.**

Summary of the recovery and precision data for sample A (n = 4).

Analyte	Enantiomer	Recovery, % (RSD%)	Intra day, RSD%			Inter day, RSD%		
			Sample A	Spike level 0.5 µg/mL	Spike level 5.0 µg/mL	Sample A	Spike level 0.5 µg/mL	Spike level 5.0 µg/mL
Ala	D-	88.7 (18.7)	ND <sup>a</sup>	5.9	2.3	ND	3.0	8.8
	L-	93.5 (3.8)	4.2	5.5	1.6	6.8	4.8	7.0
Arg	D-	95.0 (13.2)	ND	3.9	2.1	ND	13.9	5.6
	L-	92.7 (11.9)	7.4	2.0	2.6	6.2	1.9	7.3
Asn	D-	89.2 (19.6)	ND	6.7	0.4	ND	3.5	18.0
	L-	115.3 (16.7)	3.9	4.6	1.3	7.4	3.4	7.1



Asp	D-/L-	108.4 (23.1)	2.8	8.5	2.2	11.9	1.3	8.9
Cys	D-	114.8 (3.3)	ND	6.2	4.0	ND	3.4	11.7
	L-	80.5 (20.2)	ND	6.3	1.1	ND	3.6	6.4
Glu	D-/L-	92.3 (6.0)	3.9	7.1	6.5	8.4	1.5	0.8
Gln	D-	80.3 (15.9)	ND	5.9	2.0	ND	1.7	13.4
	L-	85.2 (3.8)	0.9	10.5	1.3	13.8	19.7	11.6
Gly	-	99.0 (19.1)	2.9	5.4	3.2	0.7	0.5	2.7
His	D-/L-	97.2 (11.0)	3.4	4.5	2.3	21.7	7.6	1.8
Leu/Iso	D-	95.1 (13.0)	ND	6.1	1.2	ND	1.3	5.1
	L-	98.8 (6.6)	5.9	5.8	1.5	8.9	1.8	8.8
Lys	D-	78.4 (7.2)	ND	5.6	2.1	ND	7.8	15.6
	L-	101.3 (8.9)	8.0	1.6	0.7	11.7	12.7	2.7
Met	D-	86.6 (10.9)	ND	8.6	2.8	ND	8.6	7.7
	L-	93.4 (21.7)	4.3	10.1	3.0	12.4	1.1	12.3
Phe	D-	79.8 (15.1)	ND	3.9	1.4	ND	4.6	6.4
	L-	81.0 (6.5)	7.3	7.6	2.8	0.6	6.7	9.4
Pro	D-	98.7 (6.0)	8.3	10.9	2.7	6.7	13.4	14.0
	L-	96.6 (15.5)	6.9	5.7	1.2	13.8	1.0	9.8
Ser	D-	95.4 (7.1)	ND	2.6	1.7	ND	5.2	18.1
	L-	97.6 (19.0)	7.4	7.0	2.4	10.0	0.0	2.7
Thr	D-	73.4 (11.4)	ND	4.9	1.7	ND	5.7	15.5
	L-	102.0 (13.5)	8.1	6.6	1.7	6.4	0.5	8.8
Trp	D-	106.2 (16.0)	ND	4.1	2.2	ND	5.6	9.8
	L-	116 (6.0)	7.6	7.9	6.6	8.1	8.7	5.0
Tyr	D-	98.7 (21.9)	ND	16.4	3.8	ND	2.7	14.0
	L-	97.0 (15.5)	3.7	7.7	4.6	19.5	3.0	14.6
Val	D-	91.1 (13.4)	ND	5.4	0.9	ND	4.3	5.0
	L-	99.4 (1.8)	4.7	7.4	1.8	5.5	0.5	10.5

<sup>a</sup>ND = Not detected.

### 3.6. Sample Analysis

Developed HILIC-MS/MS method was employed for the identification of protein amino acids in four commercial biological fertilizers of natural origin: Aminocat30<sup>TM</sup>, Razormin<sup>TM</sup>, Zytron<sup>TM</sup>, and Canelys<sup>TM</sup>. The first two are produced by seaweed hydrolysis, Zytron<sup>TM</sup> is the extract of citric plant seeds and Canelys<sup>TM</sup> is cinnamon tree extract. Manufacturer (Atlantica Agricola, Spain) claims that all of these bio stimulants contain free  $\alpha$ -amino acids.

A brief extraction optimization experiment was initially performed. The isolation of protein amino acids from biological matrices usually involves

extraction with acidified aqueous or aqueous/organic solutions [95-97]. In this study three acids (HCOOH, CH<sub>3</sub>COOH and HCl) as additives to aqueous/acetonitrile 1:5 (v/v) extractant were compared for the best extraction efficiency. The results showed that for the same samples acetic acid provided slightly higher peak areas for most of the analyzed amino acids (Figure 3.23).

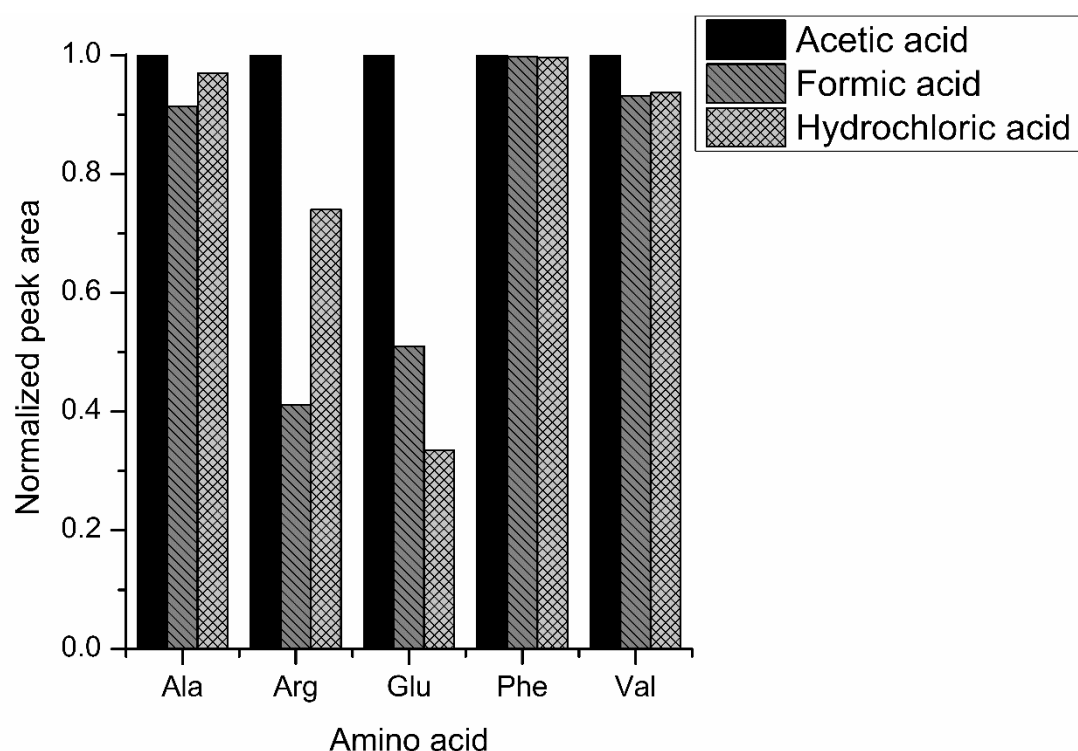


**Figure 3.23.** Effect of acid (1 mol/L) nature on the extraction efficiency (peak areas) of selected amino acids.

The optimized extraction protocol was as follows: 0.50 g of the crude fertilizer sample was extracted with 10 mL of an aqueous/acetonitrile (1:5, v/v) solution containing 1 mol/L CH<sub>3</sub>COOH in an ultrasonic bath for 10 min, then 1:1 (v/v) diluted with acetonitrile and centrifuged for 2 min at 10 000 rpm. 1 mL of the supernatant was filtered through a 0.2 µm nylon syringe filter, diluted with initial mobile phase and analyzed.

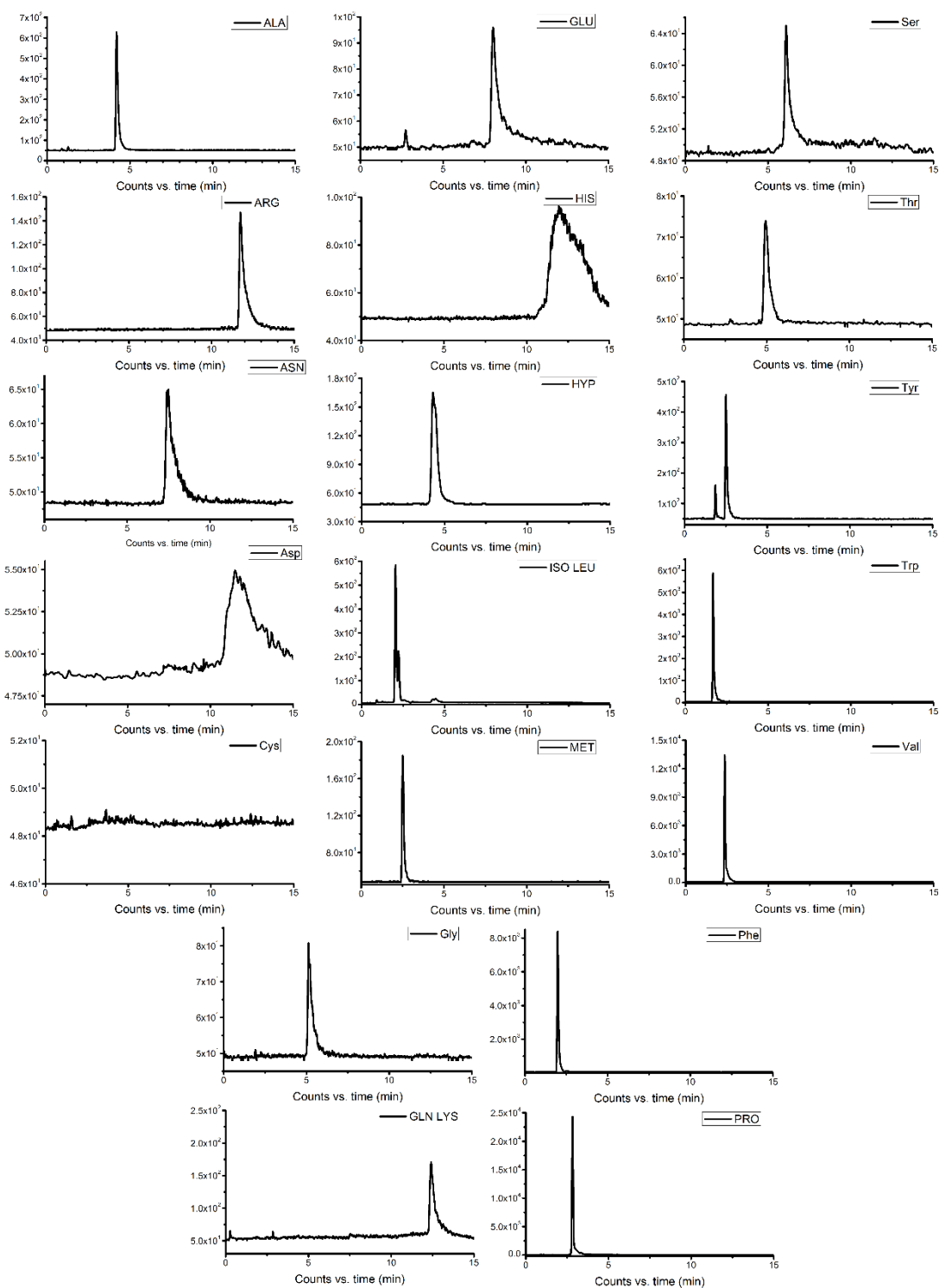


**Figure 3.24.** MRM chromatograms (only higher intensity MRM) obtained for Aminocat30™ extract.

MRM chromatogram of Aminocat30™ is presented in Figure 3.24 and the results are summarized in Table 3.10. Aminocat30™ and Razormin™ fertilizers

contained most of the protein amino acids whereas the other two fertilizers (i.e., extracts of cinnamon and citrus fruit seeds) contained only traces of some amino acids.

**Table 3.10.**

Identification of the amino acids in commercially available biological fertilizers of natural origin.

Amino acid	Aminocat30 <sup>TM</sup> Sample 1	Razormin <sup>TM</sup> Sample 2	Zytron <sup>TM</sup> Sample 3	Canleys <sup>TM</sup> Sample 4
Ala	+ <sup>a</sup>	+	+	+
Arg	+	+	+	+
Asn	+	ND	+	ND
Asp	+	+	ND	ND
Cys	ND <sup>b</sup>	ND	ND	ND
Gly	+	+	+	ND
Gln	+	ND	ND	ND
Glu	+	+	ND	ND
His	+	+	+	+
Hyp	+	+	ND	ND
Ile	+	+	+	+
Leu	+	+	+	+
Lys	+	+	+	+
Met	+	+	ND	ND
Phe	+	+	+	+
Pro	+	+	+	+
Ser	+	+	+	+
Thr	+	+	+	+
Tyr	+	+	+	+
Trp	+	+	+	+
Val	+	+	+	+

<sup>a</sup>+ - analyte was identified.  
<sup>b</sup>ND - not detected.

Finally, particular enantiomers of amino acids were quantified in five commercially available HPF samples using optimized chiral LC-MS/MS technique. For quantitative analysis the validated sample extraction procedure was adopted as it was described by Alarcon-Flores et al. [94]. Only stability of the analytes during the extraction procedure was checked and no racemization

was observed. Because of low or no enantiomeric resolution, aspartic acid, glutamic acid, and histidine were determined as the sum of D- and L-enantiomers, whereas for unresolved isobaric D-Iso/D-Leu and L-Iso/L-Leu, only the sum of L-Iso and L-Leu as well as D-Iso and D-Leu amounts was measured. As an example, MRM chromatograms of Protifert LMW8<sup>TM</sup> extract are presented in Figure 3.25.

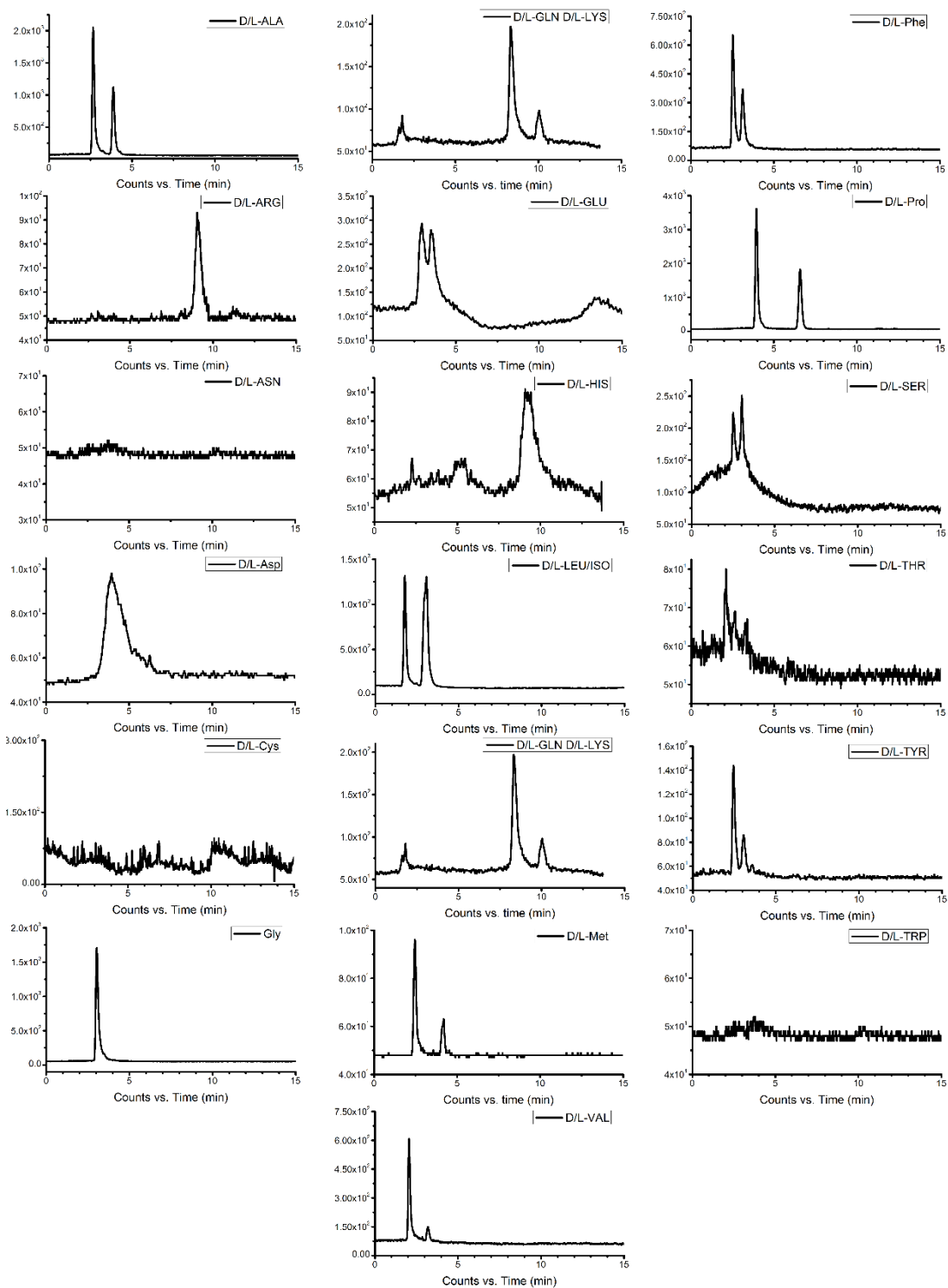


**Figure 3.25.** MRM chromatograms (only transitions used for quantification) obtained for Protifert LMW8™ (Sample D).

Determined concentrations of the individual amino acid enantiomers are summarized in Table 3.11. The obtained total amounts of D- and L-amino acids

were compared to those declared by the manufacturer (Table 3.12.). Unfortunately, composition of sample E was not specified. As seen, for samples A, B, and D, the determined values agree well with the amounts provided by manufacturers. The majority of the amino acids in sample C most likely exist in bonded form. Samples A and B had the highest enantiomeric purity, whereas in sample D, at least one-fourth of the total amino acid amount was the D-enantiomer.

**Table 3.11.**

Determined concentrations of the D- and L-amino acids in the commercial fertilizers (n = 3).

Analyte	Enantiomer	Determined amount, mg/g ( $\pm$ SD)				
		Sample A	Sample B	Sample C	Sample D	Sample E
Ala	D-	ND <sup>a</sup>	0.3 (0.1)	1.7 (0.2)	14.0 (0.3)	2.1 (0.3)
	L-	9.2 (0.2)	7.8 (0.7)	2.7 (0.3)	15.9 (0.4)	3.9 (0.3)
Arg	D-	ND	ND	ND	ND	ND
	L-	7.1 (1.4)	9.5 (1.7)	0.82 (0.01)	1.1 (0.1)	1.2 (0.3)
Asn	D-	ND	ND	ND	ND	ND
	L-	1.9 (0.5)	1.8 (0.4)	0.07 (0.02)	ND	ND
Asp	D-/L-	10.9 (0.8)	14.9 (0.5)	0.25 (0.05)	12.5 (1.5)	ND
Cys	D-	ND	ND	ND	ND	ND
	L-	ND	ND	ND	ND	ND
Glu	D-/L-	151.6 (5.5)	34.4 (5.0)	0.50 (0.1)	11.5 (0.6)	31.9 (1.5)
Gln	D-	ND	ND	ND	ND	ND
	L-	0.6 (0.1)	2.8 (0.5)	0.05 (0.02)	ND	1.72 (0.5)
Gly	-	18.8 (0.6)	38.0 (5.0)	5.3 (0.2)	68.2 (5.0)	11.2 (1.5)
His	D-/L-	5.7 (0.3)	9.3 (2.0)	0.30 (0.05)	2.6 (0.1)	1.49 (0.2)
Leu/Iso	D-	ND	ND	ND	5.5 (0.5)	0.55 (0.1)
	L-	3.4 (0.7)	2.7 (0.2)	0.63 (0.04)	2.0 (0.1)	0.49 (0.05)
Lys	D-	ND	ND	ND	5.8 (0.5)	ND
	L-	27.7 (0.9)	24.8 (1.3)	0.52 (0.01)	6.1 (1.0)	2.4 (0.4)
Met	D-	ND	ND	ND	0.62 (0.1)	ND
	L-	0.4 (0.1)	0.4 (0.1)	0.25 (0.1)	0.63 (0.1)	0.4 (0.2)
Phe	D-	ND	0.6 (0.1)	0.03 (0.01)	1.5 (0.1)	0.35 (0.1)
	L-	4.3 (0.4)	4.6 (0.1)	0.37 (0.1)	1.7 (0.1)	0.68 (0.2)
Pro	D-	1.0 (0.2)	2.1 (0.3)	0.18 (0.03)	10.8 (0.3)	1.6 (0.3)
	L-	5.9 (1.0)	6.6 (1.0)	0.18 (0.04)	11.4 (0.2)	1.9 (0.3)
Ser	D-	ND	ND	ND	1.5 (0.2)	ND
	L-	8.6 (0.1)	7.3 (1.6)	0.24 (0.1)	0.56 (0.05)	2.0 (0.2)
Thr	D-	ND	ND	ND	ND	ND
	L-	7.7 (0.1)	7.9 (0.4)	0.8 (0.3)	ND	0.6 (0.1)

Trp	D-	ND	ND	ND	ND	ND
	L-	1.4 (0.4)	1.4 (0.5)	0.07 (0.01)	ND	0.25 (0.03)
Tyr	D-	ND	ND	ND	0.80 (0.1)	ND
	L-	3.0 (0.4)	3.0 (0.4)	0.20 (0.03)	1.7 (0.1)	0.70 (0.1)
Val	D-	ND	ND	0.02 (0.01)	1.1 (0.1)	0.03 (0.01)
	L-	2.0 (0.3)	7.7 (0.4)	0.61 (0.1)	1.6 (0.2)	0.42 (0.01)

<sup>a</sup>ND - not detected.

**Table 3.12.**

Declared and determined amounts of free amino acids in commercial fertilizers  
(n = 3).

Sample	Brand	Declared amount (w/w) of amino acids	Determined amount <sup>a</sup> (w/w) of L-amino acids, % (±SD)	Determined amount (w/w) of D-amino acids, % (±SD)
A	Aminocat30 <sup>TM</sup>	Contains 30% free L- amino acids + glycine.	27.0 (1.4)	<0.1
B	Terra Sorb Complex <sup>TM</sup>	Contains 20% free L- amino acids+ glycine.	18.5 (2.2)	0.3
C	ILSA Drip Forte <sup>TM</sup>	Total amino acids > 50%. Contains free amino acids, mainly in L- form.	1.4 (0.2)	0.2
D	Protifert LMW8 <sup>TM</sup>	Total amino acids 50%, free amino acids 15 %. Polarization – no information.	12.3 (0.2)	4.2 (0.2)
E	Rutter <sup>TM</sup>	No information.	6.1 (0.6)	0.5 (0.1)

<sup>a</sup>Amounts of enantiomerically unresolved amino acids and glycine were included to L-amino acids.



## CONCLUSIONS

1. Among three HILIC stationary phases (Atlantis HILIC, BEH HILIC and BEH Amide) investigated, BEH Amide provides the best performance for the separation of amino acids. This can be attributed to lower density of free silanols which leads to reduced secondary ion exchange interactions.
2. The results suggest that neither adsorption nor partition dominates the retention processes of amino acids in HILIC separation mode. The retention is caused by the mixed partition/adsorption retention mechanism and can be best described ( $R^2 \geq 0.993$ ) by the model which considers analyte-mobile phase-stationary phase interactions.
3. Amino acids on teicoplanin based chiral stationary phase exhibit typical HILIC retention behavior. The retention is caused by the mixed partition/adsorption retention mechanism in which adsorption predominates over partition.
4. For most amino acids the resolution of enantiomers increases as the column temperature decreases because of the negative enthalpy difference for the transfer of enantiomers from the mobile phase to the stationary phase.
5. Positive ESI ionization tandem mass spectrometry operating in MRM mode provides specific and sensitive detection of protein amino acids.
6. HILIC-MS/MS method exhibits excellent specificity for the identification of amino acids in biological matrices. The retention time RSD values in spiked samples were less than 1%. The method was successfully applied for the identification of the amino acids in commercial fertilizers.
7. Chiral HPLC-MS/MS method is robust against sample matrix: signal suppression was in the range 92.0–112.6%. The recoveries ranged from 73.4% to 115.3% with acceptable reproducibility ( $RSD \leq 21.9\%$ ). Individual amino acid enantiomers were quantified in five commercial fertilizer samples. For most samples the determined values agreed well with the declared amounts.

## **Publications summarized in doctoral dissertation**

### **Articles in journals:**

1. **Taujenis L.**, Valasinavičiūtė I., Olšauskaitė V., Padarauskas A. Identification of  $\alpha$ -amino acids by hydrophilic interaction chromatography-tandem mass spectrometry in fertilizers. *Chemija*, 2014, Vol. 25, No. 2, p. 101-106.
2. **Taujenis L.**, Olšauskaitė V., Padarauskas A. Enantioselective Determination of Protein Amino Acids in Fertilizers by Liquid Chromatography-Tandem Mass Spectrometry on Chiral Teicoplanin Stationary Phase. *Journal of Agricultural and Food Chemistry*, 2014, 62, 11099-11108.

### **Published contributions to academic conferences:**

1. **Taujenis L.**, Olšauskaitė V., Padarauskas A. Enantioselective Determination of Essential  $\alpha$ -Amino Acids in Fertilizers by HPLC-MS/MS. In: 8th International Scientific Conference, „The Vital Nature Sign“, Kaunas, Lithuania, 2014 May 15-17, L-13, p. 24, oral presentation.
2. **Taujenis L.**, Olšauskaitė V., Padarauskas A. Amino Acid Identification by HILIC-MS/MS and Enantioselective determination by Chiral Chromatography-MS/MS in Hydrolyzed Protein Fertilizes Samples. In: International Conference of Lithuanian Chemical Society, Chemistry and Chemical Technology 2015, Vilnius, Lithuania, 2015 January 23, PP-72, p. 219-222.

## **ACKNOWLEDGEMENT**

I am grateful to Research Council of Lithuania for the financial support.

My gratitude goes to my chemistry teacher Virginija Savickaitė; to my bachelor supervisor Povilas Adomėnas together with the colleagues from Fine Synthesis; to my masters supervisor doc. dr. Evaldas Naujalis; most important to my doctoral dissertation supervisor prof. Audrius Padarauskas and all the colleagues from Department of Analytical and Environmental Chemistry and other, who

were not mentioned but contributed to my personal development in the field of chemistry.

## REFERENCES

1. H. Engelhardt, *J. Chromatogr. B*, 800 (2004) 3-6.
2. L.S. Ettre, *LC-GC Europe*, (2003) 1-15.
3. M. Tswett, *Ber. Deutsch. Bot. Ges.*, 24 (1906) 384-391.
4. A. Winterstein, G. Stein, *Physiol. Chem.*, 220 (1933) 247-263.
5. P. Hemström, K. Irgum, *J. Sep. Sci.*, 29 (2006) 1784-1821.
6. P. Jandera, *Anal. Chim. Acta*, 692 (2011) 1-25.
7. T. Greibrokk, *J. Sep. Sci.*, 27 (2004) 1249-1257.
8. R. Consden, A. H. Gordon, A. Martin, *Biochemical Journal*, 38 (1944) 224-232.
9. J.C. Linden, C.L. Lawhead, *J. Chromatogr. A*, 105 (1975) 125-133.
10. B. Buszewski, S. Noga, *Anal. Bioanal. Chem.*, 402 (2012) 231-247.
11. Z.L. Nikolov, P.J. Reilly, *J. Chromatogr.*, 325 (1985) 287-293.
12. W. Muller, G. Kutemeier, *Eur. J. Biochem.*, 128 (1982) 231-238.
13. G.J. Annas, S. Elias, *Am. J. Public Health*, 89 (1999) 98-101.
14. M. Kotake, T. Sakan, N. Nakamura, S. Senoh, *J. Am. Chem. Soc.*, 73 (1951) 2973-2974.
15. B. Chankvetadze, *J. Chromatogr. A*, 1269 (2012) 26-51.
16. W.J. Lough, *J. Chromatogr. B.*, 968 (2014) 1-7.
17. I.W. Wainer, *Trends Anal. Chem.*, 6 (1987) 787-793.
18. M. Lämmerhofer, *J. Chromatogr. A*, 1217 (2010) 814-856.
19. E. Francotte, W. Lindner, *Chirality in Drug Research*. Wiley-VCH. 2006.
20. G. Hesse, R. Hagel, *Chromatographia*, 6 (1973) 277-280.
21. G. Subramanian, *Chiral Separation Techniques: A Practical Approach*. Wiley-VCH. 2007.

22. E. Yashima, C. Yamamoto, Y. Okamoto, *Synlett*, 336 (1998) 344-360.
23. Y. Okamoto, E. Yashima, *Angew. Chemie Int. Ed.*, 37 (1998) 1020-1043.
24. S. Ma, S. Shen, H. Lee, M. Eriksson, X. Zeng, J. Xu, K. Fandrick, N. Yee, C. Senanayake, N. Grinberg, *J. Chromatogr. A*, 1216 (2009) 3784-3793.
25. J. Szejtli, *Starch/Stärke*, 39 (1987) 357-362.
26. S. Allenmark, V. Schurig, *J. Mater. Chem.*, 7 (1997) 1955-1963.
27. T. Koscielski, D. Sybilska, J. Jljrczak, *Notes*, 280 (1983) 131-134.
28. D. Sybliska, T. Kościelski, *J. Chromatogr. A*, 261 (1983) 357-362.
29. E. Takahisa. *Modified cyclodextrins as chiral stationary phases for capillary gas chromatographic separation of enantiomers*. PhD thesis, University Munchen. (2005).
30. A.R. Khan, P. Forgo, K.J. Stine, V.T. D'Souza, *Chem. Rev.*, 98 (1998) 1977-1996.
31. F. Bressolle, M. Audran, T. Pham, J. Vallon, *J. Chromatogr. B*, 687 (1996) 303-336.
32. L. He, T.E. Beesley, *J. Liq. Chromatogr. Relat. Technol.*, 28 (2005) 1075-1767.
33. M. Tang, J. Zhang, S. Zhuang, W. Liu, *TrAC - Trends Anal. Chem.*, 39 (2012) 180-194.
34. W.H. Pirkle, D.W. House, J.M. Finn, *J. Chromatogr.*, 192 (1980) 143-158.
35. W.H. Pirkle, C.J. Welch, B. Lamm, *J. Org. Chem.*, 57 (1992) 3854-3860.
36. W.H. Pirkle, C.J. Welch, *J. Liq. Chromatogr.*, 15 (1992) 1947-1955.
37. A. Cavazzini, L. Pasti, A. Massi, N. Marchetti, F. Dondi, *Anal. Chim. Acta*, 706 (2011) 205-222.
38. D.W. Armstrong, Y. Tang, S. Chen, C. Bagwlll, J. Chen, *Anal. Chem.*, 66

- (1994) 1473-1484.
39. D.W. Armstrong, Y. Liu, K.H. Ekborgott, *Chirality*, 7 (1995) 474-497.
  40. D.W. Armstrong, U.B. Nair, *Electrophoresis*, 18 (1997) 2331-2342.
  41. V. Maier, V. Ranc, M. Švidrnoch, J. Petr, J. Ševčík, E. Tesařová, D.W. Armstrong, *J. Chromatogr. A*, 1237 (2012) 128-132.
  42. K.H. Ekborg-Ott, G. a. Zientara, J.M. Schneiderheinze, K. Gahm, D.W. Armstrong, *Electrophoresis*, 20 (1999) 2438-2457.
  43. R. Bhushan, D. Gupta, *Biomed. Chromatogr.*, 19 (2005) 474-478.
  44. K.H. Ekborg-Ott, J.P. Kullman, X. Wang, K. Gahm, L. He, D.W. Armstrong, *Chirality*, 10 (1998) 627-660.
  45. T.J. Ward, A.B. Farris, *J. Chromatogr. A*, 906 (2001) 73-89.
  46. S. Dixit, J.H. Park, *Biomed. Chromatogr.*, 28 (2014) 10-26.
  47. I. Ilisz, R. Berkecz, A. Péter, *J. Chromatogr. A*, 1216 (2009) 1845-1860.
  48. K.H. Ekborg-ott, Y. Liu, D.W. Armstrong, *Chirality*, 483 (1998) 434-483.
  49. I. Ilisz, Z. Pataj, Z. Gecse, Z. Szakonyi, F. Fülöp, W. Lindner, A. Péter, *Chirality*, 393 (2014) 385-393.
  50. I. Ilisz, R. Berkecz, A. Péter, *J. Sep. Sci.*, 29 (2006) 1305-1321.
  51. J.J. Thomson, *Nature*, 79 (1913) 52-56.
  52. S. Maher, F.P.M. Jjunju, S. Taylor, *Rev. Mod. Phys.*, 87 (2015) 113-135.
  53. K. Blaum, Y. a. Litvinov, *Int. J. Mass Spectrom.*, 349-350 (2013) 1-2.
  54. W. Bleakney, *Phys. Rev.*, 34 (1929) 157-162.
  55. M. Yamashita, J.B. Fenn, *J. Phys. Chem.*, 88 (1984) 4451-4463.
  56. T.C. Rohner, N. Lion, H.H. Girault, *Phys. Chem. Chem. Phys.*, 6 (2004) 3056-3068.

57. P. Kebarle, U.H. Verkerk, *A Brief Overview of the Mechanisms Involved in Electrospray Mass Spectrometry*. Wiley-VCH. 2010.
58. J. Laskin, C. Lifshitz, F. Sobott, V.C. Robinson. *Principles of Mass Spectrometry Applied to Biomolecules*. J. Wiley & Sons. 2006.
59. N.B. Cech, C.G. Enke, *Mass Spectrom. Rev.*, 20 (2002) 362-387.
60. P. Kebarle, M. Peschke, *Anal. Chim. Acta*, 406 (2000) 11-35.
61. S. Nguyen, J.B. Fenn, *Proc. Natl. Acad. Sci.*, 104 (2007) 11111-11117.
62. P. Kebarle, U.H. Verkerk, *Mass Spectrom. Rev.*, 28 (2009) 898-917.
63. F.J. Andrade, J.T. Shelley, W.C. Wetze, M.R. Webb, G. Gamez, S.J. Ray, G.M. Hieftje, *Anal. Chem.*, 80 (2008) 2646-2653.
64. C. Wang, *Austin Chromatogr.*, 2 (2015) 2-8.
65. L. Burlingame, R.K. Boyd, S.J. Gaskell. *Mass Spectrometry; A Textbook*. 2ed Edn., Springer. 1996.
66. E. De Hoffmann. *Kirk-Othmer Encyclopedia of Chemical Technology*. John Wiley & Sons, Inc. 2005.
67. P. Wolfgang, *Electromagnetic Traps for Charged and Neutral Particles*. Physkalisches Institut der Universitat Bonn. 1989.
68. P. Wolfgang, *Reviews Mod. Phys.*, 62 (1990) 531-540.
69. P.S.H. Wong, *Rapid Commun. Mass Spectrom.*, 54 (1994) 237-267.
70. R.E. March, *J. Mass Spectrom.*, 32 (1997) 351-369.
71. Q. Hu, R.J. Noll, H. Li, A. Makarov, M. Hardman, R. Graham Cooks, *J. Mass Spectrom.*, 40 (2005) 430-443.
72. J. de Gouw, C. Warneke, *Mass Spectrom. Rev.*, 26 (2007) 223-257.
73. I. V. Chernushevich, A. V. Loboda, B. a. Thomson, *J. Mass Spectrom.*, 36 (2001) 849-865.

74. A.K. Shukla, J.H. Futrell, *J. Mass Spectrom.*, 35 (2000) 1069.
75. D.E. Goeringer, S. a McLuckey, *Rapid Commun. Mass Spectrom.*, 10 (1996) 328-334.
76. F. Lermyte, A. Konijnenberg, J.P. Williams, J.M. Brown, D. Valkenburg, F. Sobott, *J. Am. Soc. Mass Spectrom.*, 25 (2014) 343-350.
77. R. a. Zubarev, *Curr. Opin. Biotechnol.*, 15 (2004) 12-16.
78. M.S. Kim, A. Pandey, *Proteomics*, 12 (2012) 530-541.
79. B. Domon, *Science*, 312 (2006) 212-217.
80. K. Araki, T. Ozeki, *Kirk-Othmer Encyclopedia of Chemical Technology*. John Wiley & Sons, Inc. 1991.
81. R. Paleckiene, A. Sviklas, R. Šlinkšienė, *Russ. J. Appl. Chem.*, 80 (2007) 352.
82. R. Dromantienė, I. Pranckietienė, G. Šidlauskas, V. Pranckietis, S. Grigaitytė, *Rural Development*, (2011) 178-183.
83. Timothy Allan Stemwedel. 20080302151 U. S. Patent. 2007.
84. M. Jie, W. Raza, Y.C. Xu, Q.R. Shen, *J. Plant Nutr.*, 31 (2008) 571-582.
85. M. Friedman, *J. Agric. Food Chem.*, 47 (1999) 3457-3479.
86. O. Forsum, H. Svennerstam, U. Ganeteg, T. Nasholm, *New Phytol.*, 179 (2008) 1058-1069.
87. H. Svennerstam, U. Ganeteg, C. Bellini, T. Näsholm, *Plant Physiol.*, 143 (2007) 1853-1860.
88. G. C. Barret. *Chemistry and Biochemistry of the Amino Acids*. Champman and Hall, 1985.
89. D. Spaey, D. Traon, *Study on options to fully harmonise the EU legislation on fertilising materials including technical feasibility, environmental, economic and social impacts*. European Commission.



- (2012) 1-150.
90. M. Zhao, Y. Ma, L. Dai, D. Zhang, J. Li, W. Yuan, Y. Li, H. Zhou, *Food Anal. Methods*, 6 (2012) 69-75.
  91. S. Jia, Y.P. Kang, J.H. Park, J. Lee, S.W. Kwon, *J. Chromatogr. A*, 1218 (2011) 9174-9182.
  92. S. Samy, J. Robinson, M.D. Hays, *Anal. Bioanal. Chem.*, 401 (2011) 3103-3113.
  93. X. Yao, G. Zhou, Y. Tang, H. Pang, Y. Qian, S. Guo, X. Mo, S. Zhu, S. Su, D. Qian, C. Jin, Y. Qin, J. Duan, *J. Sep. Sci.*, 36 (2013) 2878-2887.
  94. M.I. Alarcón-Flores, R. Romero-González, A.G. Frenich, J.L. Martínez Vidal, R.C. Reyes, *Anal. Methods*, 2 (2010) 1745-1751.
  95. Y. Xu, L. Yang, F. Yang, Y. Xiong, Z. Wang, Z. Hu, *Metabolomics*, 8 (2011) 475-483.
  96. M.K.R. Mudiam, C. Ratnasekhar, R. Jain, P.N. Saxena, A. Chauhan, R.C. Murthy, *J. Chromatogr. B*, 907 (2012) 56-64.
  97. Y.C. Fiamegos, C.G. Nanos, C.D. Stalikas, *J. Chromatogr. B.*, 813 (2004) 89-94.
  98. C.W. Gehrke, H. Nakamoto, R.W. Zumwalt, *J. Chromatogr. A*, 45 (1969) 24-29.
  99. J.A.S. John, A. Grunau, *J. Chromatogr. A*, 594 (1992) 1992-2000.
  100. G. Kesiunaite, E. Naujalis, A. Padarauskas, *J. Chromatogr. A*, 1209 (2008) 83-87.
  101. A. Orentienė, V. Olšauskaitė, V. Vičkačkaitė, A. Padarauskas, *J. Chromatogr. A*, 1218 (2011) 6884-6891.
  102. M. Dołowy, A. Pyka, *Biomed. Chromatogr.*, 28 (2014) 84-101.
  103. I. Ilisz, R. Berkecz, A. Péter, *J. Pharm. Biomed. Anal.*, 47 (2008) 1-15.

104. I. Ilisz, A. Aranyi, A. Péter, *J. Chromatogr. A*, 1296 (2013) 119-139.
105. G. Torok, A. Peter, *J. Chromatogr. A*, 793 (1998) 283-296.
106. I. Poplewska, R. Kramarz, W. Piatkowski, A. Seidel-Morgenstern, D. Antos, *J. Chromatogr. A*, 1192 (2008) 130-138.
107. T.E. Beesley, J.-T. Lee, *J. Liq. Chromatogr. Relat. Technol.*, 32 (2009) 1733-1767.
108. L. Cavani, C. Ciavatta, C. Gessa, *J. Chromatogr. A*, 985 (2003) 463-469.
109. N.S. Serra, A.L. Crego, *J. Agric. Food. Chem.*, 61 (2013) 5022-5030.
110. Validation of Analytical Procedures: Text and Methodology Q2(R1), *ICH Harmonised Tripartite Guideline*, (1994) 1-13.
111. E.S. Grumbach, D.M. Diehl, U.D. Neue, *J. Sep. Sci.*, 31 (2008) 1511-1518.
112. P. Nikitas, A. Pappa-Louisi, *J. Chromatogr. A*, 971 (2002) 47-60.
113. G. Jin, Z. Guo, F. Zhang, X. Xue, Y. Jin, X. Liang, *Talanta*, 76 (2008) 522-527.
114. M. Schlauch, A.W. Frahm, *J. Chromatogr. A*, 868 (2000) 197-207.
115. A. Berthod, Y. Liu, C. Bagwill, D.W. Armstrong, *J. Chromatogr. A*, 731 (1996) 123-137.
116. V. Backovska, P. Jandera, M. Skavrada, K. Klemmova, *J. Chromatogr. A*, 917 (2001) 123-133.
117. E. Tesarová, Z. Bosáková, V. Pacáková, *J. Chromatogr. A*, 838 (1999) 121-129.
118. A. Péter, E. Vékes, D.W. Armstrong, *J. Chromatogr. A*, 958 (2002) 89-107.
119. M. Schlauch, O. Kos, A.W. Frahm, *J. Pharm. Biomed. Anal.*, 27 (2002) 409-419.

120. A. Berthod, B.L. He, T.E. Beesley, *J. Chromatogr. A*, 1060 (2004) 205-2014.
121. M.G. Schmid, N. Grobuschek, V. Pessenhofer, A. Klostius, G. Gübitz, *J. Chromatogr. A*, 990 (2003) 83-90.
122. L. Dillen, W. Cools, L. Vereyken, W. Lorrenyne, T. Huybrechts, R. Vries, H. Ghobarah, F. Cuyckens, *Bioanalysis*, 4 (2012) 565-579.
123. M. Thompson, S.L.R. Ellison, R. Wood, *Pure Appl. Chem.*, 74 (2002) 835-855.
124. M. Thompson, S.L.R. Ellison, A. Fajgelj, P. Willetts, R. Wood, *Pure Appl. Chem.*, 71 (1999) 337-348.
125. P.J. Taylor, *Clin. Biochem.*, 38 (2005) 328-334.
126. A. Kruve, R. Rebane, K. Kipper, M.-L. Oldekop, H. Evard, K. Herodes, P. Ravio, I. Leito, *Anal. Chim. Acta*, 870 (2015) 8-28.
127. A. Kruve, R. Rebane, K. Kipper, M.-L. Oldekop, H. Evard, K. Herodes, P. Ravio, I. Leito, *Anal. Chim. Acta*, 870 (2015) 29-44.